online issn: 1307-6892

irc 2024
XVIII. international research conference
proceedings

open science index 18 2024

february 05-06, 2024 amsterdam netherlands
international scholarly and scientific research & innovation

Open Science

Open Science Philosophy

Open science encompasses unrestricted access to scientific research articles, access to data from public research, and collaborative research enabled by information and communication technology tools, models, and incentives. Broadening access to scientific research publications and data is at the heart of open science. The objective of open science is to make research outputs and its potential benefits available to the entire world and in the hands of as many as possible:

- Open science promotes a more accurate verification of scientific research results. Scientific inquiry and discovery can be sped up by combining the tools of science and information technologies. Open science will benefit society and researchers by providing faster, easier, and more efficient availability of research outputs.
- Open science reduces duplication in collecting, creating, transferring, and re-using scientific material.
- Open science increases productivity in an era of tight budgets.
- Open science results in great innovation potential and increased consumer choice from public research.
- Open science promotes public trust in science. Greater citizen engagement leads to active participation in scientific experiments and data collection.

Open Science Index

The Open Science Index (OSI) currently provides access to over thirty thousand full-text journal articles and is working with member and non-member organizations to review policies to promote and assess open science. As part of the open science philosophy, and by making open science a reality; OSI is conducting an assessment of the impact of open science principles and restructuring the guidelines for access to scientific research. As digitalization continues to accelerate science, Open science and big data hold enormous promise and present new challenges for policymakers, scientific institutions, and individual researchers.

OSI is helping the global scientific research community discover, evaluate, and access high-quality research output. Renowned for its editorially curated and refereed collection of the highest-quality publications, OSI has always been and will remain free-of-charge.

OSI provides an efficient and thorough discovery process to the open science research database and provides links and free access to full-text articles. There are 50 open access journal categories that are curated and refereed by international scientific committees, the in-house editorial team, and trusted partners. Since its inception in 2007, OSI has made more than thirty thousand peer-reviewed open access full-text journal articles (PDF versions) freely available online without cost, barriers, or restrictions.

Open Science Access

With the Open Science Index, researchers can discover and access trusted peer-reviewed open access full-text scientific research articles with confidence. OSI helps researchers find appropriate non-profit open access journals to publish their work.

OSI gives one-click access to online full-text PDFs and expands the reach to global society by giving users free access from anywhere around the globe. Through cutting-edge open science collaboration, in an innovative public partnership, the non-profit OSI is devoted to making science open and reusable.

To learn more, visit online at waset.org

Open Science

Open Society

An open society allows individuals to change their roles and to benefit from corresponding changes in status. Open science depends to a greater or lesser extent on digital technologies and innovations in structural processes by an open society. When realized, open science research and innovation can create investment opportunities for new and better products and services and therefore increase competitiveness and employment. Open science research and innovation is a key component of thematic open science priorities. Central to the open science digital infrastructure is enabling industry to benefit from digital technology and to underpin scientific advances through the development of an open society. Open science research and innovation can also contribute to society as a global actor because scientific relations can flourish even where global relations are strained. Open science has a critical role across many areas of decision making in providing evidence that helps understand the risks and benefits of different open science choices. Digital technology is making the conduct of open science and innovation more collaborative, more global, and more open to global citizens. Open society must embrace these changes and reinforce its position as the leading power for science, for new ideas, and for investing sustainably in the future.

It is apparent in open society that the way science works is fundamentally changing, and an equally significant transformation is taking place in how organizations and societies innovate. The advent of digital technology is making research and innovation more open, collaborative, and global. These exchanges are leading open society to develop open science and to set goals for research and innovation priority. Open science goals are materializing in the development of scientific research and innovation platforms and greater acceptance of scientific data generated by open science research. Open science research and innovation do not need help from open society to come up with great ideas, but the level of success ideas ultimately reach is undoubtedly influenced by regulation, financing, public support, and market access. Open society is playing a crucial role in improving all these success factors.

Open Science

Open science represents a new approach to the scientific process based on cooperative work and new ways of diffusing knowledge by using digital technologies and collaborative tools. These innovations capture a systemic change to the way science and research have been carried out for the last fifty years. Science is shifting from the standard practice of publishing research results in scientific publications after the research and reviews are completed. The shift is towards sharing and using all available knowledge at an earlier stage in the research process. Open science is to science what digital technology is to social and economic transactions: allowing end users to be producers of ideas, relations, and services and in doing so, enabling new working models, new social relationships and leading to a new modus operandi for science. Open science is as important and disruptive as e-commerce has been for the retail industry. Just like e-commerce, the open science research paradigm shift affects the whole business cycle of doing science and research. From the selection of research subjects to the carrying out of research, to its use and re-use, to the role of universities, and that of publishers are all dramatically changed. Just as the internet and globalization have profoundly changed the way we do business, interact socially, consume culture, and buy goods, these changes are now profoundly impacting how one does research and science.

The discussion on broadening the footprint of science and on novel ways to produce and spread knowledge gradually evolved from two global trends: Open Access and Open Source. The former refers to online, peer-reviewed scholarly outputs, which are free to read, with limited or no copyright and licensing restrictions, while open source refers to software created without any proprietary restriction and which can be accessed and freely used. Although open access became primarily associated with a particular publishing

or scientific dissemination practice, open access already sought to induce a broader practice that includes the general re-use of all kinds of research products, not just publications or data. It is only more recently that open science has coalesced into the concept of a transformed scientific practice, shifting the focus of researchers' activity from publishing as fast as possible to sharing knowledge as early as possible. Open science is defined as the idea that scientific knowledge of all kinds should be openly shared as early as is practical in the discovery process. As a result, the way science is done in the future will look significantly different from the way it is done now. Open science is the ongoing evolution in the modus operandi of doing research and organizing science. This evolution is enabled by digital technology and is driven by both the globalization of the scientific community and increasing public demand to address the societal challenges of our times. Open science entails the ongoing transitions in the way research is performed, researchers collaborate, knowledge is shared, and science is organized.

Open science impacts the entire research cycle, from the inception of research to its publication, and on how this cycle is organized. The outer circle reflects the new interconnected nature of open science, while the inner circle shows the entire scientific process, from the conceptualization of research ideas to publishing. Each step in the scientific process is linked to ongoing changes brought about by open science, including the emergence of alternative systems to establish a scientific reputation; changes in the way quality and impact of research are evaluated; the growing use of scientific blogs; open annotation; and open access to data and publications. All institutions involved in science are affected, including research organizations, research councils, and funding bodies. The trends are irreversible, and they have already grown well beyond individual projects. Theses changes predominantly result from a bottom-up process driven by a growing number of researchers who increasingly employ social media in their research and initiate globally coordinated research projects while sharing results at an early stage in the research process.

Open science is encompassed in five schools of thought:

- the infrastructure school, concerned with technological architecture
- the public school, concerned with the accessibility of knowledge creation
- the measurement school, concerned with alternative impact assessment
- the democratic school, concerned with access to knowledge
- the pragmatic school, concerned with collaborative research

According to the measurement school, the reputation and evaluation of individual researchers are still mainly based on citation-based metrics. The h-index is an author-level metric that attempts to measure both the productivity and citation impact of the publications of a scientist or scholar. The impact factor is a measure reflecting the average number of citations to articles published in an academic journal and is used as a proxy for the relative importance of a journal.

Numerous criticisms have been made of citation-based metrics, primarily when used, and often misused, to assess the performance of individual researchers. These metrics:

- are often not applicable at the individual level
- do not take into account the broader social and economic function of scientific research
- are not adapted to the increased scale of research
- cannot recognize new types of work that researchers are performing

Web-based metrics for measuring research output, popularized as altmetrics, have recently received much attention: some measure the impact at the article level, others make it possible to assess the many outcomes of research in addition to the number of scientific articles and references. The current reputation and evaluation system has to adapt to the new dynamics of open science and acknowledge and incentivize

engagement in open science. Researchers engaging in open science have growing expectations that their work, including intermediate products such as research data, will be better rewarded or taken into account in their career development. Vice-versa, the use, and reuse of open data will require appropriate codes of conduct requiring, for example, the proper acknowledgment of the original creator of the data.

These ongoing changes are progressively transforming scientific practices with innovative tools to facilitate communication, collaboration, and data analysis. Researchers that increasingly work together to create knowledge can employ online tools and create a shared space where creative conversation and collaboration can occur. As a result, the problem-solving process can be faster, and the range of problems that can be solved can be expanded. The ecosystem underpinning open science is evolving very rapidly. Social network platforms for researchers already attract millions of users and are being used to begin and validate more research projects.

Furthermore, the trends towards open access are redefining the framework conditions for science and thus have an impact on how open innovation is produced by encouraging a more dynamic circulation of knowledge. It can enable more science-based startups to emerge thanks to the exploitation of openly accessible research results. Open science, however, does not mean free science. It is essential to ensure that intellectual property is protected before making knowledge publicly available in order to subsequently attract investments that can help translate research results into innovation. If this is taken into account, fuller and broader access to scientific publications and research data can help to accelerate innovation. Investments that boost research and innovation in open science would benefit society with fewer barriers to knowledge transfer, open access to scientific research, and greater mobility of researchers. In this context, open access can help overcome the barriers that innovative organizations face in accessing the results of research funded by the public.

Open innovation

An open society is the largest producer of knowledge, but the phenomenon of open science is changing every aspect of the scientific method by becoming more open, inclusive, and interdisciplinary. Ensuring open society is at the forefront of open science means promoting open access to scientific data and publications alongside the highest standards of research integrity. There are few forces in this globe as engaging and unifying as science. The universal language of science maintains open channels of communication globally. Open society can maximize its gains through maintaining its presence at the highest level of scientific endeavor, and by promoting a competitive edge in the knowledge society of the information age. The ideas and initiatives described in this publication can stimulate anyone interested in open science research and innovation. It is designed to encourage debate and lead to new ideas on what and open society should do, should not do, or do differently.

An open society can lead to a research powerhouse; however, open society rarely succeeds in turning research into innovation and in getting research results to the global market. Open society must improve at making the most of its innovation talent, and that is where open innovation comes into play. The basic premise of open innovation is to open up the innovation process to all active players so that knowledge can circulate more freely and be transformed into products and services that create new markets while fostering a stronger culture of entrepreneurship. Open innovation is defined as the use of purposive inflows and outflows of knowledge to accelerate internal innovation. This original notion of open innovation was primarily based on transferring knowledge, expertise, and even resources from one company or research institution to another. This notion assumes that firms can and should use external ideas as well as internal ideas, and internal and external paths to market, as they seek to improve their performance. The concept of open innovation is continually evolving and is moving from linear, bilateral transactions and collaborations

towards dynamic, networked, multi-collaborative innovation ecosystems. This means that a specific innovation can no longer be seen as the result of predefined and isolated innovation activities but rather as the outcome of a complex co-creation process involving knowledge flows across the entire economic and social environment. This co-creation takes place in different parts of the innovation ecosystem and requires knowledge exchange and absorptive capacities from all the actors involved, whether businesses, academia, financial institutions, public authorities, or citizens.

Open innovation is a broad term, which encompasses several different nuances and approaches. Two main elements underpin the most recent conceptions of open innovation: the users are in the spotlight and invention becomes an innovation only if users become a part of the value creation process. Notions such as user innovation emphasize the role of citizens and users in the innovation processes as distributed' sources of knowledge. This kind of public engagement is one of the aims of open science research and innovation. The term 'open' in these contexts has also been used as a synonym for 'user-centric'; creating a well-functioning ecosystem that allows co-creation and becomes essential for open innovation. In this ecosystem, relevant stakeholders are collaborating along and across industry and sector-specific value chains to co-create solutions for socio-economic and business challenges. One important element to keep in mind when discussing open innovation is that it cannot be defined in absolutely precise terms. It may be better to think of it as a point on a continuum where there is a range of context-dependent innovation activities at different stages, from research to development through to commercialization, and where some activities are more open than others. Open innovation is gaining momentum thanks to new large-scale trends such as digitalization and the mass participation and collaboration in innovation that it enables. The speed and scale of digitalization are accelerating and transforming the way one designs, develops, and manufactures products, the way one delivers services, and the products and services themselves. It is enabling innovative processes and new ways of doing business, introducing new cross-sector value chains and infrastructures.

Open society must ensure that it capitalizes on the benefits that these developments promise for citizens in terms of tackling societal challenges and boosting business and industry. Drawing on these trends, and with the aim of helping build an open innovation ecosystem in open society, the open society's concept of open innovation is characterized by:

- combining the power of ideas and knowledge from different actors to co-create new products and find solutions to societal needs
- creating shared economic and social value, including a citizen and user-centric approach
- capitalizing on the implications of trends such as digitalization, mass participation, and collaboration

In order to encourage the transition from linear knowledge transfer towards more dynamic knowledge circulation, experts agree that it is essential to create and support an open innovation ecosystem that facilitates the translation of knowledge into socio-economic value. In addition to the formal supply-side elements such as research skills, excellent science, funding and intellectual property management, there is also a need to concentrate on the demand side aspects of knowledge circulation, making sure that scientific work corresponds to the needs of the users and that knowledge is findable, accessible, interpretable and reusable. Open access to research results aims to make science more reliable, efficient, and responsive and is the springboard for increased innovation opportunities, e.g. by enabling more science-based startups to emerge. Prioritizing open science does not, however, automatically ensure that research results and scientific knowledge are commercialized or transformed into socio-economic value. In order for this to happen, open innovation must help to connect and exploit the results of open science and facilitate the faster translation of discoveries into societal use and economic value.

Open Science

Collaborations with global partners represent important sources of knowledge circulation. The globalization of research and innovation is not a new phenomenon, but it has intensified in the last decade, particularly in terms of collaborative research, international technology production, and worldwide mobility of researchers and innovative entrepreneurs. Global collaboration plays a significant role both in improving the competitiveness of open innovation ecosystems and in fostering new knowledge production worldwide. It ensures access to a broader set of competencies, resources, and skills wherever they are located, and it yields positive impacts in terms of scientific quality and research results. Collaboration enables global standard-setting, allows global challenges to be tackled more effectively, and facilitates participation in global value chains and new and emerging markets.

To learn more, visit online at waset.org

Open Science

Scholarly Research Review

The scholarly research review is a multidimensional evaluation procedure in which standard peer review models can be adapted in line with the ethos of scientific research, including accessible identities between reviewer and author, publishing review reports and enabling greater participation in the peer review process. Scholarly research review methods are employed to maintain standards of quality, improve performance, provide credibility, and determine suitability for publication. *Responsible Peer Review Procedure:* Responsible peer review ensures that scholarly research meets accepted disciplinary standards and ensures the dissemination of only relevant findings, free from bias, unwarranted claims, and unacceptable interpretations. Principles of responsible peer review:

• Honesty in all aspects of research
• Accountability in the conduct of research
• Professional courtesy and fairness in working with others
• Good stewardship of research on behalf of others

The responsibilities of peer review apply to scholarly researchers at all stages of peer review: Fairness, Transparency, Independence, Appropriateness and Balance, Participation, Confidentiality, Impartiality, Timeliness, Quality and Excellence, Professionalism, and Duty to Report.

Scholarly Research Review Traits:
• Scholarly Research Review Identities: Authors and reviewers are aware of each other's identity

• Scholarly Research Review Reports: Review reports are published alongside the relevant article

• Scholarly Research Review Participation: The wider academic community is able to contribute to the review process

• Scholarly Research Review Interaction: Direct reciprocal discussion between author(s) and reviewers, and/or between reviewers, is allowed and encouraged

• Scholarly Research Pre-review Manuscripts: Manuscripts are made immediately available in advance of any formal peer review procedures

• Scholarly Research Review Final-version Reviewing: Editorial revision of the language and format is conducted on the final version of the manuscript for publication

• Scholarly Research Review Platforms: The scholarly research review process is independent of the final publication of the manuscript and it is facilitated by a different organizational entity than the venue of publication

All submitted manuscripts are subject to the scholarly research review process, in which there are three stages of evaluation for consideration: pre-review manuscripts, chair-review presentation, and final-review manuscripts. All submitted full text papers, that may still be withstand the editorial review process, are presented in the conference proceedings. Manuscripts are tracked and all actions are logged by internal and external reviewers according to publication policy. External reviewers' editorial analysis consists of the evaluation reports of the conference session chairs and participants in addition to online internal and external reviewers' reports. Based on completion of the scholarly research review process, those manuscripts meeting the publication standards are published 10 days after the event date.

To learn more, visit online at waset.org

TABLE OF CONTENTS

Numerical Study of Laminar Separation Bubble Over an Airfoil Using γ-$Re_{\theta t}$ SST Turbulence Model on Moderate Reynolds Number

Y. El khchine [*], M. Sriti

[*] *Materials, Energy and Sustainable Development Laboratory, National High School of Arts and Crafts, Moulay Ismail University of Meknes*

Materials, Energy and Sustainable Development Laboratory, National High School of Arts and Crafts, Moulay Ismail University of Meknes

Corresponding author: y.elkhchine@umi.ac.ma

Abstract:

A parametric study has been conducted to analyse the flow around S809 airfoil of wind turbine in order to better understand the characteristics and effects of laminar separation bubble (LSB) on aerodynamic design for maximizing wind turbine efficiency. Numerical simulations were performed at low Reynolds number by solving the Unsteady Reynolds Averaged Navier-Stokes (URANS) equations based on C-type structural mesh and using γ-$Re_{\theta t}$ turbulence model. Two-dimensional study was conducted for the chord Reynolds number of 1×10^5 and angles of attack (AoA) between 0 and 20.15 degrees. The simulation results obtained for the aerodynamic coefficients at various angles of attack (AoA) were compared with XFoil results. A sensitivity study was performed to examine the effects of Reynolds number and free-stream turbulence intensity on the location and length of laminar separation bubble and aerodynamic performances of wind turbine. The results show that increasing the Reynolds number leads to a delay in the laminar separation on the upper surface of the airfoil. The increase in Reynolds number leads to an accelerate transition process and the turbulent reattachment point move closer to the leading edge owing to an earlier reattachment of the turbulent shear layer. This leads to a considerable reduction in the length of the separation bubble as the Reynolds number is increased. The increase of the level of free-stream turbulence intensity leads to a decrease in separation bubble length and an increase the lift coefficient while having negligible effects on the stall angle. When the AoA increased, the bubble on the suction airfoil surface was found to moves upstream to leading edge of the airfoil that causes earlier laminar separation.

Keywords: laminar separation bubble, turbulence intensity, S809 airfoil, transition model, Reynolds number.

Identification of Candidate Gene for Root Development and Its Association with Plant Architecture and Yield in Cassava

Abiodun Olayinka, Daniel Dzidzienyo, Pangirayi Tongoona, Samuel Offei, Edwige Gaby Nkouaya Mbanjo, Chiedozie Egesi, Ismail Yusuf Rabbi

***Abstract*—** Cassava (Manihot esculenta Crantz) is a major source of starch for various industrial applications. However, the traditional cultivation and harvesting methods of cassava are labour-intensive and inefficient, limiting the supply of fresh cassava roots for industrial starch production. To achieve improved productivity and quality of fresh cassava roots through mechanized cultivation, cassava cultivars with compact plant architecture and moderate plant height are needed. Plant architecture-related traits, such as plant height, harvest index, stem diameter, branching angle, and lodging tolerance, are critical for crop productivity and suitability for mechanized cultivation. However, the genetics of cassava plant architecture remain poorly understood. This study aimed to identify the genetic bases of the relationships between plant architecture traits and productivity-related traits, particularly starch content. A panel of 453 clones developed at the International Institute of Tropical Agriculture, Nigeria, was genotyped and phenotyped for 18 plant architecture and productivity-related traits at four locations in Nigeria. A genome-wide association study (GWAS) was conducted using the phenotypic data from a panel of 453 clones and 61,238 high-quality Diversity Arrays Technology sequencing (DArTseq) derived Single Nucleotide Polymorphism (SNP) markers that are evenly distributed across the cassava genome. Five significant associations between ten SNPs and three plant architecture component traits were identified through GWAS. We found five SNPs on chromosomes 6 and 16 that were significantly associated with shoot weight, harvest index, and total yield through genome-wide association mapping. We also discovered an essential candidate gene that is co-located with peak SNPs linked to these traits in M. esculenta. A review of the cassava reference genome v7.1 revealed that the SNP on chromosome 6 is in proximity to Manes.06G101600.1, a gene that regulates endodermal differentiation and root development in plants. The findings of this study provide insights into the genetic basis of plant architecture and yield in cassava. Cassava breeders could leverage this knowledge to optimize plant architecture and yield in cassava through marker-assisted selection and targeted manipulation of the candidate gene.

***Keywords*—** manihot esculenta crantz, plant architecture, dartseq, snp markers, genome-wide association study.

Abiodun Fatai Olayinka is with the University of Ghana, Ghana (e-mail: aolayinka@wacci.ug.edu.gh).

Identification of Impact Load and Partial System Parameters Using 1D-CNN

Xuewen Yu and Danhui Dan

Abstract—The identification of impact load and some hard-to-obtain system parameters is crucial for the activities of analysis, validation, and evaluation in the engineering field. This paper proposes a method that utilizes neural networks based on 1D-CNN to identify the impact load and partial system parameters from measured responses. To this end, forward computations are conducted to provide datasets consisting of the triples $(parameter\ \theta, input\ u, output\ y)$. Then neural networks are trained to learn the mapping from input to output, $f_{u|\{\theta\}} : y \rightarrow u$, as well as from input and output to parameter, $f_\theta : (u, y) \rightarrow \theta$. Afterward, feeding the trained neural networks the measured output response, the input impact load and system parameter can be calculated, respectively. The method is tested on two simulated examples and shows sound accuracy in estimating the impact load (waveform and location) and system parameter.

Keywords—Convolutional neural network, impact load identification, system parameter identification, inverse problem.

I. Introduction

THE identification of impact load [1] plays an important role in structure design, vibration analysis, disaster recognition, and structural health monitoring in aerospace, mechanical, civil, and other engineering fields. In general, the direct measurement by device is unavailable due to the contingency and destructiveness of the impact load itself, e.g., the burst load. The widely used means are estimating the impact load from the structural responses [2]. With the development of sensing and communication techniques, it's cheaper and easier to obtain the responses. However, it is still a challenging inverse problem to identify the impact load given the measured output, featured by the difficulties of ill-condition and non-linearity.

Many studies have focused on this issue, with the direct inverse method being the most natural approach [3]. To mitigate the effects of an ill-conditioned matrix, regularization techniques that incorporate the priors of impact loads (e.g., sparsity in a transformed domain) are frequently employed [4], [5], [6], [7]. And linearization is necessary for nonlinear structures to construct corresponding system matrices. To avoid the computation of a large-scale matrix inversion, the impact load is represented by a weighted superposition of basis functions. The problem is transformed into seeking a set of weights that minimize the gap between the measured responses and the calculated responses under basis functions. This classic optimization problem can be solved by the least square method or heuristic searching/evolutionary computing, e.g., genetic algorithm [8], [9], [10], [11]. However, the results greatly depend on the number and form of selected basis functions.

Recently, artificial neural networks (ANNs) have emerged as a promising approach for identifying the impact load. Due to the strong representation ability of ANN, the nonlinear relationship between the input impact load and output response can be learned through the training of a large number of prepared data pairs. In addition, neural networks are much more flexible in manipulating data dimensions than heuristic and evolutionary optimization algorithms. On the premise that the ANN model enjoys good generalization performance, it can estimate the impact load very fast in the inference stage. This is charming for online tracking, evaluating, or monitoring of structures. Zhou et al. [12] used a deep recurrent neural network (RNN) model based on long short-term memory (LSTM) layers to identify the impact load of nonlinear structures, showing the capability for identifying the complex impact load even if the impact location is unknown. Li et al. [13] employed Kriging interpolation combined with BP neural network (K-BP) to improve the accuracy of strain field inversion and load identification for carbon fiber reinforced plastic (CFRP). Baek et al. [14] proposed a multi-layered perceptron (MLP) based method to identify impact points and magnitudes of a submerged floating tunnel (SFT) and validated it through numerical simulations and experimental tests. Guo et al. [15] utilized three kinds of machine learning models, gradient boosting decision trees (GBDT) model, convolutional neural network (CNN) model, and bidirectional long short-term memory (BLSTM) model to identify and locate impact loads according to dynamic response. The performance of different models was compared with a thin-walled cylinder. However, in the context of existing works relying on ANNs, the limitation arises from the fact that the system is fully predefined during the dataset construction for training. That is the form of the governing equation is fixed, as well as the parameter values within the equation. As a result, the mapping relationship learned from output to input is only suitable for the specific condition. While in practical scenarios, it is difficult to obtain or measure some system parameters, such as damping, and these parameters could also exhibit variations during operation. Therefore, in this paper, the authors attempt to calculate the system outputs under impact loads concerning different system parameters, forming the dataset consisting of the triple variables of system parameter θ_i, input impact load u_i, and output response y_i: $\{(\theta_i, u_i, y_i)\}$. Two neural network models denoted as impact load identification network $\mathcal{N}_u$ and system parameter estimation network $\mathcal{N}_\theta$ based on the 1D-CNN layer are trained separately. The former is used to learn the mapping from output response to input impact load by

X. Yu is with the School of Civil Engineering, Tongji University, Shanghai, CO 200092 CHN (corresponding author, e-mail: xuewen_yu@tongji.edu.cn).

D. Dan is with the School of Civil Engineering, Tongji University, Shanghai, CO 200092 CHN (corresponding author, e-mail: dandanhui@tongji.edu.cn).

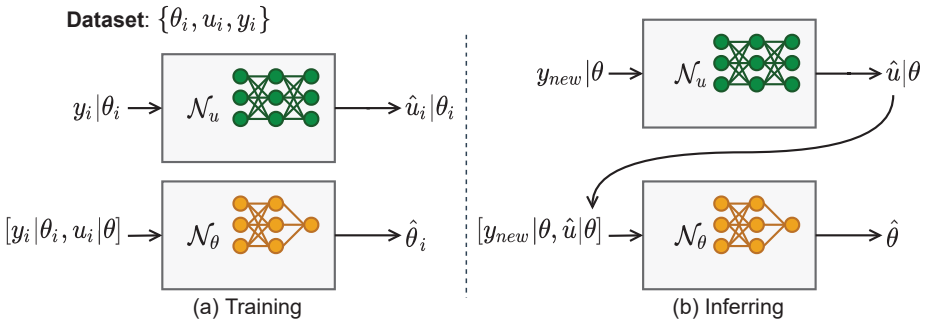

Fig. 1. Framework of the proposed method

arranging the dataset as $\{(y_i; u_i)|\theta_i\}$, and the latter is used to learn the mapping from input impact and output response to system parameter by organizing the dataset as $\{(y_i, u_i; \theta_i)\}$. Thus, the network can grasp the relationship between the input and output when the system parameter varies within a certain range. Once the output is determined, the network can further estimate the system parameter.

The proposed method is verified through a nonlinear duffing oscillator and a cantilever beam. The results demonstrate its capability of identifying the impact load from the response considering the indetermination of system parameter, and to determine the system parameter in reverse when the impact load is estimated.

II. 1D-CNN BASED IMPACT LOAD AND SYSTEM PARAMETER IDENTIFICATION

A. The Proposed Method

For a dynamic system

$$dy/dt = f_\theta(y, u) = f(y, u; \theta), \tag{1}$$

where y, u, and θ represent the system input, output, and parameters, respectively, denoting the solution as

$$y = g(u; f_\theta), \tag{2}$$

the key to identifying the impact load u from the measured output y of the dynamic system f_θ is to determine the inverse transform

$$u = g^{-1}(y; f_\theta). \tag{3}$$

However, in a nonlinear system or an undetermined linear system observed, g^{-1} is hard to obtain explicitly and directly. So, a 1D-CNN layer based neural network is utilized in this paper to represent g^{-1}.

On account of the uncertainty of the structure itself, at the stage of collecting the dataset, the input and output pairs are calculated by taking different system parameters within a certain range, as shown in Fig. 2. The dataset $\{(\theta_i, u_i, y_i)\}$ is utilized in two aspects (Fig. 1(a)), one is to train the impact load identification network $\mathcal{N}_u$ and another is to train the system parameter identification network $\mathcal{N}_\theta$. The impact load identification network $\mathcal{N}_u$ could be regarded as a superset of many possible system models, and the distribution of system parameters is embedded in the network. The architectures of networks will be introduced in the following sections II-B and II-C. When finishing the training of the two networks, they can be used to identify the impact load and system parameter as shown in Fig. 1(b).

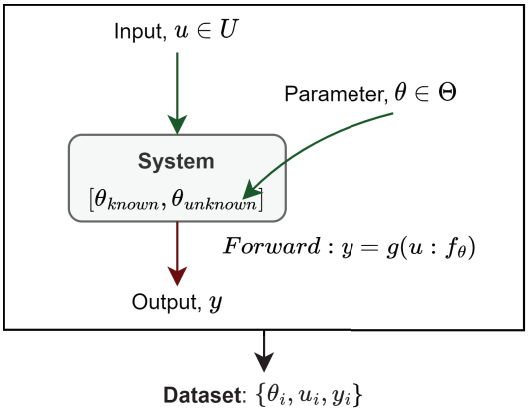

Fig. 2. Construction of dataset

B. Impact Load Identification Network

The impact load identification network $\mathcal{N}_u$ consists of three CNN blocks and flows with a ReLU activate function (Fig. 3). Two skip connections are added between the CNN blocks, as drawn in the figure. The CNN block is shown in the enlarged box. It consists of a 1D-CNN layer with a kernel size denoted as K_i that maps the channels from C into O_i, a ReLU layer, and another 1D-CNN layer with a kernel size of K_i that maps the channels from O_i back to C. Zero padding is adopted in each 1D-CNN layer to make the sequence length L unchanged. To finally determine the network, it has to set the size parameters of $\{\underbrace{O_1, K_1}_{\text{1st block}}; \underbrace{O_2, K_2}_{\text{2nd block}}; \underbrace{O_3, K_3}_{\text{3rd block}}\}$.

The loss function is defined as the mean square root (MSE) of the predicted and the true impact load as

$$\mathcal{L}_u = \frac{1}{N}\sum_{i=1}^{N}\left(\frac{1}{CL}\sum_{j=1}^{C}\sum_{k=1}^{L}\left(\hat{u}_{j,k}^{i} - u_{j,k}^{i}\right)^2\right) \tag{4}$$

where, N is the total number of samples, C and L are the number of channels and the length of sequence of the impact load time-history, respectively.

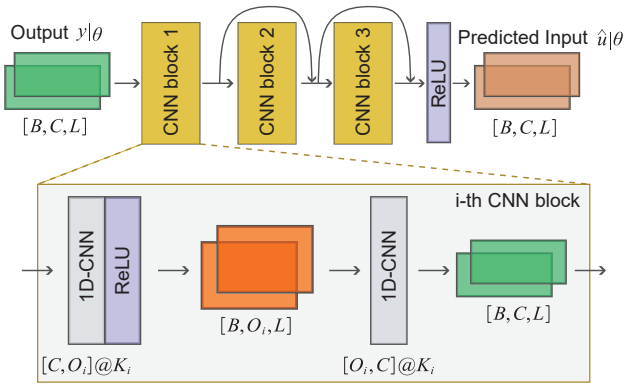

Fig. 3. Impact load identification network $\mathcal{N}_u$

C. System Parameter Identification Network

The system parameter identification network $\mathcal{N}_\theta$ maps the concatenate of input and output (multi-channel input/output requires vectorization) into the desired parameter. The network consists of three sets of 1D-CNN layer and ReLU layer, finally follows a linear layer (Fig. 4). The three 1D-CNN layers with a kernel size of K transform the channels from 1 to O and back to 1, as depicted in the figure. In order to gradually reduce the dimension, a stride with a size of S is utilized in the 1D-CNN layers. The input size of the linear layer is derived accordingly. To completely determine the network, it has to set the parameters of $\{O, K, S\}$.

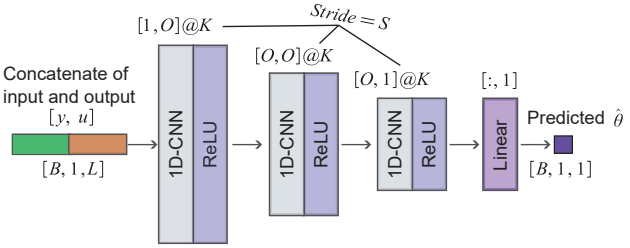

Fig. 4. System parameter identification network $\mathcal{N}_\theta$

The loss function is defined as the MSE of the predicted and the true system parameters as

$$\mathcal{L}_\theta = \frac{1}{N}\sum_{i=1}^{N}\left(\hat{\theta}-\theta\right)^2 \tag{5}$$

where N is the total number of samples.

III. Numerical Experiment

To generate the dataset $\{(\theta_i, u_i, y_i)\}$, three kinds of impact loads, triangular, half-sine[10], and Gaussian [12] forms are utilized (Fig. 5). The expressions are written in (6), (7), and (8), respectively.

$$u_{tri}(t) = \begin{cases} 0, & 0 \le t < t_a, t \ge t_b \\ p_{max}\left(t-t_a\right)/\left(t_c-t_a\right), & t_a \le t < t_c, \\ p_{max}\left(t_b-t\right)/\left(t_b-t_c\right), & t_c \le t < t_b, \end{cases} \tag{6}$$

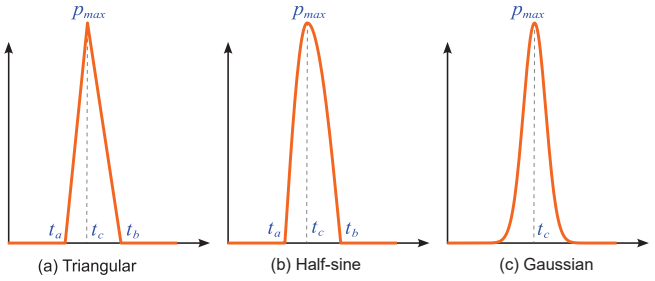

Fig. 5. The forms of impact load considered

where t_a and t_b are the start time and stop time of the impact load, and t_c is the time corresponding to the maximum impact load p_{max}.

$$u_{sin}(t) = \begin{cases} 0, & 0 \le t < t_a, t \ge t_b \\ p_{max}\sin\left(2\pi\omega_1\left(t-t_a\right)\right), & t_a \le t < t_c, \\ p_{max}\sin\left(2\pi\omega_2\left(t-2t_c+t_b\right)\right) & t_c \le t < t_b, \end{cases} \tag{7}$$

where $\omega_1 := 1/4(t_c - t_a)$ $\omega_2 := 1/4(t_b - t_c)$

$$u_{Gau}(t) = p_{max}\exp\left(-\left(t-t_c\right)^2/\left(2\sigma^2\right)\right) \tag{8}$$

where σ is the standard deviation of Gaussian distribution.

These impact load expressions are parameterized, and the parameters are uniformly sampled in the corresponding range

$$\begin{aligned} t_a &\sim U(0, 0.1), \\ t_b &\sim t_a + U(0.01, 0.1), \\ t_c &\sim U(t_a, t_b), \\ p_{max} &\sim U(100, 1000), \\ \sigma &\sim U(0.005, 0.01). \end{aligned} \tag{9}$$

A. Duffing Oscillator

The duffing oscillator expressed as

$$m\ddot{y} + c\dot{y} + \kappa y + \alpha y^3 = u(t) \tag{10}$$

is utilezed to valid the proposed method, where $m = 1$, $\kappa = 10000$, $\alpha = 10000$, and the parameter c is regarded as not determined that uniformly sampled from $U(1, 10)$. The force u is sampled from the three types of impact loads in (6), (7), and (8), and the parameters of force are sampled according to (9). There are a total of 3000 samples $\{(c_i, u_i, y_i)\}$ are generated. The sampling frequency is 1000 Hz, and the analysis duration is 1 s.

The parameters of the impact load indentification network $\mathcal{N}_u$ are set as $\{O_1, K_1; O_2, K_2; O_3, K_3\} = \{16, 128; 16, 64; 16, 32\}$, and that of the parameter identification network $\mathcal{N}_\theta$ are set as $\{O, K, S\} = \{4, 64, 4\}$.

In the training of the networks $\mathcal{N}_u$ and $\mathcal{N}_\theta$, the dataset is divided into training data, validation data, and testing data with a ratio of 70%:15%:15%. The batch size is set as 20 and 10, respectively. The Adam optimizer [16] is used. The initial learning rate is set as 0.001 and it is multiplied by a factor of 0.95 when the current loss of the validation dataset is greater

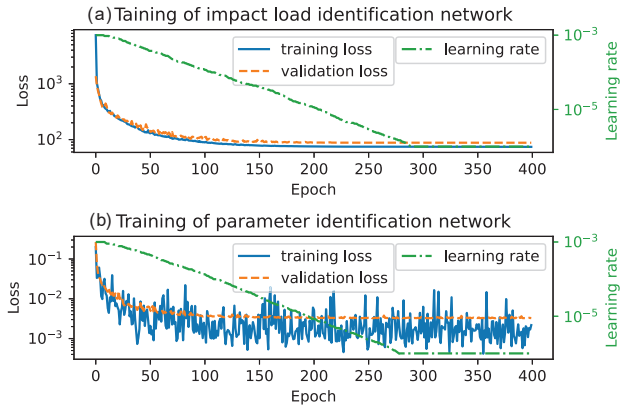

Fig. 6. Training process of duffing oscillator case.

than the previous one. Once the learning rate is lower than 0.000001, it will stop decreasing.

Fig. 6 plots the training and validation losses. After about 200 epochs, the losses tend to converge. The results of the trained networks on the test dataset are shown in Fig. 7. The MSE and relative error (RE) are defined as

$$\text{MSE} = \|\hat{u} - u\|_2^2 / \|u\|_2^2 \times 100\%, \tag{11}$$

and

$$\text{RE} = |\hat{\theta} - \theta| / \theta \times 100\%. \tag{12}$$

It is found that the maximum MSE of the impact load identification is about 10%, and the mean of MSE is 0.50% in the 450 tests. The maximum identification RE of the parameter c is about 20%, and the mean of RE is 2.19%.

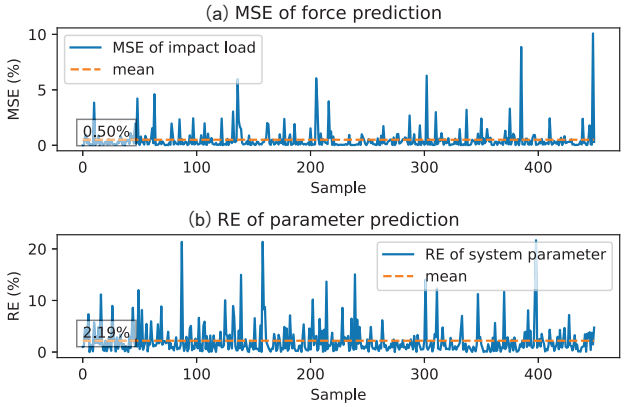

Fig. 7. Test results of duffing oscillator case.

B. Cantilever Beam

In this section, a cantilever beam (Fig. 8) is analyzed. The structural parameters are listed in TABLE I. Forward computations for preparing the dataset are carried out using finite element method (FEM). The beam is divided into 20 elements, and the nodes 5, 9, 13, 17, and 21 are observed.

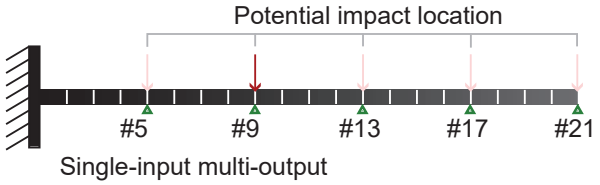

Fig. 8. The cantilever beam model

TABLE I
PARAMETERS OF THE CANTILEVER BEAM

Length	Width	Height	Young's modulus	Mass
5.0m	0.4m	0.2m	205GPa	2450kg/m^3

In the FEM model, rayleigh damping is adopted, and regard the damping ratio c as an uncertain system parameter. Parameter c is sampled from a uniform distribution $U(0.001, 0.05)$; the impact load is sampled in the same way in Section III-A, and it is randomly located at one of the five observed nodes. The other nodes with no impact loads are set as zeros. The responses at all the five observed nodes are measured. And there are a total of 10000 samples $\{(c_i, u_i, y_i)\}$ are collected. The sampling rate is 1000 Hz, and the total duration of analysis is 0.5 s.

The parameters of network $\mathcal{N}_u$ and $\mathcal{N}_\theta$ are also set as $\{O_1, K_1; O_2, K_2; O_3, K_3\} = \{16, 128; 16, 64; 16, 32\}$ and $\{O, K, S\} = \{4, 64, 5\}$. The related settings of network training are kept the same as that in the case of duffing oscillator (see in Section III-A).

The training and validation losses are plotted in Fig. 9. After about 300 epochs, the losses are converged.

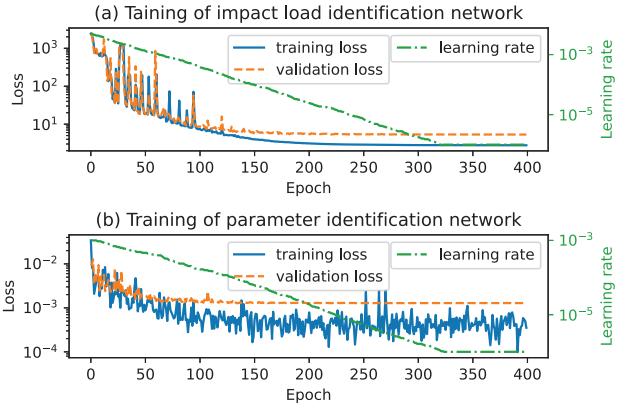

Fig. 9. Training process of cantilever beam case

Fig. 10 shows the test results of this example. It suggests that the maximum MSE of the impact load identification is about 10%, and the mean of MSE is 0.18% among 1500 trials. The maximum identification RE of the damping ratio c exceeds 50%, but the mean of RE is 2.55%. In this case, the input dimension of the concatenation of input load and output response is $5 \times 1000 \times 0.5 \times 2 = 5000$. It's relatively large, which brings more difficulties in the fitting and generalization of the network.

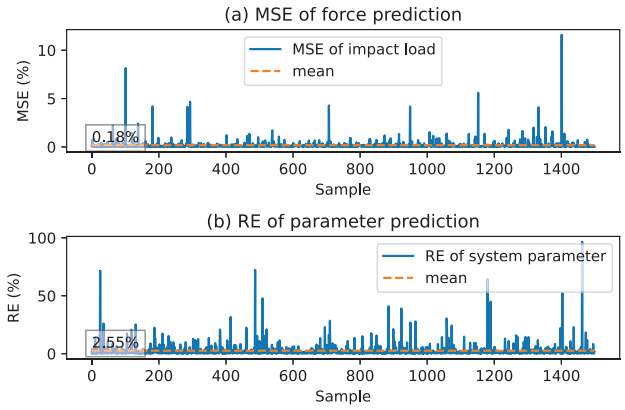

Fig. 10. Test results of cantilever beam case

Fig. 11 dives into the results of two tests. The waveforms of the predicted impact loads match well with the actual ones. And the method can also locate the positions of the impact loads.

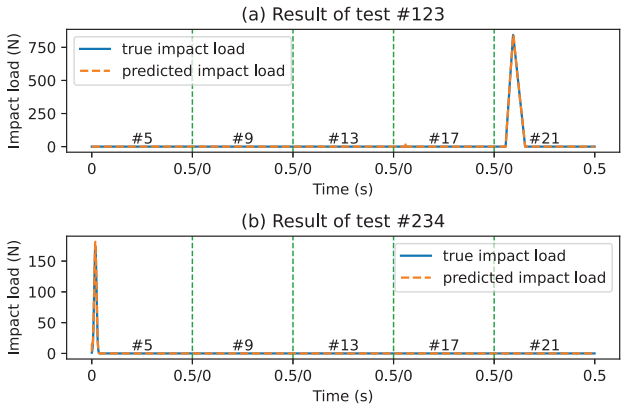

Fig. 11. Diving into the results of two tests of cantilever beam case

IV. Conclusion

This paper proposes a method using a 1D-CNN based neural network to identify the impact load considering the uncertainty of system parameters and a method to further estimate the unknown system parameter based on the identified impact load and the measured response utilizing another 1D-CNN based neural network. Two numerical examples, i.e., a nonlinear single-DOF duffing oscillator and a 5-DOF linear cantilever beam, are utilized to prove the method. On the testing dataset, the mean MSEs of impact load identification in the two cases are 0.50% and 0.18%, respectively, and the mean REs of system parameter identification are 2.19% and 2.55%, respectively.

In future works, the authors will exploit the proposed method on noise robustness and explore its performance on experimental or realistic structures.

Acknowledgment

The authors would like to thank the support of the Project of China Railway Engineering Design and Consulting Group Co., Ltd., “Research and development of bridge management and maintenance system based on perception neural network”; the Fundamental Research Funds for the Central Universities, China (20210205); the National Natural Science Foundation of China (51878490).

References

[1] R. Liu, E. Dobriban, Z. Hou, and K. Qian, ”Dynamic load identification for mechanical systems: a review,” *Arch. Comput. Methods Eng.*, 1–33, 2021.

[2] T.S. Jang, H. Baek, S.L. Han, and T. Kinoshita, ”Indirect measurement of the impulsive load to a nonlinear system from dynamic responses: inverse problem formulation,” *Mech. Syst. Sig. Process.*, 24 (6), 1665–1681, 2010.

[3] H. Inoue, N. Ikeda, K. Kishimoto, T. Shibuya, and T. Koizumi, ”Inverse analysis of the magnitude and direction of impact force,” *JSME Int. J. Ser. A, Mech. Mater. Eng.*, 38 (1), 84–91, 1994.

[4] G. Yan, H. Sun, and O. Büyüköztürk, ”Impact load identification for composite structures using Bayesian regularization and unscented Kalman filter,” *Struct. Control Health Monit.*, 24, e1910, 2017.

[5] J. Jiang, H. Tang, M.S. Mohamed, S. Luo, and J. Chen, ”Augmented Tikhonov Regularization Method for Dynamic Load Identification,” *Appl. Sci.*, 10, 6348, 2020.

[6] Y. Li, X. Wang, Y. Xia, and L. Sun, ”Sparse Bayesian technique for load identification and full response reconstruction,” *J. Sound Vib.*, 553, 117669, 2023.

[7] Y. Liu, L. Wang, ”A two-step weighting regularization method for stochastic excitation identification under multi-source uncertainties based on response superposition-decomposition principle,” *Mech. Syst. Signal Process.*, 182, 109565, 2023.

[8] B. Qiao, X. Zhang, C. Wang, H. Zhang, and X. Chen, ”Sparse regularization for force identification using dictionaries,” *J. Sound Vib.*, 368, 71–86, 2016.

[9] J. Liu, X. Sun, X. Han, C. Jiang, and D. Yu, ”A novel computational inverse technique for load identification using the shape function method of moving least square fitting,” *Comput. Struct.*, 144, 127–137, 2014.

[10] G. Yan and L. Zhou, ”Impact load identification of composite structure using genetic algorithms,” *J. Sound Vib.*, 319, 869–884, 2009.

[11] R. Hashemi and M. Kargarnovin, ”Vibration base identification of impact force using genetic algorithm,” *Int. J. Mech. Syst. Sci. Eng.*, 1 (4), 204–210, 2007.

[12] J. Zhou, L. Dong, W. Guan, J. Yan, ”Impact load identification of nonlinear structures using deep Recurrent Neural Network,” *Mech. Syst. Signal Process.*, 133, 106292, 2019.

[13] J. Li, J. Yan, J. Zhu, and X. Qing, ”K-BP neural network-based strain field inversion and load identification for CFRP,” *Measurement*, 187, 110227, 2022.

[14] S.-M. Baek, J.-C. Park, and H.-J. Jung, ”Impact load identification method based on artificial neural network for submerged floating tunnel under collision,” *Ocean Eng.*, 286, 115641, 2023.

[15] C. Guo, L. Jiang, F. Yang, Z. Yang, and X. Zhang, ”Impact load identification and localization method on thin-walled cylinders using machine learning,” *Smart Mater. Struct.*, 32, 065018, 2023.

[16] D. P., Kingma, and J. Ba, ”Adam: A method for stochastic optimization,” *arXiv preprint*, arXiv:1412.6980, 2014.

Determination of Micronutrients in the Fruit of Cydonia Oblonga Miller

Madrakhimova Sakhiba[1]., Matmurotov Bakhtishod[2]., Boltaboyava Zilola., Matchanov Alimjan[1]

[1]PhD, Institute of Bioorganic Chemistry, Academy of Sciences of the Republic of Uzbekistan., Orcid ID:0000-0002-9742-8251., E-mail:bioorganic86@mail.ru
[2]teacher of the Department of Medical and Biological Chemistry of the Tashkent Medical Academy.,Orcid ID:0000-0002-9742-8251.,E-mail: b.matmurotov@mail.ru+998946459166
[3]Student of Urganch State University.,
[1]Dr of Chemical Sciences leading Reasearcher., Institute of Bioorganic Chemistry, Academy of Sciences of the Republic of Uzbekistan

Abstract

Analyzing the chemical composition of food products that are consumed every day is one of the urgent problems today. Considering this, in this work, we analyzed the micronutrient composition of Cydonia oblonga Miller (COM) fruit, which is common in all continents of the world, using mass spectrometry method combined with ISP MS. Among the macroelements contained in the fruit of the plant, it is observed that the amount of potassium and phosphorus is higher. Trace elements strontium and barium were found to be more abundant than other trace elements. It was observed that the amount of trace elements contained in COM fruit does not exceed the permissible standards. Therefore, it can be recommended to eat this fruit every day to prevent various diseases that occur in the human body (the results of the analysis are presented in Figure 1).

Keywords: Cydonia oblonga Miller (COM), macroelement, microelement, inductively coupled mass spectrometry (ISP MS),

Objective: Cydonia oblonga Miller fruit micronutrient (macro-micronutrient) content was analyzed using inductively coupled mass spectrometry.

Research object and subject: Cydonia oblonga Miller fruit, macro and micronutrients

Material and method: Cydonia oblonga Miller fruit, HNO3, H2O2, distilled water hydrolysis, ISP MS, mineralization, hydrolysis

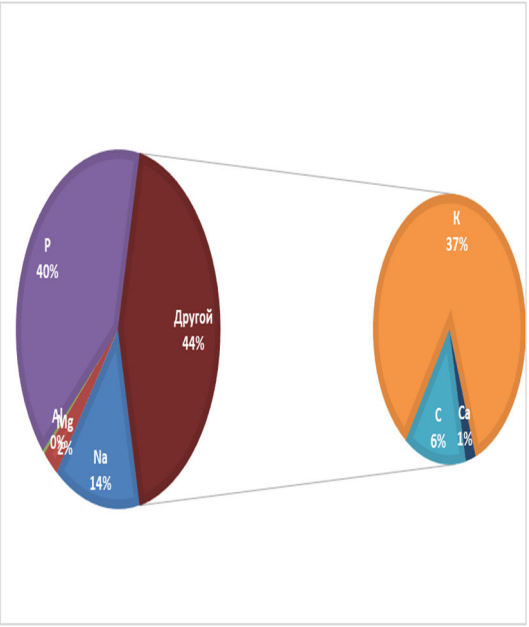

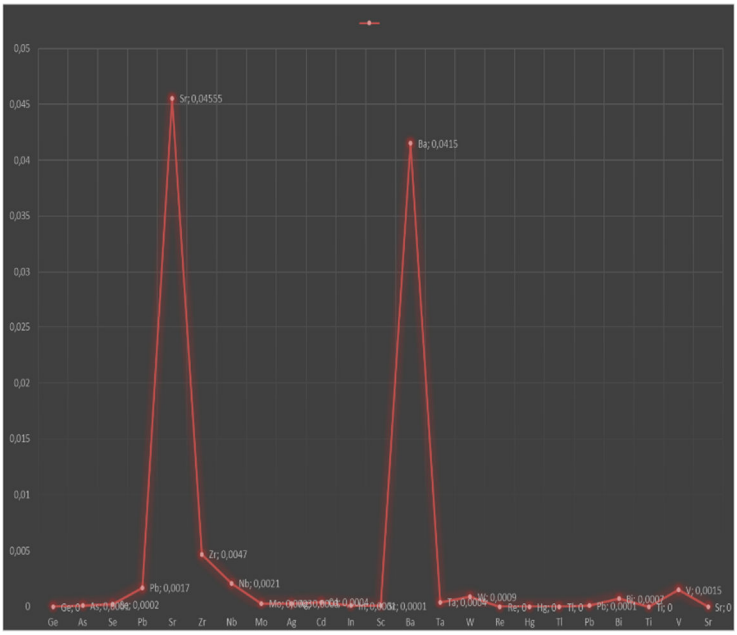

Virus and Bispecific Antibody Combinatorial Therapy amplifies T Cell-Mediated Antitumour Immunity

Swati Dhiman[1], Joel Brenner[2], Doris Hellerschmied[2], Karl S Lang[1]

Institute of Immunology, University Clinic Essen, University of Duisburg-Essen

Centre of Medical Biotechnology, University of Duisburg-Essen

Key Words: Combination immunotherapy, (Lymphocytic choriomeningitis virus) LCMV, Bispecific T cell Engager (BiTE), T cell activation, EpCAM,

Abstract

Bispecific antibodies targeting cancer cells have shown great therapeutic potential. The approval of Blinatumomab (anti CD3*anti CD19) for the treatment of Acute Lymphoblastic leukaemia and several others in clinical trials highlights the important role of bispecific antibodies. T cell targeting bispecific antibodies are called Bispecific T cell engager (BITE) and have been used to redirect T cells to kill tumour cells expressing tumour associated antigen (TAA). One such BITE, Catumaxomab (anti EpCAM* anti CD3), was approved by European Medicines Agency in 2010 but was later withdrawn from the market because of associated side effects such as cytokine release syndrome (CRS) with its usage. However, this target of tumour toxicity is underexplored. Here, we have designed a bispecific construct that consists of a CD3-specific single chain variable fragment (scFv) in frame with EpCAM – specific scFv with Human Fc tag flanking the protein at C terminal termed as CD3-EpCAM Fc (CEFc). CEFc was well expressed in mammalian cells showed binding affinity to both cognate antigens of the parental antibodies. *In vitro*, we show that CEFC mediates EpCAM+ tumour cell cytolysis via the production of effector cytokines TNFα and IFNγ and is dependent on the Effector to Target (E: T) ratio. *In vivo*, investigations have provided valuable insights into the heightened activation of T cells when combining CE-Fc with LCMV infection compared to LCMV infection alone. This combination treatment leads to superior tumour regression and is dosage dependent. Importantly, we have found that the combination significantly enhances tumour targeting and therapeutic efficacy compared to monotherapy, manifesting synergistic treatment effects.

OR

Bispecific antibodies targeting cancer cells have exhibited considerable therapeutic potential. Notably, the approval of Blinatumomab (comprising anti-CD3 and anti-CD19 components) for the treatment of Acute Lymphoblastic Leukaemia, along with several others currently undergoing clinical trials, underscores the pivotal role played by bispecific antibodies in oncology. Specifically, T-cell-targeting bispecific antibodies, referred to as Bispecific T Cell Engagers (BiTEs), have been harnessed to redirect T cells towards the eradication of tumour cells expressing tumour-associated antigens (TAAs). Notably, Catumaxomab (comprising anti-EpCAM and anti-CD3 components) received approval from the European Medicines Agency in 2010. However, it was subsequently withdrawn from the market due to associated adverse effects, notably cytokine release syndrome (CRS), linked to its usage. Nevertheless, the phenomenon of on-target, off-tumour toxicity remains an area warranting deeper investigation.

In this study, we have meticulously designed a bispecific construct, denoted as CD3-EpCAM Fc (CEFc), which features a CD3-specific single-chain variable fragment (scFv) linked to an EpCAM-specific scFv, flanked by a Human Fc tag at the C-terminal region. CEFc has been successfully expressed in mammalian cells and has demonstrated binding affinity to both cognate antigens corresponding to the parental antibodies. *In vitro* experimentation has corroborated that CEFc facilitates cytolysis of EpCAM-positive tumour cells through the production of effector cytokines such as TNFα and IFNγ, with its efficacy being contingent upon the Effector-to-Target (E:T) ratio. Furthermore, our *in vivo* investigations have provided valuable insights into the heightened activation of T cells when combining CE-Fc with LCMV infection compared to LCMV infection alone. This combination treatment leads to superior tumour regression and is dosage dependent. Importantly, we have found that the combination significantly enhances tumour targeting and therapeutic efficacy compared to monotherapy, manifesting synergistic treatment effects.

OR

Bispecific antibodies show promise in targeting cancer cells, exemplified by Blinatumomab's approval for Acute Lymphoblastic Leukaemia and ongoing clinical trials. T-cell-targeting Bispecific T Cell Engagers (BiTEs) redirect T cells to eliminate tumour cells with tumour-associated antigens (TAAs). Catumaxomab, with anti-EpCAM and anti-CD3 components, received approval but was withdrawn due to adverse effects, like cytokine release syndrome (CRS).

In our study, we've designed CD3-EpCAM Fc (CEFc), a bispecific construct with a CD3-specific scFv linked to an EpCAM-specific scFv, bearing a Human Fc tag at the C-terminus. CEFc effectively binds to both target antigens. *In vitro* experiments confirm CEFc's ability to induce the cytolysis of EpCAM-positive tumour cells, dependent on the Effector-to-Target (E:T) ratio.

Furthermore, our *in vivo* research reveals enhanced T cell activation when combining CE-Fc with LCMV infection compared to LCMV alone. This combination treatment results in better tumour regression, depending on the dosage. Importantly, it significantly improves tumour targeting and therapeutic efficacy compared to monotherapy, showing synergistic treatment effects.

Or

Immunotherapy has been a game changer in cancer treatment. The approval of checkpoint inhibitor monoclonal antibodies to manipulate the host immune response to enhance immune surveillance has been named the breakthrough in 2013. Despite this, there are limitations to use of immunotherapy. Insufficient intratumoral T cell infiltration, downregulation of Tumour associated neoantigens and lack of tumour specific immune monitoring in tumour microenvironment (TME) puts limitations to immunotherapy. In this study, we've designed CD3-EpCAM Fc (CEFc), a bispecific construct with a CD3-specific scFv linked to an EpCAM-specific scFv, bearing a Human Fc tag at the C-terminus. CEFc effectively binds to both target antigens. *In vitro* experiments confirm CEFc's ability to induce the cytolysis of EpCAM-positive tumour cells, dependent on the Effector-to-Target (E:T) ratio.

Furthermore, our in vivo research reveals enhanced T cell activation when combining CE-Fc with LCMV infection compared to LCMV alone. This combination treatment results in better tumour regression, depending on the dosage. Importantly, it significantly improves tumour targeting and therapeutic efficacy compared to monotherapy, showing synergistic treatment effects.

Or

Immunotherapy has emerged as a paradigm-shifting approach within the landscape of cancer therapeutics. Notably, the approval of checkpoint inhibitor monoclonal antibodies aimed at modulating the host immune response to augment immune surveillance was recognized as a pivotal milestone in 2013. However, it is imperative to acknowledge that the application of immunotherapy is encumbered by certain constraints. These encompass inadequate intratumoral T cell infiltration, the downregulation of tumour-associated neoantigens, and the absence of tumour-specific immune surveillance within the tumour microenvironment (TME). These factors collectively impose restrictions on the full realization of the potential of immunotherapeutic interventions. In the context of this study, we have devised a novel construct known as CD3-EpCAM Fc (CEFc). This bispecific entity is composed of a CD3-specific single-chain variable fragment (scFv) linked to an EpCAM-specific scFv, featuring a Human Fc tag at the C-terminus. CEFc demonstrates an exceptional affinity for both target antigens. Our in vitro experiments affirm the capability of CEFc to induce cytolysis in EpCAM-positive tumor cells, with the degree of cytolysis being contingent on the Effector-to-Target (E:T) ratio. Moreover, our in vivo investigations unveil augmented T cell activation when CEFc is combined with LCMV infection, in comparison to LCMV administration in isolation. This combination therapy results in more pronounced tumour regression, the extent of which is contingent on the dosage administered. Crucially, it significantly enhances tumor targeting and therapeutic efficacy when contrasted with monotherapy, thereby demonstrating profound synergistic effects in the treatment regimen.

Materials and Methods:

Cell Lines

Human embryonic kidney cell HEK293, mouse mammary carcinoma 4T1 cells were obtained from the American Type Culture Collection (ATCC, USA). ExpiCHO-S™ suspension cells were obtained from ThermoFisher Scientific (Cat. No. A29127). HEK293 cells were cultured in DMEM media supplemented with 10% fetal bovine serum (FBS) (Cat. No.) and 1% Pen-Strep-Glutamine, whereas 4TI cells were cultured in RPMI 1640 medium (Cat. No.) supplemented with 10% FBS and 1% Pen-Strep-Glutamine solution.. Suspension cells were culture in ExpiCHO™ Expression medium obtained from ThermoFisher Scientific (Cat. No. A2910001). All cells were maintained in a humidified incubator with an atmosphere containing 5% CO_2 at 37°C except suspension cells, which were grown at 8% CO_2.

Expression and Purification of Bispecific Antibody

The AbCE-Fc is a recombinant anti-mouse CD3ε and anti-mouse EpCAM (CD3 x EpCAM) bispecific antibody generated from transient transfection of Expi CHO-S (Cat. Code A29127, ThermoFisher SCIENTIFIC) cell expression system. The sequence of variable heavy chain and light chain of antibody against mouse CD3ε 2C11 clone was obtained from PDB (RCSB PDB - 3R06: Crystal structure of anti-mouse CD3epsilon antibody 2C11 Fab fragment). The sequence of anti EpCAM is from clone G8.8 which was retrieved from a patent (US 2015/0010567 A1). The protein sequences were reverse translated into the DNA sequence using ExPasy (BackTranseq program). These coding gene sequences were synthesized by company Eurofins, inserted into the pFUSE-hIgG1-Fc2 vector (Cat. code pfuse-hg1fc2, InvivoGen, Germany), and verified by sequencing the entire vectors by Microsynth (Germany). Subsequently, the expression vector was transfected into the Expi CHO S cells using Expifectamine Transfection kit (Cat. code A29129, ThermoFisher SCIENTIFIC) according to the manufacturer's protocols using Max titer protocol. After culturing for 13 days, the supernatant was collected after centrifugation at 4000 rcf for 20min. HALT Proteases inhibitor 100X (Cat. code 78429, ThermoFisher SCIENTIFIC) is added to the supernatant to a final conc. of 1X and stored at -80°C.

The CD3 x EpCAM fragments were purified by Protein A based affinity chromatography (Cytiva, Uppsala, Sweden) through the AKTA pureTM 25 L system (Cat. No. 29018224 Cytiva, Uppsala, Sweden). The supernatant was centrifuged and filtered through a 0.45 μm filter membrane. The column was loaded with binding buffer (20 mM sodium phosphate, pH 7.0), supernatants, wash buffer (20 mM sodium phosphate, pH 7.0), and eluted with elution buffer (0.1 M Glycine, pH 2.5). The elution was neutralized to pH 7.0 with Tris-HCl buffer (1 M, pH 8.5).

The eluent was further processed to exchange the neutralizing buffer to PBS using Sepharose Buffer Exchange columns (Cat No. 17508701 HiPrep 26/10 Desalting Columns).

Flow Cytometry

To evaluate binding of CD3*EpCAM BsAb to its target antigens CD3 and EpCAM, CD3+ T cells containing mouse splenocytes and 4TI EpCAM high mouse tumour cell line was used. To check binding of BsAb to EpCAM, 10^4 cells per well in 96 U bottom plate were incubated with different conc. of BsAb diluted in FACS buffer for 30 min at 4℃ in the dark. Followed by two washes with FACS buffer, it was incubated with monoclonal antibody against Human Fc-FITC (Cat. No.) conjugated antibody for 30min. at 4℃ in the dark. The cells were washed with FACS buffer to remove the unbound antibody. The cells were finally resuspended in 150ul FACS buffer and immediately detected by Flow Cytometry. To check the binding of BsAb to CD3, mouse splenocytes were taken and resuspended to have 10^5 cells per well in 96 U bottom plate. Different conc. of BsAb diluted in FACS buffer were added onto the cells for 30 min at 4℃ in the dark. Followed by two washes with FACS buffer, it was incubated with monoclonal antibody against Human Fc-FITC, CD4-APC (Cat. No.) and CD8-PE-Cy7 (Cat. No.) conjugated antibody for 30min. at 4℃ in the dark. The cells were washed with FACS buffer to remove the unbound antibody. The cells were finally resuspended in 150ul FACS buffer and immediately detected by Flow Cytometry

For *in vitro* T cell activation assay, a single suspension from mice spleen was prepared using 70 mm strainer. The cells were then centrifuged at 300g for 5 min, resuspended in 1ml erythrocyte lysis buffer for 2min. at RT, followed by single wash with Complete RPMI medium to deactivate the lysis buffer and centrifugation at 300g for 5min. and finally resuspended in 1ml Complete RPMI media. Different amounts of 4T1 cells (1000, 5000, 10000, 50000, 10000) per well in triplicates were seeded in 96-well U bottom plates. $4*10^5$ Splenocytes were added to the tumour cells in each well, followed by co-incubation with 50ul of 10ug/ml purified CE-Fc protein. After 24, 48, 72 hours, the cells were stained for CD4- (Clone, Cat), CD8a- (Clone Cat), CD25- (Clone, Cat. No.), CD69- (Clone, Cat,) TNFα (Clone, Cat) and IFNγ (Clone Cat. No.) and analysed by flow cytometry.

In vivo, the extracted tumours, spleen and lymph node were smashed and passed through filter and resuspended in complete RPMI-1640 (). Tumour tissues were filtered to make single-cell suspensions and stained with the following antibodies:

In vitro Cytotoxicity Assay

Different amounts of 4T1 Tumour cells (1000, 5000, 10000, 50000, 10000) per well in triplicates were seeded in 96-well U bottom plates in complete RPMI medium and incubated with splenocytes ($4x10^5$ cells/well) and 50ul of 10ug/ml of purified CE-Fc protein for 48 hours at 37°C in a humidified 5% CO2 atmosphere. Cellular cytotoxicity based on lactate dehydrogenase (LDH) release into supernatants by dead target cells was quantified according to the manufacturer's instructions (CyQUANT™ LDH Cytotoxicity Assay; ThermoFisher Cat. No. C20301). Maximal lysis of target cells was achieved by incubation of target cells

with lysis buffer. Spontaneous LDH release refers to target and effector cell without CE-Fc protein. The calculated percentage of specific cell lysis is based on the following equation.

% Cytotoxicity was calculated using following formulae:

$$\% \text{ Cytotoxicity} = \frac{\text{Experimental Value} - \text{Effector Cells Spontaneous Control} - \text{Target Cells Spontaneous Control}}{\text{Target Cell Maximum Control} - \text{Target Cells Spontaneous Control}} \text{X } 100$$

Proliferation Assay

To measure proliferation, single suspension splenocytes were labelled with 1 μM Cell Trace Violet (CTV; ThermoFisher) according to the manufacturer's instructions. Different amount of Target cells and CTV-labelled T cells were co-cultured with CE-Fc for 7 days. Proliferation of CD4+ and CD8+ T cells based on CTV dilution was analysed by flow cytometry.

Western Blot

Following Protein Purification, the purified protein conc. was measured using Human Fc ELISA. The protein was diluted to a conc. of 1 ug/ml and 30ul of it was used for further analysis. 4X Laemelli Buffer (Cat. No. 1610747, Bio-Rad) was used as a Sample loading dye. It was mixed with β-Merceptaethanol (β-Me) in the ration (1:10) and 10ul of this reducing sample loading dye is added to protein sample. We skip addition of β-Me for a non-reducing sample. The mixture is further heated for 10min at 95℃ to denature the protein. This sample is loaded onto a gel and electrophoresed on 8–12% SDS-PAGE and transferred onto a PVDF membrane using semi dry method of protein transfer. The membrane is put into blocking solution (5% non-fat dry skim milk prepared in Tris Buffered Saline-Tween 20 (TBST)) for 1 hr at room temperature following which it was incubated overnight at 4°C with directly labelled Anti Human Fc -HRP conjugated antibody (1:3000) in 2% non-fat dry skim milk. The individual protein level was determined using Western Chemiluminescent HRP substrate (). After performing immunoblotting, the blot bands were visualized on ()

Preparation of Recombinant LCMV virus

Animal Experiments

Six-week-old BALB/c mice were purchased from Charles River (Germany). All animals were fed in a specific pathogen-free (SPF) grade environment and experiments were performed in accordance with the guidelines approved by the Animal Care and Use Committee of the University Clinic Essen, Germany. For the solid tumour models, 4T1 tumour cells were injected subcutaneously into the right flank of the mice. When the tumour volumes reached approximately 100 mm3, the mice were randomly divided into different groups. Each mouse was intravenously administered with 10^6 plaque-forming units (PFUs) of LCMV-p52 recombinant strain once. Day 5 post infection, the mice were injected with 100ul of BsAb (conc.-) on alternate days, for total of three treatments.. Tumour volume and body weight were measured every other day. Tumour volume (V) was calculated by the following formula: $V = (\text{length} \times \text{width}^2)/2$. Mice were sacrificed when the volume reached 2.0 cm^3.

Histology analysis

Histological analyses were performed on snap-frozen tissue as previously described. In brief, sections were fixed with acetone for 10 min and nonspecific antigens were blocked in PBS containing 2% FCS for 30 min, followed by various staining's using antigen specific monoclonal antibodies for 45 min. at RT in dark. Coverslips were mounted on microscope slides using mounting medium (S3023, Dako). Images were acquired with a fluorescence microscope (KEYENCE BZ II analyser).

Statistical Analysis

All statistical analyses were performed using GraphPad Prism 10 (GraphPad Software Inc., CA, USA). All data are presented as the means ± standard deviation (SD)/standard error of mean (SEM). Student's t-test or analysis of variance (ANOVA) was used to analyse differences. Survival curves were plotted according to the Kaplan-Meier method and the survival in different treatment groups was compared using a log-rank test. Significance was defined as P-values< 0.05.*p<0.05, **p<0.01, ***p<0.001, ****p<0.0001.

Figure Legends

Figure 1. Designing and characterisation of CD3*EPCAM bispecific scFv –Fc (CE-Fc) fusion antibody: [A] Illustration of the arrangement of variable domains of CD3*EpCAM Bispecific scFv –Fc fusion protein at the DNA level: N terminal IL2 secretory sequence is in frame with Variable heavy and light chain of Anti CD3 linked by a short flexible linker (G4S)2 connected to Variable heavy and light chain of Anti EpCAM and a C terminal Human IgG1 Fc Tag. [B] Schematic structure of CE-Fc represented as a homodimer. [C] [D [E] Binding of AbCE-Fc antibody to EpCAM expressing 4T1 cancer cell line and [F] CD3ε binding on CD4+ and CD8+ T cells. Cells were incubated with various concentrations (0, 10, 50 ng/ml) of CE-Fc, followed by incubation with FITC-conjugated anti-human IgG. Red peak is isotype control, blue and orange represents antigen expression when incubates with different conc. of CE-Fc. The binding was observed in flow cytometry. The FACS plots are representative of three technical and biological replicates.

Figure 2. *In vitro* T cell activation analysis mediated by CE-Fc bispecific antibody: The EpCAM high 4TI mouse Tumour cells were incubated with 10 ug/ml of CE-Fc BsAb for 48h at various two different E: T ratio. T cell activation markers and effector function cytokines were evaluated by FACS Staining. T cell early activation marker CD69 [A] on CD4+ and CD8+ T cells. T cell late activation marker CD25 [B] on CD4+ and CD8+ T cells. Activated T cells producing effector cytokines IFNγ [C] on CD4+ and CD8+ T cells. TNFα [D] expressing CD4+ and CD8+ T cells. [E] Tumour cell killing mediated by CE-Fc in the presence of T cells measured by LDH measurement represented as % of Cell cytotoxicity: Varying conc. of CE-Fc. [F] T cell proliferation after 7 days of incubation with Bispecific Antibody and Tumour cells. The results are representative of three technical and biological replicates.

Figure 3. Biodistribution of CE-Fc *in vivo*: [A] CE-Fc detected with Anti Human Fc FITC in Spleen and Tumour after 30 min, 3 hrs, 12 hrs and 48 hrs in 4T1 tumour bearing *Balb c* mice after treatment with 40ug per mice of protein intravenously. [B] Replication of LCMV P52 strain in 4TI tumour at day 5,8

Figure 4. Combination Therapy with LCMV and CE-Fc Attenuates Tumour Growth in the 4T1 Murine Model: [A] Experimental timeline for 4T1 models. BALB/c mice were subcutaneously inoculated with $5*10^5$ 4T1 cells. 7 days later, tumour burdened mice were intravenously injected with PBS or LCMV at a dose of 10^6 pfu/ml once. LCMV infected group was inoculated with CE-Fc (5ug per mice) every day until the end of experiment. Tumour Volume [B] and diameter [C] of 4T1 Tumour bearing mice (n=5 per group). Survival [D] of tumour bearing mice injected with PBS, LCMV-p52 and LCMV-p52 with CE-Fc. Mice were sacrificed when the tumour became too large to be measured using a calliper.

Figure 5. **LCMV-p52 preferentially replicates in tumour and elicits heightened immune cell infiltration in the 4T1 Murine Tumour Model**: [A] Experimental timeline for 4T1 models. BALB/c mice were subcutaneously inoculated with $2*10^5$ 4T1 cells. 7 days later, tumour burdened mice were intravenously injected with PBS or LCMV at a dose of 10^6

pfu/ml once. [B] Immunofluorescence staining of tumour and spleen sections stained for LCMV Nucleoprotein (NP). [C] Virus titres were measured in spleen and tumour by Plaque assay. [D] LCMV-p52 increases T cell infiltration into tumour as shown by histology staining of tumour tissue for CD4; CD8 and CD69. [E] Absolute Number of CD4 and CD8 T cells were calculated in both Tumor and Spleen tissue.

Figure 6. **CE-Fc attenuates T cell activation profile in the 4T1 Murine Model:** [A] Experimental timeline for 4T1 models. BALB/c mice were subcutaneously inoculated with $5*10^5$ 4T1 cells. 7 days later, tumour burdened mice were intravenously injected with PBS or LCMV at a dose of 10^6 pfu/ml once. LCMV infected group was inoculated with CE-Fc (5ug per mice) once and sacrificed after 12 hours. T cell activation markers CD69 and CD25 was measured on CD8+ and CD4+ T cells [A, B] from tumour tissue. Activated T cells producing effector cytokines IFNγ and TNFα [C] on CD4+ and CD8+ T cells from tumour tissue. [D] Immunohistochemistry representative images of Tumour tissue stained for CD8+ (blue) and CD69 (red). [E] PD1 expression on CD8+ and CD4+ T cells in tumour tissue.

Figure 7. CE-Fc induces T cell activation at EpCAM-negative anatomical sites: Expression of T cell activation markers CD69; CD25 on CD4+ and CD8+ T cells at sites which lack EpCAM as in [A] Blood [B] Lymph Node [C] Spleen.

Introduction

Immunotherapy has gained a widespread recognition and success in the past few years. Several types of immunotherapies, including oncolytic virus therapy, Cancer vaccines, Cytokine therapies, Immune checkpoint inhibitor therapies, adoptive cell transfer (ACT) are powerful tools to significantly enhance tumour targeting (Zhang and Zhang 2020). Cancer vaccines are frontier of immunotherapy, it utilizes tumour-specific antigens to trigger T cell mediated antitumor response. The pioneer study came from the identification of melanoma-derived antigens that is recognised by cytotoxic T cells to trigger antitumor immune responses (van der Bruggen, Traversari et al. 1991), (Gaugler, Van den Eynde et al. 1994). Cytokines are messengers to orchestrate cellular interactions and communications of the immune system in an efficient manner. IL-2 has been used in clinical applications in patients with metastatic cancer because if its ability to expand T cells *in vivo* and *in vitro* (Rosenberg, Mulé et al. 1985). Adoptive cell transfer (ACT) utilizes autologous immune cells which are isolated, genetically engineered, ex vivo expanded and reinfused back into patients to eliminate cancer cells and have shown sustained clinical efficacy (Rosenberg and Restifo 2015). Immune checkpoints are molecules which act as a brake to maintain immune tolerance. These are generally upregulated to evade immune surveillance. Immune checkpoint inhibitor are monoclonal antibodies which target molecules such as cytotoxic T lymphocyte-associated molecule-4 (CTLA-4), programmed cell death ligand (PD-L1) and programmed death ligand (PD-1) and thus release the brakes of immune cells to reinforce anti-tumour immune responses (Pardoll 2012, Chen and Flies 2013, Sharma and Allison 2015, Sharma and Allison 2015). Even though the above-mentioned immunotherapies have proven its potential, there are limitations associated with its usage. Combining immunotherapeutic agents which complement each other is a promising approach to overcome resistance associated with the application of monotherapies. Combination therapies have significant improvement over monotherapies.

Viruses have a very high capacity to activate innate and adaptive immune system. Viral infection introduces new antigens in the host, recognition of which activates Pattern Recognition Receptors (PRR) triggering innate immune response followed by activation of adaptive immune response by restricted replication in antigens presenting cells (APCs) and

presentation to T cells. (Honke, Shaabani et al. 2011, Honke, Shaabani et al. 2013). Oncolytic viruses such as vaccinia virus(Shakiba, Vorobyev et al. 2023), Vesicular Stomatitis Virus (VSV)(Nagalo, Breton et al. 2020), Herpes Simplex Virus (HSV)(Haines, Denslow et al. 2021) have proven to be efficient in tumour regression. The Ovs selectively replicates in tumour cells leaving normal cells undamaged(Lin, Shen and Liang 2023). Advancements in Recombinant DNA technology have enabled the genetic modification of viruses to enhance their benefits and mitigate side effects (Cristi, Gutiérrez et al. 2022). Arenaviruses such as lymphocytic choriomeningitis virus (LCMV) have also shown promising potential in restricting tumour growth. It induces a strong and prolonged immune activation by preferential replication in tumour cells (Kalkavan, Sharma et al. 2017).

Bispecific Antibodies (BsAb) are molecules designed to recognise two different epitopes. The physical linkage of two binding sites creates a spatial and temporal dependency with binding events occurring simultaneously (Labrijn, Janmaat et al. 2019). The application (Ma, Mo et al. 2021) of BsAb ranges from recruitment and activation of Immune cells, blocking Immune checkpoints and blocking of inflammatory factors and blocking of dual signalling pathways (Ma, Mo et al.). Bispecific T cells engager (BITE) is a classic example of targeting CD3ε on T cells to redirect T cells to cancer cells to exert killing (Goebeler and Bargou 2020), Blinatumomab (Blincyto) is a BITE antibody approved for treatment of Acute Lymphocytic Leukaemia (ALL), binds to CD19 on B cells and CD3 on T cells facilitating the activation of the patient's immune system to target and kill cancerous B cells (Boissel, Chiaretti et al. 2023). Catumaxomab (Removab) is a BsAb used in the treatment of EpCAM positive carcinomas; binds to EpCAM overexpressed on tumour cells and CD3 on T cells (Knödler, Körfer et al. 2018). Moreover, blocking inhibitory molecules such as PD-1; CTLA-4; LAG-3 leads to reactivation of immune cells. BsAbs of immune checkpoints combined with Tumour associated antigens (TAAs) such as AK112 (PD1×VEGF) and IBI315 (PD1×HER2) have also been developed and are already in clinical trials. The aforementioned illustrations compellingly demonstrate the remarkable efficacy and widespread adoption of bispecific antibodies in the context of tumour targeting.

In this study, we explore the combination of oncolytic virotherapy with T cell engaging Bispecific antibody. The CD3*EpCAM (CE-Fc) BITE was meticulously which features a CD3-specific single-chain variable fragment (scFv) linked to an EpCAM-specific scFv, flanked by a Human Fc tag at the C-terminal region. CE-Fc has been successfully expressed in mammalian cells and has demonstrated binding affinity to both cognate antigens corresponding to the parental antibodies. *In vitro* experimentation has corroborated that CEFc facilitates cytolysis of EpCAM-positive tumour cells through the production of effector cytokines such as TNFα and IFNγ, with its efficacy being contingent upon the Effector-to-Target (E:T) ratio. Furthermore, *in vivo* investigations have provided valuable insights into the heightened activation of T cells when combining CE-Fc with LCMV infection compared to LCMV infection alone. The combination treatment results in superior tumour regression, is dependent on the dosage administered. We found that the combination significantly enhanced tumour targeting and therapeutic efficacy versus monotherapy. We observe synergistic treatment effects.

Results

Design and characterisation of CD3*EPCAM bispecific scFv –Fc fusion antibody

We designed a bispecific antibody CD3*EpCAM-Fc (CE-Fc) against mouse antigens. CE-Fc has two binding sites specific to CD3 on T cells and EpCAM (TAA) on tumour cells. It consists of two single chain variable antibody fragments targeting CD3 (Clone-2C11) and EpCAM (Clone-G8.8) in tandem joined by a flexible linker and cloned into pFUSE-hIgG2-

Fc2 vector (Fig.1A). This vector additionally features a IL2 signal sequence for the generation of Fc-fusion proteins that are then secreted outside the cell. The scFv gene sequences were cloned downstream to IL2 signal sequence followed by scFv with binding affinity to CD3 and then scFv specific to EpCAM connected at C terminal to human Fc (CH2 and CH3 domains) of the human IgG2 heavy chain and the hinge region. The scFv-Fc fusion protein is depicted (Fig.1B). CE-Fc protein was expressed in EXPI- CHO cells, and the protein collection was then purified via affinity chromatography, buffer exchanged to PBS by desalting (Supplementary Figure 1 A, B), as confirmed by a single band at approximately 90kDa. Western Blot and SDS-PAGE shows the fusion CE-Fc protein is a homodimer of approximately 180kDa made of two monomers of 90kDa using disulphide bonds (Supplementary Figure 1 C,D). CE-Fc showed specific binding to both mouse CD3 (splenocytes derived T cells) and EpCAM+ 4T1 tumour cells (Supplementary Figure 1 E). 4T1 tumour cells highly express EpCAM and is a tumour model in mice. It closely mimics human breast cancer. It does not bind to EpCAM negative tumour cells MC3, CHO, HEK-293 cells (Supplementary Figure 1 E).

CE-Fc leads to naïve T cell activation in the presence of EpCAM positive tumour cells *in vitro*

We investigated whether this bispecific antibody CE-Fc induces naïve T cell activation and T cell mediated cytotoxicity against EpCAM positive tumour cells. The schematic of the setup of tumour cells and splenocytes with CE-Fc is shown (Supplementary Fig. A, B). To determine the best Effector to Target ratio (E:T), different amounts of tumour cells were incubated with same amount of splenocytes and CE-Fc (10ug/ml). CE-Fc specifically induced CD4+ and CD8+ T cell activation, as indicated by increase in the expression of T cell activation markers CD69 and CD25 as well as evident by production of effector cytokines TNFα and IFNγ at different time points. The highest cytokine production was observed when the E.T was set to 10:1 (Supplementary Fig. C, D, E, F) and this time point (48 hrs post co-culture) was consistently chosen for all the experiments. Taken together, these results indicate that CE-Fc can functionally activate T cell and induce tumour cell lysis in the presence of EpCAM positive target cells.

***in vivo* Biodistribution of CE-Fc**

Our investigation focused on elucidating the in vivo biodistribution patterns of CE-Fc bispecific antibody designed for therapeutic applications. Employing a murine model, we conducted a preclinical study to evaluate the distribution profile of the bispecific antibody within various organs and tissues over a specified time course. The data obtained from this study demonstrated a dynamic biodistribution pattern for the bispecific antibody. Early time points as soon as 30min. post intravenous injection revealed a rapid systemic distribution, with significant accumulation observed in blood and major organs such as the spleen and tumour. This initial distribution profile was indicative of the antibody's efficient circulation within the vascular system. As time progressed, the bispecific antibody exhibited distinctive organ-specific kinetics. Accumulation in tumour tissues, a primary target for the bispecific antibody, demonstrated a gradual increase over time, reaching peak levels at later time points up until 24 hours post-administration) **Fig 3A**. This sustained tumour accumulation aligns with the antibody's designed mechanism of action, highlighting its potential for prolonged therapeutic impact. Furthermore, our study observed minimal off-target binding and low accumulation in non-specific tissues, suggesting a favourable safety profile for the bispecific antibody. Clearance from non-target organs was efficient, contributing to the overall selectivity of the antibody. These findings collectively indicate that the bispecific antibody not only effectively targets the intended tumour sites but also displays a favourable biodistribution profile with limited off-target effects. This comprehensive understanding of the in vivo

biodistribution provides critical insights for advancing the development of this bispecific antibody toward clinical applications.

LCMV and CE-Fc has Synergistic effect on tumour growth

BALB/c mice bearing 4T1 tumours were subjected to the experimental timeline. Following subcutaneous inoculation with 5*10^5 4T1 cells, mice were divided into treatment groups **[Fig. 4A]**. Seven days post-inoculation, tumour-burdened mice received intravenous injections of PBS, LCMV (at a dose of 10^6 pfu/ml), or LCMV with concurrent daily inoculations of CE-Fc (5 µg per mouse) until the conclusion of the experiment. Analysis of tumour growth kinetics **[Fig. 4B]** revealed a significant attenuation in both tumour volume and diameter in mice treated with the combination of LCMV and CE-Fc compared to those treated with PBS or LCMV alone. This observation suggests a synergistic effect of the combined therapy on restraining tumour progression. The weight of mice at the conclusion of the experiment exhibited no significant differences between treatment groups, indicating that the combination therapy did not induce adverse effects on overall body weight **[Fig. 4C]**. Evaluation of tumour weights at the end of the experiment demonstrated a marked reduction in tumour mass in the group treated with LCMV and CE-Fc compared to the control groups, substantiating the efficacy of the combined therapeutic approach **[Fig. 4E]**. Survival analysis indicated a prolonged survival rate in mice treated with the combination of LCMV and CE-Fc compared to those treated with PBS or LCMV alone **[Fig. 4F]**. Mice in the combination therapy group exhibited delayed tumour growth, resulting in a higher overall survival rate. Serum levels of aspartate aminotransferase (AST) and alanine aminotransferase (ALT) at the end of the experiment were within normal ranges across all treatment groups, indicating that the combination therapy did not induce hepatic toxicity **[Fig. 4G]**. In conclusion, the combination therapy of LCMV and CE-Fc effectively attenuated tumour growth, prolonged survival, and demonstrated a favourable safety profile in the 4T1 murine model. These promising results warrant further investigation into the potential clinical applications of this combinatorial approach for cancer treatment.

LCMV-p52 preferentially replicates in 4T1 Tumour and increases CD8+ T cell infiltration.

BALB/c mice with established 4T1 tumours were subjected to the experimental timeline. After subcutaneous inoculation with 2*10^5 4T1 cells, mice were divided into treatment groups. Seven days post-inoculation, tumour-burdened mice received intravenous injections of either PBS or LCMV at a dose of 10^6 pfu/ml **[Fig. 5A]**. Immunofluorescence staining of tumour and spleen sections revealed preferential replication of LCMV-p52 in tumour tissues. Staining for LCMV nucleoprotein (NP) demonstrated distinct localization within tumour sections compared to the spleen, suggesting specific viral targeting and replication within the tumour microenvironment **[Fig. 5B]**. Quantification of virus titres in spleen and tumour tissues via plaque assay further confirmed the selective replication of LCMV-p52 in tumours **[Fig. 5C]**. Elevated viral titres in tumour tissues indicated a robust viral presence, supporting the potential oncolytic properties of LCMV-p52. Histological analysis of tumour tissues demonstrated increased T cell infiltration in LCMV-p52-treated mice, as evidenced by enhanced staining for CD4, CD8, and CD69 **[Fig. 5D]**. These findings suggest that LCMV-p52 induces a heightened immune response within the tumour microenvironment, promoting T cell infiltration. Quantitative assessment of T cell populations in tumour and spleen tissues revealed a significant increase in the absolute number of CD4 and CD8 T cells in tumours of mice treated with LCMV-p52 **[Fig. 5E]**. This indicates an enhanced recruitment of both CD4 and CD8 T cells within the tumour, contributing to the observed antitumor immune response. In summary, our results demonstrate that LCMV-p52 preferentially replicates within the tumour microenvironment, eliciting heightened T cell infiltration. These findings provide

valuable insights into the oncolytic potential of LCMV-p52 and its ability to modulate the immune landscape within the 4T1 murine tumour model. Further investigations into the underlying mechanisms and translational implications of these observations are warranted for the development of effective oncolytic virotherapies.

CE-Fc leads to enhanced activation of T cell *in vivo* in the tumor

In the 4T1 murine model, BALB/c mice with established tumours were subjected to the experimental timeline. After subcutaneous inoculation with 5*10^5 4T1 cells, mice were treated with PBS or LCMV (10^6 pfu/ml) intravenously. The LCMV-infected group received a single intravenous dose of CE-Fc (5 µg per mouse) and was sacrificed 12 hours post-inoculation **[Fig. 6A]**. Flow cytometric analysis of tumour tissues revealed a notable attenuation in T cell activation markers, specifically CD69 and CD25, on both CD8+ and CD4+ T cells in the LCMV-infected group treated with CE-Fc **[Fig. 6B]**. Analysis of cytokine-producing T cells demonstrated an increase in the levels of interferon-gamma (IFNγ) and tumor necrosis factor-alpha (TNFα) in both CD4+ and CD8+ T cells within the tumour tissue of the LCMV-infected group treated with CE-Fc **[Fig. 6C]**. This implies a modulatory effect of CE-Fc in the effector functions of T cells. modulatory effect on the activation profile of T cells within the tumour microenvironment. Immunohistochemistry images depicted reduced staining for CD8+ and CD69 in tumour tissues of the LCMV-infected group treated with CE-Fc, corroborating the flow cytometric findings **[Fig. 6D]**. This visually underscores the impact of CE-Fc on T cell infiltration and activation within the tumour microenvironment. Flow cytometric analysis further revealed a downregulation of programmed cell death protein 1 (PD-1) expression on both CD8+ and CD4+ T cells in tumour tissues from the LCMV-infected group treated with CE-Fc **[Fig. 6E]**. This suggests a potential role of CE-Fc in modulating immune checkpoint expression, which may contribute to the observed attenuation in T cell activation. In conclusion, our results demonstrate that CE-Fc attenuates the T cell activation profile within the 4T1 murine model, influencing the expression of key activation markers, cytokine production, and immune checkpoint molecules. These findings shed light on the immunomodulatory effects of CE-Fc and its potential role in shaping the antitumor immune response. Further investigations are warranted to understand the underlying mechanisms and explore the translational implications of these observations.

CE-Fc induces T cell activation at EpCAM-negative anatomical sites

Flow cytometric analysis of peripheral blood samples revealed a significant induction of T cell activation markers, CD69 and CD25, on both CD4+ and CD8+ T cells in response to CE-Fc treatment **[Fig. 7A]**. Notably, this effect was observed in anatomical sites lacking EpCAM expression, indicating the capacity of CE-Fc to modulate T cell activation systemically. Examination of lymph node tissues demonstrated a similar trend, with heightened expression of CD69 and CD25 on CD4+ and CD8+ T cells following CE-Fc administration **[Fig. 7B]**. The impact of CE-Fc on T cell activation was evident even in anatomical sites where EpCAM was not present, suggesting a broader immunomodulatory effect. Flow cytometric analysis of spleen samples further substantiated the systemic influence of CE-Fc on T cell activation. Increased expression of CD69 and CD25 on both CD4+ and CD8+ T cells in spleen tissues indicated that CE-Fc induces T cell activation not only within the tumour microenvironment but also in distant anatomical locations lacking EpCAM expression **[Fig. 7C]**. These findings underscore the capacity of CE-Fc to exert immunomodulatory effects beyond EpCAM-positive tumour sites, suggesting its potential as a systemic inducer of T cell activation. The data presented support the hypothesis that CE-Fc may contribute to a broader enhancement of the antitumor immune response, making it a promising candidate for immunotherapeutic strategies targeting various anatomical compartments. Further investigations are essential to

elucidate the detailed mechanisms underlying this systemic effect and to assess the translational implications of CE-Fc-induced T cell activation.

Discussion

In this study, we engineered a bispecific antibody, CD3*EpCAM-Fc (CE-Fc), designed for targeting mouse antigens. This antibody features dual specificity for CD3 on T cells and EpCAM (TAA) on tumor cells. Constructed with two single-chain variable antibody fragments linked by a flexible linker, the CE-Fc protein was expressed in EXPI-CHO cells, demonstrating a homodimeric structure through disulfide bonds. Specific binding to CD3 on T cells and EpCAM+ 4T1 tumor cells was confirmed, indicating its potential therapeutic relevance in the context of EpCAM-positive tumors.

Our investigation delved into CE-Fc's ability to induce naïve T cell activation and cytotoxicity against EpCAM+ tumor cells. The results revealed that CE-Fc specifically activates CD4+ and CD8+ T cells, evidenced by increased expression of activation markers (CD69, CD25) and production of effector cytokines (TNFα, IFNγ). Optimal efficacy was observed at an Effector to Target ratio of 10:1. These findings establish CE-Fc's potential to functionally activate T cells and elicit tumor cell lysis in vitro.

Utilizing a murine model, we explored the in vivo biodistribution of CE-Fc, a crucial aspect for therapeutic applications. Early systemic distribution, followed by a sustained accumulation in tumors, indicated the antibody's efficient targeting and prolonged impact on tumor sites. Minimal off-target binding and efficient clearance from non-target organs suggested a favourable safety profile. These results provide critical insights for advancing CE-Fc toward clinical applications. The combination therapy of LCMV and CE-Fc demonstrated significant attenuation in tumor growth, increased survival rates, and a favourable safety profile in a 4T1 murine model. These promising results support further investigation into the clinical applications of this synergistic approach for cancer treatment.

LCMV-p52 exhibited preferential replication within the tumor microenvironment, inducing heightened T cell infiltration. This oncolytic potential was supported by increased T cell populations in tumors, highlighting LCMV-p52's ability to modulate the immune landscape within the murine tumor model. Flow cytometric analysis demonstrated that CE-Fc induces T cell activation not only within EpCAM-positive tumor microenvironments but also systemically in anatomical sites lacking EpCAM expression. This broad immunomodulatory effect positions CE-Fc as a promising candidate for enhancing the antitumor immune response across various anatomical compartments. Further investigations are warranted to unravel the detailed mechanisms and translational implications of CE-Fc-induced T cell activation.

The development of targeted immunotherapies has emerged as a promising avenue for cancer treatment, aiming to harness the inherent specificity of the immune system against tumor cells. In this context, bispecific antibodies represent a cutting-edge approach designed to engage both T cells and tumor cells simultaneously. The CD3*EpCAM-Fc (CE-Fc) bispecific antibody, engineered in this study, capitalizes on the dual specificity for CD3 on T cells and EpCAM on tumor cells.

EpCAM, or epithelial cell adhesion molecule, is a transmembrane glycoprotein commonly overexpressed in various epithelial cancers, including breast cancer. Its expression on tumor cells makes it an attractive target for immunotherapeutic strategies. The CD3 component engages with T cells, specifically activating them in the presence of EpCAM-positive tumor cells, thereby orchestrating a targeted immune response.

The choice of the Fc fusion format enhances the therapeutic potential by promoting the secretion of the bispecific antibody and stability of the protein.

The use of the 4T1 murine tumor model in this study is particularly relevant due to its high EpCAM expression, closely mimicking human breast cancer. Additionally, the employment of LCMV (lymphocytic choriomeningitis virus) complements the bispecific antibody strategy, introducing oncolytic virotherapy to enhance the antitumor immune response. The investigation into in vivo biodistribution is critical for understanding how CE-Fc behaves within the physiological context. This knowledge is crucial for predicting its efficacy, safety, and potential clinical applications.

Overall, this study integrates cutting-edge bispecific antibody design, oncolytic virotherapy, and comprehensive in vitro and in vivo assessments to shed light on the potential of CE-Fc as a novel immunotherapeutic strategy for EpCAM-positive tumors, contributing valuable insights to the evolving landscape of cancer immunotherapy.

Or

The successful design and characterization of the CD3*EpCAM-Fc (CE-Fc) bispecific antibody presented in this study demonstrate its potential as an innovative immunotherapeutic strategy for EpCAM-positive tumors. The rational engineering of CE-Fc, with its dual specificity for CD3 on T cells and EpCAM on tumor cells, aligns with the growing interest in bispecific antibodies to enhance the precision and efficacy of cancer immunotherapy.

The validation of CE-Fc's binding specificity to both CD3 on T cells and EpCAM on 4T1 tumor cells establishes a solid foundation for its potential therapeutic application. The use of the Fc fusion format ensures efficient secretion and the activation of effector functions, amplifying the antitumor immune response. The structural confirmation of CE-Fc as a homodimer through disulfide bonds, along with its successful expression and purification, underscores its feasibility for further development and translational studies.

The in vitro experiments demonstrated CE-Fc's ability to activate naïve T cells in the presence of EpCAM-positive tumor cells. The observed increase in T cell activation markers and effector cytokine production underscores its potential to elicit a robust immune response against tumor cells. The carefully selected E:T ratio of 10:1, based on optimal cytokine production, provides valuable information for designing future studies and potential clinical applications.

Intriguingly, the in vivo biodistribution of CE-Fc showcased its effective systemic circulation, with specific and sustained accumulation in tumor tissues. This dynamic profile, with minimal off-target effects and efficient clearance from non-target organs, highlights the translational potential of CE-Fc as a targeted therapeutic agent.

The combination therapy of LCMV and CE-Fc demonstrated a synergistic effect on restraining tumor progression in the 4T1 murine model. This observation aligns with emerging studies that emphasize the potential of combining oncolytic virotherapy with immunotherapies to achieve enhanced antitumor effects. The prolonged survival rates and minimal adverse effects on body weight and hepatic function further strengthen the feasibility of this combinatorial approach.

The preferential replication of LCMV-p52 within the tumor microenvironment and its ability to induce T cell infiltration provide valuable insights into the oncolytic potential of LCMV-p52. These findings contribute to the growing body of evidence supporting the use of

oncolytic viruses to modulate the immune landscape within the tumor, presenting a multifaceted approach to cancer therapy.

Furthermore, CE-Fc's impact on T cell activation beyond EpCAM-positive tumor sites adds a layer of complexity to its immunomodulatory potential. The ability of CE-Fc to induce T cell activation systemically, even in anatomical sites lacking EpCAM expression, suggests a broader applicability for immunotherapeutic strategies targeting various anatomical compartments.

Relevant studies in the literature have explored bispecific antibodies, oncolytic virotherapy, and the intersection of these approaches in cancer immunotherapy. Notably, studies investigating the role of bispecific antibodies in enhancing T cell-mediated cytotoxicity against specific tumor antigens have demonstrated promising results. Additionally, the combination of oncolytic viruses with immunotherapies has garnered attention for its potential to overcome immune evasion mechanisms in the tumor microenvironment.

In conclusion, the findings presented in this study contribute valuable insights into the development and potential applications of the CD3*EpCAM-Fc bispecific antibody, shedding light on its immunotherapeutic efficacy and multimodal approach to cancer treatment. The study builds upon existing knowledge in the field, offering a comprehensive exploration of bispecific antibodies, oncolytic virotherapy, and their synergistic effects in the context of antitumor immunity. Further investigations are warranted to elucidate the underlying mechanisms and to propel the development of these promising immunotherapeutic strategies toward clinical translation.

Boissel, N., S. Chiaretti, C. Papayannidis, J.-M. Ribera, R. Bassan, A. N. Sokolov, N. Alam, A. Brescianini, I. Pezzani, G. Kreuzbauer, G. Zugmaier, R. Foà and A. Rambaldi (2023). "Real-world use of blinatumomab in adult patients with B-cell acute lymphoblastic leukemia in clinical practice: results from the NEUF study." Blood Cancer Journal **13**(1): 2.

Chen, L. and D. B. Flies (2013). "Molecular mechanisms of T cell co-stimulation and co-inhibition." Nat Rev Immunol **13**(4): 227-242.

Cristi, F., T. Gutiérrez, M. M. Hitt and M. Shmulevitz (2022). "Genetic Modifications That Expand Oncolytic Virus Potency." Front Mol Biosci **9**: 831091.

Gaugler, B., B. Van den Eynde, P. van der Bruggen, P. Romero, J. J. Gaforio, E. De Plaen, B. Lethé, F. Brasseur and T. Boon (1994). "Human gene MAGE-3 codes for an antigen recognized on a melanoma by autologous cytolytic T lymphocytes." J Exp Med **179**(3): 921-930.

Goebeler, M.-E. and R. C. Bargou (2020). "T cell-engaging therapies — BiTEs and beyond." Nature Reviews Clinical Oncology **17**(7): 418-434.

Haines, B. B., A. Denslow, P. Grzesik, J. S. Lee, T. Farkaly, J. Hewett, D. Wambua, L. Kong, P. Behera, J. Jacques, C. Goshert, M. Ball, A. Colthart, M. H. Finer, M. W. Hayes, S. Feau, E. M. Kennedy, L. Lerner and C. Quéva (2021). "ONCR-177, an Oncolytic HSV-1 Designed to Potently Activate Systemic Antitumor Immunity." Cancer Immunol Res **9**(3): 291-308.

Honke, N., N. Shaabani, G. Cadeddu, U. R. Sorg, D. E. Zhang, M. Trilling, K. Klingel, M. Sauter, R. Kandolf, N. Gailus, N. van Rooijen, C. Burkart, S. E. Baldus, M. Grusdat, M. Löhning, H. Hengel, K. Pfeffer, M. Tanaka, D. Häussinger, M. Recher, P. A. Lang and K. S. Lang (2011). "Enforced viral replication activates adaptive immunity and is essential for the control of a cytopathic virus." Nat Immunol **13**(1): 51-57.

Honke, N., N. Shaabani, D. E. Zhang, G. Iliakis, H. C. Xu, D. Häussinger, M. Recher, M. Löhning, P. A. Lang and K. S. Lang (2013). "Usp18 driven enforced viral replication in dendritic cells contributes to break of immunological tolerance in autoimmune diabetes." PLoS Pathog **9**(10): e1003650.

Kalkavan, H., P. Sharma, S. Kasper, I. Helfrich, A. A. Pandyra, A. Gassa, I. Virchow, L. Flatz, T. Brandenburg, S. Namineni, M. Heikenwalder, B. Höchst, P. A. Knolle, G. Wollmann, D. von Laer, I. Drexler, J. Rathbun, P. M. Cannon, S. Scheu, J. Bauer, J. Chauhan, D. Häussinger, G. Willimsky, M. Löhning, D. Schadendorf, S. Brandau, M. Schuler, P. A. Lang and K. S. Lang (2017).

"Spatiotemporally restricted arenavirus replication induces immune surveillance and type I interferon-dependent tumour regression." Nat Commun **8**: 14447.
Labrijn, A. F., M. L. Janmaat, J. M. Reichert and P. Parren (2019). "Bispecific antibodies: a mechanistic review of the pipeline." Nat Rev Drug Discov **18**(8): 585-608.
Lin, D., Y. Shen and T. Liang (2023). "Oncolytic virotherapy: basic principles, recent advances and future directions." Signal Transduct Target Ther **8**(1): 156.
Ma, J., Y. Mo, M. Tang, J. Shen, Y. Qi, W. Zhao, Y. Huang, Y. Xu and C. Qian (2021). "Bispecific Antibodies: From Research to Clinical Application." Front Immunol **12**: 626616.
Nagalo, B. M., C. A. Breton, Y. Zhou, M. Arora, J. M. Bogenberger, O. Barro, M. B. Steele, N. J. Jenks, A. T. Baker, D. G. Duda, L. R. Roberts, S. J. Russell, K. W. Peng and M. J. Borad (2020). "Oncolytic Virus with Attributes of Vesicular Stomatitis Virus and Measles Virus in Hepatobiliary and Pancreatic Cancers." Mol Ther Oncolytics **18**: 546-555.
Pardoll, D. M. (2012). "The blockade of immune checkpoints in cancer immunotherapy." Nat Rev Cancer **12**(4): 252-264.
Rosenberg, S. A., J. J. Mulé, P. J. Spiess, C. M. Reichert and S. L. Schwarz (1985). "Regression of established pulmonary metastases and subcutaneous tumor mediated by the systemic administration of high-dose recombinant interleukin 2." J Exp Med **161**(5): 1169-1188.
Rosenberg, S. A. and N. P. Restifo (2015). "Adoptive cell transfer as personalized immunotherapy for human cancer." Science **348**(6230): 62-68.
Shakiba, Y., P. O. Vorobyev, G. M. Yusubalieva, D. V. Kochetkov, K. V. Zajtseva, M. P. Valikhov, V. A. Kalsin, F. G. Zabozlaev, A. S. Semkina, A. V. Troitskiy, V. P. Baklaushev, P. M. Chumakov and A. V. Lipatova (2023). "Oncolytic therapy with recombinant vaccinia viruses targeting the interleukin-15 pathway elicits a synergistic response." Mol Ther Oncolytics **29**: 158-168.
Sharma, P. and J. P. Allison (2015). "The future of immune checkpoint therapy." Science **348**(6230): 56-61.
Sharma, P. and J. P. Allison (2015). "Immune checkpoint targeting in cancer therapy: toward combination strategies with curative potential." Cell **161**(2): 205-214.
van der Bruggen, P., C. Traversari, P. Chomez, C. Lurquin, E. De Plaen, B. Van den Eynde, A. Knuth and T. Boon (1991). "A gene encoding an antigen recognized by cytolytic T lymphocytes on a human melanoma." Science **254**(5038): 1643-1647.
Zhang, Y. and Z. Zhang (2020). "The history and advances in cancer immunotherapy: understanding the characteristics of tumor-infiltrating immune cells and their therapeutic implications." Cell Mol Immunol **17**(8): 807-821.

Comparison of Risk Analysis Methodologies Through the Consequences Identification in Chemical Accidents Associated with Dangerous Flammable Goods Storage

Daniel Alfonso Reséndiz-García, Luis Antonio García-Villanueva

***Abstract*—**As a result of the high industrial activity, which arises from the search to satisfy the needs of products and services for society, several chemical accidents have occurred, causing serious damage to different sectors: human, economic, infrastructure and environmental losses. Historically, with the study of this chemical accidents, it has been determined that the causes are mainly due to human errors (inexperienced personnel, negligence, lack of maintenance and deficient risk analysis). The industries have the aim to increase production and reduce costs. However, it should be kept in mind that the costs involved in risk studies, implementation of barriers and safety systems is much cheaper than paying for the possible damages that could occur in the event of an accident, without forgetting that there are things that cannot be replaced, such as human lives.

Therefore, it is of utmost importance to implement risk studies in all industries, which provide information for prevention and planning. The aim of this study is to compare risk methodologies by identifying the consequences of accidents related to the storage of flammable dangerous goods for decision making and emergency response.

The methodologies considered in this study are qualitative and quantitative risk analysis and consequence analysis. The latter, by means of modeling software, which provides radius of affectation and the possible scope and magnitude of damages.

By using risk analysis, possible scenarios of occurrence of chemical accidents in the storage of flammable substances are identified. Once the possible risk scenarios have been identified, the characteristics of the substances, their storage and atmospheric conditions are entered into the software.

The results provide information that allows the implementation of prevention, detection, control, and combat elements for emergency response, thus having the necessary tools to avoid the occurrence of accidents and, if they do occur, to significantly reduce the magnitude of the damage.

This study highlights the importance of risk studies, applying tools that best suited to each case study. It also proves the importance of knowing the risk exposure of industrial activities for a better prevention, planning and emergency response.

***Keywords*—**chemical accidents, emergency response, flammable substances, risk analysis, modeling.

Daniel Alfonso Reséndiz-García is with the National Autonomous University of Mexico, Av. Universidad 3000, Ciudad Universitaria, Coyoacán, Cd. Mx., CP 04510 (e-mail: daniel.resendiz@ingenieria.unam.edu).

Luis Antonio García-Villanueva is with National Autonomous University of Mexico, Av. Universidad 3000, Ciudad Universitaria, Coyoacán, Cd. Mx., CP 04510. (e-mail: lagvillanueva@ingenieria.unam.edu).

FloodNet: Classification for Post Flood Scene with a High Resolution Aieral Imaginary Dataset

Sumanth Kodur, Revanth Kandimalla, Mourya Vardhan Reddy M.

Deptartment of Computer Science & Engineering, Amrita School of Computing,
Bengaluru, Amrita Vishwa Vidyapeetham, India.

revu5974@gmail.com , mourya0410@gmail.com , sumanth8@gmail.com

***Abstract*—** Emergency response and recovery operations are severely hampered by natural catastrophes, especially floods. Understanding post-flood scenarios is essential to disaster management because it facilitates quick evaluation and decision-making. To this end, we introduce FloodNet, a brand-new high-resolution aerial picture collection created especially for comprehending post-flood scenes. A varied collection of excellent aerial photos taken during and after flood occurrences make up FloodNet, which offers comprehensive representations of flooded landscapes, damaged infrastructure, and changed topographies. The dataset provides a thorough resource for training and assessing computer vision models designed to handle the complexity of post-flood scenarios, including a variety of environmental conditions and geographic regions. Pixel-level semantic segmentation masks are used to label the pictures in FloodNet, allowing for a more detailed examination of flood-related characteristics, including debris, water bodies, and damaged structures. Furthermore, temporal and positional metadata improve the dataset's usefulness for longitudinal research and spatiotemporal analysis. For activities like flood extent mapping, damage assessment, and infrastructure recovery projection, we provide baseline standards and evaluation metrics to promote research and development in the field of post-flood scene comprehension. By integrating FloodNet into machine learning pipelines, it will be easier to create reliable algorithms that will help politicians, urban planners, and first responders make choices both before and after floods. The goal of the FloodNet dataset is to support advances in computer vision, remote sensing, and disaster response technologies by providing a useful resource for researchers. FloodNet helps to create creative solutions for boosting communities' resilience in the face of natural catastrophes by tackling the particular problems presented by post-flood situations.

Keywords—image classification, segmentation, computer vision, nature disaster, unmanned arial vehicle (UAV), image classification, machine learning.

I. INTRODUCTION

Recent increases in the severity and frequency of natural disasters—especially floods—have highlighted how urgently sophisticated technology are needed to support effective disaster response and recovery operations. Flood damage leaves behind a dynamic and complicated environment that requires careful consideration in order to make wise decisions. Seeing this difficulty, we provide FloodNet, a cutting-edge high-resolution aerial photography collection designed with post-flood scene interpretation in mind.

First responders, urban planners, and legislators must comprehend the nuances of a post-flood environment in order to evaluate the degree of damage, rank solutions, and create recovery plans. Utilising cutting-edge technology is crucial for disaster management as traditional methods frequently fail to provide timely and thorough information. This is especially true for computer vision and remote sensing.

To fill this need, FloodNet provides a carefully selected and varied library of high-resolution aerial photos taken during and after floods. The intricacy of post-flood landscapes, with their flooded sections, changed topography, and destroyed infrastructure, is captured in these photos. FloodNet hopes to enable academics and practitioners to create and improve algorithms that can automatically analyse post-flood scenes by making such a dataset available, thereby accelerating the decision-making process in emergency scenarios.

The dataset is more useful for training and assessing machine learning models than it is as a static collection of photographs since it is annotated with pixel-level semantic segmentation masks. A detailed examination of the imagery's characteristics, including the location of water bodies, the degree of structural damage, and the dispersion of debris, is made possible by these annotations. FloodNet also contains important metadata, such as temporal and geographical features, which allow for spatiotemporal analysis and a better understanding of the changing post-flood landscape.

We emphasise FloodNet's distinctive contributions to remote sensing and catastrophe response in this introduction. The content of the dataset, the annotation process, and possible uses will all be covered in detail in the following sections. In addition, we provide baseline standards and assessment metrics to help academics create reliable algorithms for a variety of applications, such as predicting infrastructure recovery and mapping flood extent. In the end, FloodNet is an essential tool that advances our understanding of flood scenes after they have occurred and stimulates technological innovation that makes communities more resilient to natural catastrophes.

II. LITRATURE SURVEY

Like other natural catastrophes, floods can have a significant and long-lasting effect on the environment, infrastructure, and communities. Effective disaster response and recovery depend on accurate and efficient assessment of the aftermath. The combination of cutting-edge technologies, especially deep learning methods and high-resolution aerial photos, has shown promise in recent years for post-flood scene classification.

Gangisetty along with co authors published work [1] in 2022 named “FloodNet: Underwater image restoration based on residual dense learning” where they designed residual dense blocks to learn the residual information from the input images using dense connections between convolutional layer and residual blocks. Light scattering, colour shift, suspended particles, and haze, are what make underwater picture restoration difficult and this was the only challenge faced when using their model. To address this issue they used FloodNet dataset.

Building upon the foundation laid by FloodNet, some work has been introduced [V-FloodNet: A video segmentation system for urban flood detection and quantification] in 2023 [2].This V-FloodNet system has many advantages and works wonderfully in variety of weather conditions. But accurate water segmentation from images and videos is difficult varying lighting conditions. In order to overcome this difficulty, the system employs a deep learning segmentation pipeline that combines segmentation models based on images and videos to identify and track floods and reference objects in lengthy video sequences in a variety of meteorological scenarios.

The study used cutting-edge convolutional neural network (CNN) designs, which were refined using the FloodNet dataset, according to the article. The CNN architectures evaluated in the study include EfficientNet, ResNet, VGG-16, RegNet, and Vision Transformer (ViT).This research was carried by the name “Flood or Non-Flooded: A Comparative Study of State-of-the-Art Models for Flood Image Classification Using the FloodNet Dataset with Uncertainty Offset Analysis” in the year 2023 [3].

In order to improve the quality of training samples for flood area extraction using deep learning models, Zhang et al.'s paper "A new multi-source remote sensing image sample dataset with high resolution for flood area extraction: GF-FloodNet" (Informa UK Limited, 2023) presents GF-FloodNet, a novel dataset [4]. The GF-FloodNet dataset is placed within the larger context of research on flood area extraction and multi-source remote sensing data by this review of the literature.

In the quest for high-resolution aerial imagery datasets, presented FloodNet-to-FloodGAN : Generating Flood Scenes in Aerial Images in 2022 [5]. The architecture used in this study is called FloodGAN, which is based on the Pix2Pix GAN framework .This work might offer valuable insights into the challenges of collecting, processing, and utilizing high-resolution imagery for flood scene classification, complementing FloodNet's emphasis on resolution.

Advances in underwater picture restoration [6], urban flood detection, flood image classification, flood region extraction, and flood scene production are shown by the literature review. Even though these techniques show encouraging results, problems with precise segmentation, generalizing the model, and adapting to different contexts still exist. The introduction of datasets like FloodNet and GF-FloodNet offers useful tools for training and assessing these models, opening new avenues for flood-related research and applications[7]. Subsequent investigations ought to concentrate on enhancing current frameworks, bolstering the resilience of models, and investigating more extensive uses in environmental monitoring and disaster management.

III. DATASET

Following Hurricane Harvey, the data was gathered using a small UAV platform and DJI Mavic Pro quadcopters[8]. As a Category 4 storm, storm Harvey made landfall in August 2017 close to Texas and Louisiana. The Harvey dataset is made up of images and video captured from many aircraft between August 30 and September 4, 2017, over Texas's Ford Bend County and other locations that were directly affected. There are two reasons the dataset is distinct. One is fidelity: the data represents the current state of practise and what may be reasonably expected to be acquired following a disaster since it includes imagery from unmanned aerial vehicles (sUAVs) obtained during the emergency response phase.

It is the exclusive database of sUAV imagery for catastrophes, which brings us to our second point[9]. Keep in mind that there are alternative databases out there. Though bigger, fixed-wing aircraft that operate above the 400 feet AGL (Above Ground Level) restriction of sUAVs, such as National Guard Predators or Civil Air Patrol, there are alternative databases of images from human and unmanned aerial assets captured during catastrophes that are now available. Unlike human assets, which typically fly at 500 feet AGL or higher, all flights were conducted at 200 feet AGL. Compared to existing datasets for natural catastrophes, our photos are unique because they have a very high spatial resolution of around 1.5 cm at a height of 200 feet. Every picture shows the post-flooded damage to the impacted locations[10]. These pictures depict a variety of items, such as roads and constructions, as well as associated characteristics, such as the condition of an object—such as whether it is flooded or not following Hurricane Harvey. These factors are taken into consideration for the development of this dataset for semantic segmentation and VQA. Downloads for the FloodNet dataset are available at https://github.com/BinaLab/FloodNet-Supervised_v1.0.

Annotations:

Nine classes—building-flooded, building-non-flooded, road-flooded, road-non-flooded, water, tree, vehicle, pool, and grass—have been applied to a total of 2343 photos. When a building's side is in contact with floodwater, it is considered to be flooded. A class called "water" has been designed to represent any natural water feature, such as a river or lake, even if there are classes for flooded structures and roads that help distinguish between natural water and flood water. Every image in the classification job is categorized as either "flooded" or "non-flooded." An area is categorized as flooded if it contains more than 30% flood water; otherwise, it is categorized as non-flooded. We have a lot of photos. An hour or so is needed on average to annotate each image. We used an iterative approach to the annotation process, conducting a two-level quality check for each class to guarantee good quality. Table 2 displays the number of photos and instances that match to the various classes[11]. In order to facilitate semantic segmentation and classification, the pictures are annotated using the V7 Darwin platform. On the V7 Darwin platform, annotation duties are completed in two phases. An annotator is randomly allocated to the image in the first stage. The reviewers receive the photographs after the annotation is finished. The photographs are either approved or returned to the annotators with comments, based on how well the annotation is done. The loop of evaluation and feedback doesn't stop until the annotation is of a high caliber.

The dataset was divided into three subsets: 70% was used for training, 30% for validation, and 30% for testing. All three tasks' training, validation, and testing sets will be made available to the public.

TABLE I. IMAGES AND INSTANCES OF DIFFERENT CLASSES

Object Class	Image	Instance
Building-flooded	245	3248
Building-non-flooded	880	3427
Road-flooded	264	495
Road-non-flooded	1175	2155
Vehicle	813	4535
Pool	531	1141
Tree	1885	19682
Water	984	1374

IV. IMPLEMENTATION

Classification:

When deep neural networks were able to classify photos into multiple groups with a high degree of accuracy, its usefulness became apparent. Krizhevsky et al. primarily provided this increase, achieving state-of-the-art performance on the ImageNet dataset in 2012. Many networks were later developed that could do classification on public datasets including CIFAR, MNIST, and FashionMNIST, as this is perhaps the most basic computer vision job. Networks like VGGNet, ResNet, InceptionNet, Xception, MobileNet, and so on grew as a result[11]. These networks experimented with various skip connections, residual learning, multi-level feature extraction, separable convolutions, and optimisation techniques for mobile devices. Even though these networks performed well on regular photos of cars and animals, they were rarely enough to forecast data from scientific datasets like those taken by satellites or aircraft. In this context, several image classification networks, including, have been investigated with the aim of post-disaster damage detection. Collected photographs of catastrophe locations from the ground up using crowdsourced pictures from social media. employed a Hidden Markov Model post-processing and a Support Vector Machine on top of a Convolutional Neural Network (CNN) to identify avalanches. For the purpose of detecting fires, although the dataset that was employed included pictures from ground-based hand-held cameras. Created a cutting-edge algorithm centred on using UAV photos to detect wildfires. They have put in a great deal of effort to create a CNN for emergency response to fire, flood, collapsed buildings, and auto accidents[12].

In order to categorise the photos into Flooded and Non-Flooded categories, we employed three cutting-edge networks as base models: InceptionNetv3, ResNet50, and Xception. With the introduction of novel design elements like depthwise separable convolutions in Xception, multi-scale architecture in InceptionNet, and residual blocks in ResNet, each of these networks has made a substantial contribution to the area of computer vision[13]. The output from these basic models was divided into three layers for our classification task: a fully connected layer with 1024 neurons that had rectified linear unit (RELU) activation, a global average pooling layer, and two neurons that had softmax activation. Using binary cross entropy loss, we trained our networks for 30 epochs (20 steps each epoch) after initialising them using ImageNet weights. Utilising the Adam optimizer with a 0.001 learning rate, we downsized every image to 224 × 224 pixels[14].

Segmentation:

One of the main fields of computer vision research and a crucial component of scene understanding is semantic segmentation. A number of cutting-edge models have been developed since the groundbreaking work of Fully Convolutional Network (FCN). This study addresses semantic segmentation. Two categories may be distinguished amongst segmentation models from the standpoint of contextual aggregation. Promising results have been observed on numerous segmentation benchmarks by models that perform spatial pyramid pooling at several grid sizes, such as PSPNet (Pyramid Scene Parsing Network) and DeepLab[15]. Mid-level and high-level characteristics are combined by the encoder-decoder networks to extract global context at various scales. Notable pieces that make use of this architecture include. Conversely, some models learn contextual dependencies on local features in order to gain feature representation.

Numerous researchers have offered various deep learning models for post-natural disaster damage assessment in addition to suggesting natural catastrophe datasets. In order to identify regions of greatest effect from natural disasters, authors in employ previously suggested semantic segmentation on satellite pictures to identify alterations in the structure of various man-made objects. Rahnemoonfar et al. use a densely connected recurrent neural network in to segment UAV photos semantically in order to identify flooded areas. Rudner et al. combine multisensor, multiresolution, and multitemporal satellite images and suggest a unique method called Multi3Net for quickly segmenting flooded structures. For cooperative building segmentation and damage classification, Gupta et al. provide a RescueNet in that is inspired by DeepLabv3 and DeepLabv3+. Rather than focusing on entire post-disaster sceneries, all of these suggested approaches target the semantic segmentation of certain object types, such as rivers, buildings, and roads.

The state-of-the-art semantic segmentation methods described above have mostly been used with images derived from the ground. In contrast, we use our proposed FloodNet dataset to test three cutting-edge semantic segmentation networks. We choose to use one network called ENet, one network called PSPNet that is built on encoder-decoder modules, and one final model called DeepLabv3+ that uses both types of modules[16].

We built three algorithms (DSPNet, ENet and DeepLabv3+) for semantic segmentation and tested their effectiveness using the FloodNet dataset. The backbone for PSPNet implementation was ResNet101. With a base learning rate of 0.0001, we employed a "poly" learning rate. The auxiliary loss's mass, momentum, weight decay, power, and weight were all set to 0.9, 0.0001, 0.9, and 0.4, respectively. We set the learning rate and learning rate degradation for ENet to 0.0005 and 0.1, respectively. A weight decay of 0.0002 was selected. In a similar manner, we employed poly learning rate with base learning rate 0.01 for DeepLabv3+. We configure momentum to be 0.9 and weight decay to be 0.0001. In order to prevent the models from overfitting, we employed random rotation, flipping, scaling, and shuffling throughout the picture

augmentation process. It has been demonstrated via several trials that greater "crop size" and "batch size" enhance the models' performance[17]. We scaled the photographs to 713 × 713 during training since high resolution images benefit from a big crop size. We employed mean intersection over union (mIoU) as the assessment measure for semantic segmentation.

V. RESULTS

Classification analysis:

Table 2 displays the three networks' categorization accuracies. This table shows that while the performance of all three networks is comparable, InceptionNetv3 provided the best results on the test set.

Compared to previous networks, this network's multi-scale design has successfully assisted in categorising the test photos into Flooded and Non-Flooded classes. Even though Xception performed the best on the training set, the residual architecture of ResNet50 and the depthwise separable convolutions of Xception produced somewhat lower results. This contrasts with the networks' results on the ImageNet dataset, where ResNet50 produced the best results.

Therefore, it is not really possible to utilise networks like ImageNet, which provide excellent accuracy on common pictures, to recognise image characteristics from aerial datasets that comprise more intricate urban and natural environments. As a result, distinct, innovative structures that are capable of accurately identifying urban disasters must be designed.

TABLE II. CLASSIFICATION MODELS AND ITS ACCURACY(%)

Model	Training	Validation	Testing
InceptionNetV3	95.37	92.89	**95.09**
ResNet50	93.99	92.22	93.30
Xception	**96.54**	**96.00**	94.64

Segmentation analysis:

Table 3 presents the semantic segmentation findings of PSPNet, DeepLabv3+, and ENet. The segmentation experiment clearly shows that the most challenging jobs for the segmentation networks are recognising tiny objects, such as cars and pools. The next difficult job for all three models is dealing with flooded roads and buildings. PSPNet outperforms all other segmentation models across all classes.

Interestingly, despite the fact that DeepLabv3+ and PSPNet gather global contextual data, it is still difficult for them to identify flooded buildings and flooded roads because the ability to discriminate between flooded and non-flooded objects is highly dependent on the respective contexts of the classes.

TABLE III. SEMANTIC SEGMENTATION MODEL AND ITS ACCURACY(%)

Method	Buildings flooded	Building Non Flooded	mIou
Enet	21.82	41.41	39.84
DeepLabv3+	28.10	78.10	58.61
PSPNet	**65.61**	**90.92**	**80.35**

VI. CONCLUSION

The FloodNet dataset for post-natural disaster damage assessment is presented in this study. We go over the process of gathering the dataset, its various aspects, and its statistics.

The low altitude and high resolution dataset provided by UAV photographs is very valuable for computer vision tasks. Semantic segmentation and classification annotations are present in the dataset. We carry out three computer vision tasks: semantic segmentation, and picture classification. Detailed analyses have been supplied for each of the three tasks.

Even if UAVs offer a quick and affordable alternative for any post-natural disaster damage assessment, the FloodNet dataset, which was gathered with the use of UAVs, presents a number of difficulties. Since cars and pools are the smallest of all the available classes, it would be challenging for any network model to identify them. Table 4's segmentation findings confirm how challenging it is to detect tiny things like cars and pools. Finding flooded buildings is not the only major obstacle. Estimating the extent of damage done to a building is a challenging task because UAV photos only provide a top view of the structure. Building flooding is not well detected by segmentation models.

Similar to non-flooded highways, flooded roads are difficult to identify from one another, as segmentation model findings demonstrate. The ability to discriminate between flooded and non-flooded roads and buildings is mostly dependent on the circumstances in which they are found, and current state-of-the-art models continue to perform poorly in computer vision tests conducted on FloodNet. To the best of our knowledge, no previous post-natural catastrophe dataset has tackled these three essential computer vision tasks combined.

The dataset's experiments provide significant difficulties, and we fervently hope that FloodNet will inspire and foster the creation of more complex models for post-disaster damage assessment and a deeper understanding of semantics.

REFERENCES

[1] Gangisetty, Shankar & Rai, Raghu. (2022). FloodNet: Underwater image restoration based on residual dense learning. Signal Processing: Image Communication. 104. 116647. 10.1016/j.image.2022.116647.J. Clerk Maxwell, A Treatise on Electricity and Magnetism, 3rd ed., vol. 2. Oxford: Clarendon, 1892, pp.68–73.

[2] Liang, Yongqing & Li, Xin & Tsai, Brian & Chen, Qin & Jafari, Navid. (2022). V-FloodNet: A video segmentation system for urban flood detection and quantification. Environmental Modelling & Software. 160. 105586. 10.1016/j.envsoft.2022.105586.

[3] Jackson, Jehoiada & Yussif, Sophyani & Patamia, Rutherford & Sarpong, Kwabena & Qin, Zhiguang. (2023). Flood or Non-Flooded: A Comparative Study of State-of-the-Art Models for Flood Image Classification Using the FloodNet Dataset with Uncertainty Offset Analysis. Water. 15. 875. 10.3390/w15050875.

[4] Zhang, Yuwei & Liu, Peng & Chen, Lajiao & Xu, Mengzhen & Guo, Xingyan & Zhao, Lingjun. (2023). A new multi-source remote sensing image sample dataset with high resolution for flood area extraction: GF-FloodNet. International Journal of Digital Earth. 16. 2522-2554. 10.1080/17538947.2023.2230978.

[5] Shubham Goswami, Sagar Verma, Kavya Gupta, Siddharth Gupta. FloodNet-to-FloodGAN : Generating Flood Scenes in Aerial Images. 2022. ⟨hal-03846063⟩.

[6] S. Bhorge, M. Rane, N. Rane, M. Patil, P. Saraf and J. Nilgar, "Visual AI for Satellite Imagery Perspective: A Visual Question Answering Framework in the Geospatial Domain," 2023 IEEE 8th International Conference for Convergence in Technology (I2CT), Lonavla, India, 2023, pp. 1-6, doi: 10.1109/I2CT57861.2023.10126467.

[7] F. Safavi and M. Rahnemoonfar, "Comparative Study of Real-Time Semantic Segmentation Networks in Aerial Images During Flooding Events," in IEEE Journal of Selected Topics in Applied Earth Observations and Remote Sensing, vol. 16, pp. 15-31, 2023, doi: 10.1109/JSTARS.2022.3219724.

[8] S. Lenka, B. Vidyarthi, N. Sequeira and U. Verma, "Texture Aware Unsupervised Segmentation for Assessment of Flood Severity in UAV Aerial Images," IGARSS 2022 - 2022 IEEE International Geoscience and Remote Sensing Symposium, Kuala Lumpur, Malaysia, 2022, pp. 7815-7818, doi: 10.1109/IGARSS46834.2022.9883678.

[9] U. Verma and G. Puthumanaillam, "Improved Semantic Segmentation for Identification of Flooded Regions in UAV Aerial Images: A Transformer-Based Approach," IGARSS 2023 - 2023 IEEE International Geoscience and Remote Sensing Symposium, Pasadena, CA, USA, 2023, pp. 4800-4803, doi: 10.1109/IGARSS52108.2023.10283035.

[10] A. Arjun and T. Singh, "Analysis of image segmentation methods on Amrita's Indian side face profile database," 2017 International Conference on Communication and Signal Processing (ICCSP), Chennai, India, 2017, pp. 0952-0958, doi: 10.1109/ICCSP.2017.8286512.

[11] D. Reddy, Dheeraj, Kiran, V. Bhavana and H. K. Krishnappa, "Brain Tumor Detection Using Image Segmentation Techniques," 2018 International Conference on Communication and Signal Processing (ICCSP), Chennai, India, 2018, pp. 0018-0022, doi: 10.1109/ICCSP.2018.8524235.

[12] I. K. Veetil, E. A. Gopalakrishnan, V. Sowmya and K. P. Soman, "Parkinson's Disease Classification from Magnetic Resonance Images (MRI) using Deep Transfer Learned Convolutional Neural Networks," 2021 IEEE 18th India Council International Conference (INDICON), Guwahati, India, 2021, pp. 1-6, doi: 10.1109/INDICON52576.2021.9691745.

[13] Z. Wang, "Disaster Remote Sensing Image Semantic Segmentation model with boundary constraints based on SegNeXt," 2023 3rd International Conference on Neural Networks, Information and Communication Engineering (NNICE), Guangzhou, China, 2023, pp. 734-737, doi: 10.1109/NNICE58320.2023.10105751.

[14] A. Sharma and U. Verma, "Flood Magnitude Assessment from UAV Aerial Videos Based on Image Segmentation and Similarity," TENCON 2021 - 2021 IEEE Region 10 Conference (TENCON), Auckland, New Zealand, 2021, pp. 476-481, doi: 10.1109/TENCON54134.2021.9707250.

[15] R. D. I. Puspitasari, F. Q. Annisa and D. Ariyanto, "Flooded Area Segmentation on Remote Sensing Image from Unmanned Aerial Vehicles (UAV) using DeepLabV3 and EfficientNet-B4 Model," 2023 International Conference on Computer, Control, Informatics and its Applications (IC3INA), Bandung, Indonesia, 2023, pp. 216-220, doi: 10.1109/IC3INA60834.2023.10285752.

[16] Zhou, Jing, and David De Roure. "Floodnet: Coupling adaptive sampling with energy aware routing in a flood warning system." Journal of Computer Science and Technology 22 (2007): 121-130.

[17] Blyth, K. E. N. "Floodnet: a telenetwork for acquisition, processing and dissemination of earth observation data for monitoring and emergency management of floods." Hydrological Processes 11.10 (1997): 1359-1375.

Selection of Segmentation Algorithm for Satellite Images

Edgaras Janusonis, Giruta Kazakeviciute-Januskeviciene, Romualdas Bausys

***Abstract*—** The combination of MCDM and fuzzy sets offers new potential ways to solve the challenges posed by complex image contents, such as selecting the optimal segmentation algorithm or evaluating the segmentation quality based on various parameters. Since no single segmentation algorithm can achieve the best results on satellite image datasets, it is essential to determine the most appropriate segmentation algorithm for each satellite image, the content of which can be characterized by relevant visual features. In this research, we proposed a set of visual criteria representing the fundamental aspects of satellite image segmentation. The segmentation algorithms chosen for testing were evaluated for their performance against each criterion. We introduced a new method to create a decision matrix for each image using fuzzy fusion, which combines the image content vector and the evaluation matrix of the studied segmentation algorithms. An extension of the Preference Ranking Organization Method Enrichment Evaluation (PROMETHEE) using intuitive fuzzy sets (IFSs) was applied to solve this problem. The results acquired by the proposed methodology were validated by comparing them with those obtained in expert ratings and by performing a sensitivity analysis.

***Keywords*—** satellite imagery, image segmentation, segmentation quality assessment, multiple-criteria decision-making methods, intuitionistic fuzzy set.

Edgaras Janušonis is with the VILNIUS TECH, Lithuania (e-mail: edgaras.janusonis@vilniustech.lt).

Current Starved Ring Oscillator Image Sensor

Devin Atkin, Orly Yadid-Pecht

***Abstract*—**The continual demands for increasing resolution and dynamic range in complimentary metal-oxide semiconductor (CMOS) image sensors have resulted in exponential increases in the amount of data that need to be read out of an image sensor, and existing readouts cannot keep up with this demand. Interesting approaches such as sparse and burst readouts have been proposed and show promise, but at considerable trade-offs in other specifications. To this end, we have begun designing and evaluating various readout topologies centered around an attempt to parallelize the sensor readout. In this paper, we have designed, simulated, and started testing a light-controlled oscillator topology with dual column and row readouts. We expect the parallel readout structure to offer greater speed and alleviate the trade-off typical in this topology, where slow pixels present a major framerate bottleneck.

***Keywords*—**CMOS image sensors, high-speed capture, wide dynamic range, light controlled oscillator.

I. Introduction

THERE is an ongoing push for increasing frame rate video cameras. The current industry standard for high-speed cameras, the Phantom branded cameras, can capture very high framerates, but only by sacrificing their resolution to the point of being unusable for many applications. For example, the Phantom v2640 (see [1] for the datasheet) can capture at rates up to 303,460 frames per second (fps); however, this can only be captured at a maximum resolution of 1792W x 8H. This extreme aspect ratio is a product of the sensor's readout method. It makes it challenging to utilize these cameras in many practical applications. If we want to target a more practical 640W x 480H (Video Graphics Array (VGA) resolution), the achievable framerate drops to 53,290 fps. This is because of the standard trade-off that exists between the image sensor's specifications of framerate, resolution, dynamic range, and noise. As the captured framerate increases, the other specifications tend to shrink such that the amount of data being captured remains roughly constant. This trade-off has remained throughout time and technologies, with older film-based technologies being limited by the sensitivity (ISO) of the film. A high ISO film allowed for higher captured frame rates, but also resulted in a substantial increase to the amount of film grain, the analog medium's equivalent to fixed pattern noise.

Most of the development regarding CMOS image sensors centers around modifying them to improve one of the four main steps in the sensor's operation cycle:

1) Reset: The voltage on the photodiode node is set to some known voltage. Most often, this would be the sensor's supply voltage.
2) Integration: Photocurrents are incredibly small. To detect them effectively, they will typically need to be integrated for some time, often by providing time for the photocurrent to drain the photodiode node.
3) Sample: Once the integration has reached a level by which the signal can be measured with sufficient accuracy, the integration is stopped so that the pixel can be read out.
4) Readout: The pixel signal needs to be read and converted into a usable format. Typically, the voltage on the photodiode is put through an analog-to-digital conversion and read out of the chip.

The majority of image sensors will operate with this overall loop; however, the specifics of its implementation vary infinitely. The two primary readout strategies are global and rolling shutter sensors. In rolling shutter sensors, pixels operate with a time offset from one another by row; this means that some pixels are reset, others are integrated, and others are read out at any given time. All pixels operate in unison in global shutters outside of the readout phase. Rolling shutters attempt to better utilize the readout hardware by having it active more of the time, but in doing so, they may introduce tearing as quick-moving objects move across the frame. This rubber-pencil-like effect can render the sensor useless in specific applications. Other topologies remove the reset or integration times, and can be read out at any time during the sensor operation [2]-[4]. Regardless, the readout will remain the primary bottleneck to higher framerates as the number of paths out of the chip are fundamentally finite. Substantial work in sparse and burst readout methods attempt to sidestep this issue. Sparse readout methods primarily fall into the category of address event representation (AER) image sensors [5]-[7]. These sensors only read out pixels where they have detected an event, thus substantially limiting the number of pixels that need to be read out. Some promising burst imaging sensors utilize in-situ memory to capture successive frames rapidly before reading them out of the sensor at a slower speed. The best of these sensors can achieve framerates ranging from 5 million to 1.25 billion during their burst recording [8], [9]. Some of these topologies have begun utilizing more advanced technologies to 3D stack the silicon so that digital memory and readout can be stored behind the photodiode array [10]. This technique helps maintain the pixel's fill factor when adding a large amount of digital logic to the sensor array.

II. Proposed Topology

Fig. 1 shows the proposed pixel topology. The topology consists of a current starved ring oscillator where the pixel

Devin Atkin and Orly Yadid-Pecht are with Electrical and Computer Engineering, University of Calgary, I2Sense Laboratory, Calgary, Canada (e-mail: dmatkin@ucalgary.ca, orly.yadid-pecht@ucalgary.ca).

photocurrent sets the frequency of operation. This topology is similar in concept to previously presented light controlled oscillators [3], [4], [11]; however, other implementations have operated by counting pulses generated by the sensor. This is inherently slow and may become effectively unreadable under low light conditions. The topologies have two primary differences. First, pixels in our work act as a reset for a pulse width counter instead of being used to count the frequency. This difference means that instead of measuring the number of pulses to determine the light level, we need to only measure the length of time for a single pulse to occur which can then be interpreted directly. We have also introduced a secondary readout path which is not present in the other light controlled oscillators. This strategy allows us to read slow pixels without waiting, as one readout can handle fast pixels while the other can handle slow ones through appropriate software control. This design was completed in the AMS 350nm optical process, which includes an NWELL photodiode; this necessitates the anode of the reverse biased diode to be connected directly to the ground to prevent substrate shorting. In a deep NWELL process, this may be simplified by removing the additional current mirror.

One considerable advantage of this topology is the adjustability of the readout to serve different purposes. While the initial prototype transistor sizing was kept very simple, a lot of opportunities exist to either adjust transistor sizing or make simple additions to optimize the performance further, thus opening an avenue for development. Two potential development avenues would be creating a ratio between the current mirror transistors to adjust the ring oscillator curve to run faster, or adding a settable bias voltage to allow the pixels to be calibrated. These were dismissed for the initial prototype to keep the design as simple as possible.

AER sensors where pixels generate events saying which pixel has been triggered may also operate using row and column select outputs [5], [12]. Pulses simultaneously on two buses can determine which pixel generated a specific output at any given time. Those pulses can then determine the light level hitting any given pixel. We are not employing this address-based representation because it loses the frame-based readout, which is useful and expected by most final applications. This readout requires some form of order arbitration circuitry to determine which pixels generated the event as pulses may overlap. At higher speeds, the propagation delays can become quite tricky to decide accurately on the order of pixel outputs. Although some of the AER sensors, which include arbitration systems, will also have requests and acknowledges passed between the pixel and the driver circuitry to help with this problem [6], this is a double-edged sword that prevents fast pixels blocking slower pixel's ability to read out at the cost of increasing the design complexity. In addition, this method results in increased silicon area required and operation complexity which can further contribute to the negative side of this readout method. Instead, we utilize our secondary output to account for low-light pixels by allowing us to address multiple pixels simultaneously; slower pixels can be read through one bus, while faster pixels can be read through the other.

A. Pulse Width Counter

The second element of the design is the pulse width counter. This element was somewhat of a novelty for our lab as our previous Wide Dynamic Range (WDR) works have all relied on an external analog to digital converter to produce output values. As this design creates a pulse frequency modulated signal, we needed to adapt to utilize this topology effectively and thus included a pulse width counter internal to the sensor. This component consists of an incrementing register fed by an external clock, reset by the pixel output, and latched to an output register. This setup allows the sensor to simultaneously count the time it takes for a given pixel to pulse for an entire row or column. The level of degradation between light levels is determined by the speed of the input clock and is limited primarily by the length of the included counting register.

$$f_{min} = \frac{1}{t_{max}} \tag{1}$$

$$f_{max} = \frac{1}{t_{min}} \tag{2}$$

$$t_{dist} = \frac{1}{C_{HS}} \tag{3}$$

$$t_{mdist} = (t_{dist} * 2^{reg}) \tag{4}$$

Equations (1)-(4) are the equations that determine the sensor's performance. Equation (1) the pixel's dark current frequency (the frequency when the pixel is not exposed to light) should be relatively large; if it is small, the required register size to measure it becomes excessive. Equation (2) is the maximum frequency output of the pixels in each scene; as shown in Fig. 2, it can be extremely large relative to the dark current frequency, providing the sensor with a great inherent dynamic range. Equation (3) is the shortest distinguishable time frame for a given input clock and can be adjusted in software as needed. Finally, (4) is the maximum distinguishable time, a function of the register length and the speed of the input clock. The register length is inherently set at the design time and places constraints on the discernable contrast between light levels.

$$bits\ obtainable = \log_2((t_{max} - t_{\min})/\, t_{dist}) \tag{5}$$

Equation (5) is the maximum number of effective bits obtainable for a given clock speed if the counter register does not overflow. If the counter does overflow, this indicates that the t_{dist} is too small given the counter register size, and the input clock needs to be reduced to accommodate the scene dynamic range. However, doing this will limit the available dynamic range as the effective bit count will be less than the output bit count size.

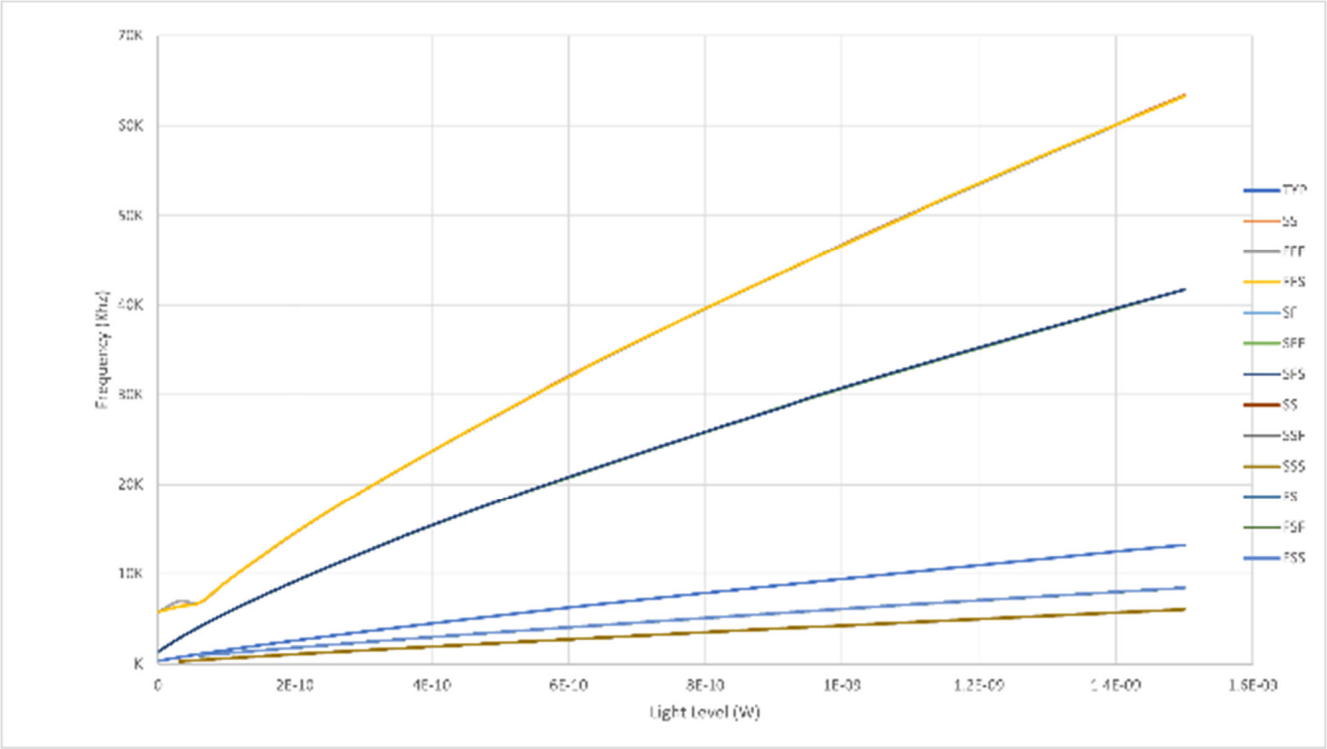

Fig. 2 Single Pixel Corner Simulation Output

III. Simulation Results

The output was simulated across different light levels on all provided silicon corners to confirm that the pixel would function as expected. The photodiode simulation input is a voltage level that represents the number of watts on the photodiode area at the optimum illumination wavelength of 850 nm. Based on this, the input power was swept between 0 W and 1.5 nW to determine the frequency behavior. Additional simulations were run up to 300 μW with the typical corner to predict the expected range of frequencies fully. The pixel did not saturate above this; however, the frequency response flattened substantially with minimal frequency change above 224.6 MHz regardless of increases to the light input. Given a maximum operating frequency of 224.6 MHz at the 300 μW input power and the dark current operating frequency of 290.5$H\ z$ we can estimate a dynamic range of roughly 271 dB using (6).

Verilog A was used to simulate varying light levels (0 W − 1.5 nW) on individual pixels in a 64 x 64 pixel array, which was modeled in Verilog A to approximate the pixel behavior. The output from this simulation was fed into MATLAB to verify the array's performance. This simulation allowed an image to be recovered using the outputs and then simulated recovered outputs based on the digital output chain. Fig. 4 shows this output with the ideal recovery based on the simulation data. Using a $f_{max} = 12.97\ Khz, f_{min} = 290.5\ Hz$, and a $C_{HS} = 13\ Khz$, if we set our maximum distinguished time to the minimum time frequency such that, $t_{mdist} = t_{max}$ we can use (4) to calculate the needed output register size of 6 bits. If we accommodate all corners, we can redo the calculations with $f_{max} = 41.32\ Khz, f_{min} = 116.2\ Hz$, and a $C_{HS} = 42\ Khz$. Using the same equation, we come to 9 bits required to capture the entire frequency range. The number of bits that the output can effectively show is 7, according to (5). Simulations and the actual results of the fabricated chip show that additional bits are required to get the needed contrast. This mistake occurs because of how the natural light levels vary compared to the calculations. More minor changes in light levels need to be distinguished to produce the appropriate contrast in natural scenes.

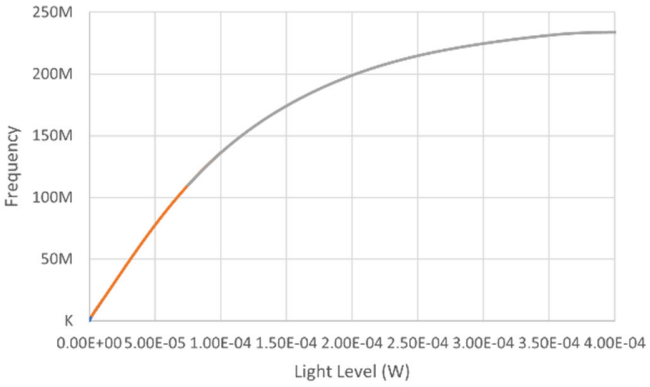

Fig. 3 Single Pixel Simulated Output

IV. Measured Outputs

The chip described above was manufactured using the AMS 350 nm Opto-Process and has undergone preliminary testing to determine the overall viability of the topology. During the

testing, several minor silicon errors were discovered with the digital output, which significantly complicated the output reading and limited the output image's performance. However, pictures from the prototype chip show promise for future chip developments despite these issues. To frame the following discussion, the readout operation is as follows:

$$DR \approx 20\log(\frac{f_{max}}{f_{min}}) \quad (6)$$

1) Reset the chip to clear the column and row select registers and the output registers. This step was intended only to be required at the beginning of operation after startup. However, in the prototype sensor, this step is necessary after each row is read out to prevent pixels from ghosting between rows. This error is due to a mistake present in the digital logic and will be corrected in future silicon.
2) Load the column and row select registers. Loading these two registers sets the X and Y of the column and row readouts. The other coordinate is selected with the output 640:10 output mux.
3) Start clocking the input at a set frequency. This step may be done at the beginning of operation or adjusted on the fly to try and maximize the scene contrast. This clock is fed into the pulse width counter to determine the frequency of the pixel outputs and should be as fast as possible without overflowing the counter register.
4) Adjust the output mux to read out each pixel in each row/ column successively. While one coordinate of the pixel being read out is set by the Column and Row registers, the other coordinate is set by the 640:10 mux connected to the output of each column. A more complicated readout algorithm should account for the dual row/column outputs to include both slow and fast outputs; however, for preliminary testing, the second output was treated primarily as a backup.
5) Read output values. Interpret these values as the varying light levels. The output value is the number of times the input clock has cycled since the last time the pixel has reset itself. The output register was too short and frequently overflows multiple times before a reset.

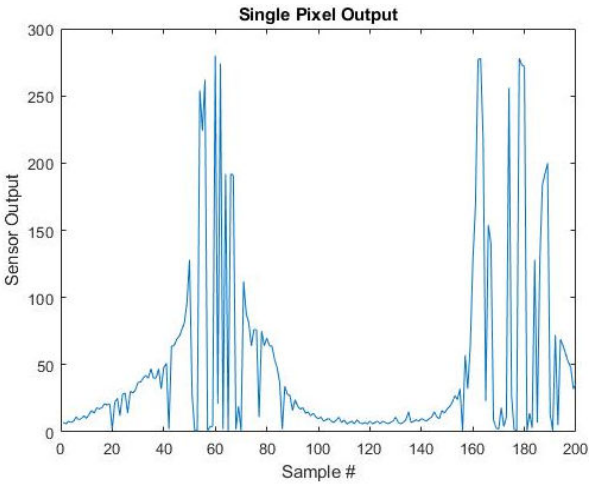

Fig. 5 Single Pixel Output

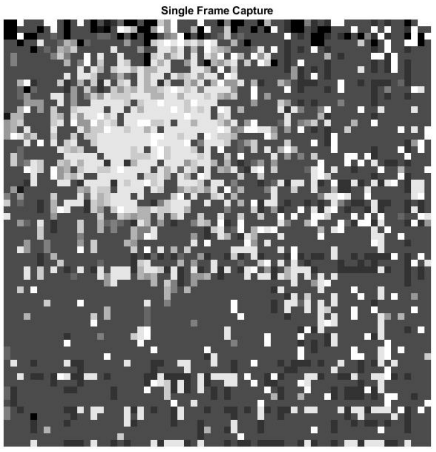

Fig. 6 Image of Lamp Light

There are a series of improvements beyond the most basic output structure. Given this basic setup, it can take quite some time to read slower pixels, with them often not resetting within the time taken to read any given row. Improvements to the design would include either increasing the dark current frequency to greater than the maximum allowable pixel time or adding additional circuitry to adjust the curve for a low light mode.

Fig. 5 shows a single pixel output over multiple samples given a constant 10 Khz input clock, with a lamp being waved in front of the sensor. The graph shows that the readout value changes depending on the light level and how the pixel frequency compares to the input clock frequency. This test revealed the first design flaw in the fabricated silicon; the output does not have a value updated signal to indicate a change. This design oversight means that if the pixel output is constant, the change in value cannot be adequately seen. Typically, the output fluctuates by 1-bit depending on how the reset lines up with the clock frequency; however, making multiple reads of a single pixel to more accurately determine its frequency is challenging. A resettable new value flag would solve this issue quickly. This test also revealed that our initial light estimates were inadequate to gain sufficient contrast; the 10-bit bus selected resulted in an overly noisy picture with insufficient bit depth in the dynamic range. Future revisions of this chip will therefore include a substantially larger pulse width counter to increase the degree to which differing light levels can be distinguished.

Fig. 6 shows an image captured of a full frame of the sensor. The output from the sensor was fed into MATLAB using a prototype board and then assembled to give the captured image. The image is very low contrast in large part due to insufficient register sizes making differing light levels challenging to distinguish. For context, the lighter-colored blob in the frame is a lamp held above the sensor.

V. Conclusion

In the above paper, we have presented an image sensor for

achieving a combination of high frame rate and high dynamic range. This initial prototype has a few minor silicon bugs discussed above, which will be fixed in a future revision of the chip. Overall, this topology has potential to improve, which will be explored in future works.

Future work will include producing a version with an increased output register to solve the contrast problem and yield more easily recognizable images. The second improvement for future iterations is the digital readout chain, which will include a more standardized interface capable of higher speed with additional flags to simplify readout. In addition, this change will allow a more thorough simulation-based test before fabrication. Finally, we will add other controls to handle the available dynamic range effectively and additional output signals to help coordinate the dual readouts cleanly. The long-term goal for this design is to integrate earlier WDR work undertaken by the I2Sense laboratory to achieve a high-speed readout alongside an easily processable frame-based image sensor.

ACKNOWLEDGMENT

The completion of this research was made possible thanks to the Natural Sciences and Engineering Research Council of Canada (NSERC) and the Alberta Informatics Circle of Research Excellence (iCORE)/Alberta Innovates - Technology Futures (AITF).

REFERENCES

[1] Vision Research and A. M. A. Division, "Phantom v2640 Datasheet and Product Page." https://www.phantomhighspeed.com/products/cameras/ultrahighspeed/v2640 (accessed Dec. 18, 2019).

[2] N. Ricquier and B. Diericks, "Pixel structure with logarithmic response for intelligent and flexible imager architectures," IEEE Conference Publication, 1992. https://ieeexplore.ieee.org/document/5435374 (accessed Dec. 19, 2019).

[3] F. Taghibakhsh and K. S. Karim, "Light controlled oscillators; pixel architecture for large area linear digital imaging using amorphous silicon," Canadian Conference on Electrical and Computer Engineering, pp. 1279–1281, 2008, doi: 10.1109/CCECE.2008.4564745.

[4] W. Yang, "Wide-dynamic-range, low-power photosensor array," in Digest of Technical Papers - IEEE International Solid-State Circuits Conference, 1994, pp. 230–231. doi: 10.1109/isscc.1994.344657.

[5] H. Zhu, M. Zhang, Y. Suo, T. D. Tran, and J. van der Spiegel, "Design of a Digital Address-Event Triggered Compressive Acquisition Image Sensor," IEEE Transactions on Circuits and Systems I: Regular Papers, vol. 63, no. 2, pp. 191–199, Feb. 2016, doi: 10.1109/TCSI.2015.2512719.

[6] E. Culurciello, R. Etienne-Cummings, and K. Boahen, "Arbitrated address event representation digital image sensor," Dig Tech Pap IEEE Int Solid State Circuits Conf, pp. 92–93, 2001, doi: 10.1109/ISSCC.2001.912560.

[7] C. Posch, D. Matolin, and R. Wohlgenannt, "A QVGA 143dB dynamic range asynchronous address-event PWM dynamic image sensor with lossless pixel-level video compression," Dig Tech Pap IEEE Int Solid State Circuits Conf, vol. 53, pp. 400–401, 2010, doi: 10.1109/ISSCC.2010.5433973.

[8] M. M. El-Desouki, O. Marinov, M. J. Deen, and Q. Fang, "CMOS active-pixel sensor with in-situ memory for ultrahigh-speed imaging," IEEE Sens J, vol. 11, no. 6, pp. 1375–1379, 2011, doi: 10.1109/JSEN.2010.2089447.

[9] L. Millet et al., "A 5 Million Frames per Second 3D Stacked Image Sensor with In-Pixel Digital Storage," in ESSCIRC 2018 - IEEE 44th European Solid State Circuits Conference, Oct. 2018, pp. 330–333. doi: 10.1109/ESSCIRC.2018.8494287.

[10] P. Vivet et al., "Advanced 3D Technologies and Architectures for 3D Smart Image Sensors," Proceedings of the 2019 Design, Automation and Test in Europe Conference and Exhibition, DATE 2019, pp. 674–679, May 2019, doi: 10.23919/DATE.2019.8714886.

[11] O. de Gaetano Ariel and D. F. Martin, "Light controlled oscillator for image sensing," 2018 2nd Conference on PhD Research in Microelectronics and Electronics Latin America, PRIME-LA 2018, pp. 1–3, May 2018, doi: 10.1109/PRIME-LA.2018.8370385.

[12] A. M. Haas, S. L. Williams, M. H. Cohen, and P. A. Abshire, "Dark address event representation imager," Midwest Symposium on Circuits and Systems, vol. 2005, pp. 388–391, 2005, doi: 10.1109/MWSCAS.2005.1594119.

Radar on Bike: Coarse Classification based on Multi-Level Clustering for Cyclist Safety Enhancement

Asma Omri, Noureddine Benothman, Sofiane Sayahi, Fethi Tlili, Hichem Besbes

***Abstract*—**Cycling, a popular mode of transportation, can also be perilous due to cyclists' vulnerability to collisions with vehicles and obstacles. This paper presents an innovative cyclist safety system based on radar technology, designed to offer real-time collision risk warnings to cyclists. The system incorporates a low-power radar sensor affixed to the bicycle and connected to a microcontroller. It leverages radar point cloud detections, a clustering algorithm, and a supervised classifier. These algorithms are optimized for efficiency to run on the TI's AWR 1843 BOOST radar, utilizing a coarse classification approach distinguishing between cars, trucks, two-wheeled vehicles, and other objects. To enhance the performance of clustering techniques, we propose a 2-Level clustering approach. This approach builds on the state-of-the-art Density-based spatial clustering of applications with noise (DBSCAN). The objective is to first cluster objects based on their velocity, then refine the analysis by clustering based on position. The initial level identifies groups of objects with similar velocities and movement patterns. The subsequent level refines the analysis by considering the spatial distribution of these objects. The clusters obtained from the first level serve as input for the second level of clustering. Our proposed technique surpasses the classical DBSCAN algorithm in terms of geometrical metrics, including homogeneity, completeness, and V-score. Relevant cluster features are extracted and utilized to classify objects using an SVM classifier. Potential obstacles are identified based on their velocity and proximity to the cyclist. To optimize the system, we used the View of Delft dataset for hyperparameter selection and SVM classifier training. The system's performance was assessed using our collected dataset of radar point clouds synchronized with a camera on an Nvidia Jetson Nano board. The radar-based cyclist safety system is a practical solution that can be easily installed on any bicycle and connected to smartphones or other devices, offering real-time feedback and navigation assistance to cyclists. We conducted experiments to validate the system's feasibility, achieving an impressive 85% accuracy in the classification task. This system has the potential to significantly reduce the number of accidents involving cyclists and enhance their safety on the road.

***Keywords*—**2-level clustering, coarse classification, cyclist safety, warning system based on radar technology.

Asma Omri is with COSIM Lab, Higher School of Communication of Tunis, Carthage University and Innovation Department, ACTIA Engineering Services, Ariana, Tunisia (e-mail: asma.omri@supcom.tn).

Noureddine Benothman is with Innovation Department, ACTIA Engineering Services, Ariana, Tunisia (e-mail: noureddine.benothman@actia-engineering.tn).

Sofiane Sayahi is with Innovation Department, ACTIA Engineering Services, Ariana, Tunisia (e-mail: sofiane.sayahi@actia-engineering.tn).

Fethi Tlili is with GRESCOM Lab, Higher School of Communication of Tunis, Carthage University, Ariana, Tunisia (e-mail: fethi.tlili@supcom.tn).

Hichem Besbes is with GRESCOM Lab, Higher School of Communication of Tunis, Carthage University, Ariana, Tunisia (e-mail: hichem.besebes@supcom.tn).

Contactless Heart Rate Measurement System based on FMCW Radar and LSTM for Automotive Applications

Asma Omri, Iheb Sifaoui, Sofiane Sayahi, Hichem Besbes

***Abstract*—**Future vehicle systems demand advanced capabilities, notably in-cabin life detection and driver monitoring systems, with a particular emphasis on drowsiness detection. To meet these requirements, several techniques employ artificial intelligence methods based on real-time vital sign measurements. In parallel, Frequency-Modulated Continuous-Wave (FMCW) radar technology has garnered considerable attention in the domains of healthcare and biomedical engineering for non-invasive vital sign monitoring. FMCW radar offers a multitude of advantages, including its non-intrusive nature, continuous monitoring capacity, and its ability to penetrate through clothing. In this paper, we propose a system utilizing the AWR6843AOP radar from Texas Instruments (TI) to extract precise vital sign information. The radar allows us to estimate Ballistocardiogram (BCG) signals, which capture the mechanical movements of the body, particularly the ballistic forces generated by heartbeats and respiration. These signals are rich sources of information about the cardiac cycle, rendering them suitable for heart rate estimation. The process begins with real-time subject positioning, followed by clutter removal, computation of Doppler phase differences, and the use of various filtering methods to accurately capture subtle physiological movements. To address the challenges associated with FMCW radar-based vital sign monitoring, including motion artifacts due to subjects' movement or radar micro-vibrations, Long Short-Term Memory (LSTM) networks are implemented. LSTM's adaptability to different heart rate patterns and ability to handle real-time data make it suitable for continuous monitoring applications. Several crucial steps were taken, including feature extraction (involving amplitude, time intervals, and signal morphology), sequence modeling, heart rate estimation through the analysis of detected cardiac cycles and their temporal relationships, and performance evaluation using metrics such as Root Mean Square Error (RMSE) and correlation with reference heart rate measurements.

For dataset construction and LSTM training, a comprehensive data collection system was established, integrating the AWR6843AOP radar, a Heart Rate Belt, and a smart watch for ground truth measurements. Rigorous synchronization of these devices ensured data accuracy. Twenty participants engaged in various scenarios, encompassing indoor and real-world conditions within a moving vehicle equipped with the radar system. Static and dynamic subject's conditions were considered. The heart rate estimation through LSTM outperforms traditional signal processing techniques that rely on filtering, Fast Fourier Transform (FFT), and thresholding. It delivers an average accuracy of approximately 91% with an RMSE of 1.01 beat per minute (bpm). In conclusion, this paper underscores the promising potential of FMCW radar technology integrated with artificial intelligence algorithms in the context of automotive applications. This innovation not only enhances road safety but also paves the way for its integration into the automotive ecosystem to improve driver well-being and overall vehicular safety.

***Keywords*—**Ballistocardiogram, FMCW Radar, vital sign monitoring, LSTM.

Asma Omri is with COSIM Lab, Higher School of Communication of Tunis, Carthage University and Innovation Department, ACTIA Engineering Services, Ariana, Tunisia (e-mail: asma.omri@supcom.tn).

Iheb Sifaoui is with Innovation Department, ACTIA Engineering Services, Ariana, Tunisia (e-mail: iheb.sifaoui@actia-engineering.tn).

Sofiane Sayahi is with Innovation Department, ACTIA Engineering Services, Ariana, Tunisia (e-mail: sofiane.sayahi@actia-engineering.tn).

Hichem Besbes is with COSIM Lab, Higher School of Communication of Tunis, Carthage University, Ariana, Tunisia (e-mail: hichem.besebes@supcom.tn).

Integrating Radar Sensors with an Autonomous Vehicle Simulator for an Enhanced Smart Parking Management System

Mohamed Gazzeh, Bradley Null, Fethi Tlili, Hichem Besbes

***Abstract*—** The burgeoning global ownership of personal vehicles has posed a significant strain on urban infrastructure, notably parking facilities, leading to traffic congestion and environmental concerns. Effective parking management systems (PMS) are indispensable for optimizing urban traffic flow and reducing emissions. The most commonly deployed systems nowadays rely on computer vision technology. This paper explores the integration of radar sensors and simulation in the context of smart parking management. We concentrate on radar sensors due to their versatility and utility in automotive applications, which extends to PMS. Additionally, radar sensors play a crucial role in driver assistance systems and autonomous vehicle development. However, the resource-intensive nature of radar data collection for algorithm development and testing necessitates innovative solutions. Simulation, particularly the monoDrive simulator, an internal development tool used by NI the Test and Measurement division of Emerson, offers a practical means to overcome this challenge. The primary objectives of this study encompass simulating radar sensors to generate a substantial dataset for algorithm development, testing, and, critically, assessing the transferability of models between simulated and real radar data. We focus on occupancy detection in parking as a practical use case, categorizing each parking space as vacant or occupied. The simulation approach using monoDrive enables algorithm validation and reliability assessment for virtual radar sensors. We meticulously designed various parking scenarios, involving manual measurements of parking spot coordinates, orientations, and the utilization of TI AWR1843 radar. To create a diverse dataset, we generated 4950 scenarios, comprising a total of 455,400 parking spots. This extensive dataset encompasses radar configuration details, ground truth occupancy information, radar detections, and associated object attributes such as range, azimuth, elevation, radar cross-section, and velocity data. The paper also addresses the intricacies and challenges of real-world radar data collection, highlighting the advantages of simulation in producing radar data for parking lot applications. We developed classification models based on Support Vector Machines (SVM) and Density-Based Spatial Clustering of Applications with Noise (DBSCAN), exclusively trained and evaluated on simulated data. Subsequently, we applied these models to real-world data, comparing their performance against the monoDrive dataset. The study demonstrates the feasibility of transferring models from a simulated environment to real-world applications, achieving an impressive accuracy score of 92% using only one radar sensor. This finding underscores the potential of radar sensors and simulation in the development of smart parking management systems, offering significant benefits for improving urban mobility and reducing environmental impact. The integration of radar sensors and simulation represents a promising avenue for enhancing smart parking management systems, addressing the challenges posed by the exponential growth in personal vehicle ownership. This research contributes valuable insights into the practicality of using simulated radar data in real-world applications and underscores the role of radar technology in advancing urban sustainability.

***Keywords*—**Autonomous Vehicle Simulator, FMCW Radar Sensors, Occupancy Detection, Smart Parking Management, Transferability of Models.

Mohamed Gazzeh is with COSIM Lab, Higher School of Communication of Tunis, Carthage University (e-mail: mohamed.gazzeh@supcom.tn).

Bradley Null is with NI the Test and Measurement Division of Emerson, Austin, Texas, USA (e-mail: bradley.null@ni.com).

Fethi Tlili is with GRESCOM Lab, Higher School of Communication of Tunis, Carthage University, Ariana, Tunisia (e-mail: fethi.tlili@supcom.tn)..

Hichem Besbes is with COSIM Lab, Higher School of Communication of Tunis, Carthage University, Ariana, Tunisia (e-mail: hichem.besebes@supcom.tn)

Assessment of Heavy Metals Contamination Levels in Groundwater: A Case Study of the Bafia Agricultural Area, Centre Region Cameroon

Carine E. Tarkang[1], Victorine N. Akenji[2], Dmitri R[3]., Josephine N[2]., Andrew A.A[2]., Franco T[4]., Ngoupayou J.R.N[5]

***Abstract*—**Groundwater is the major water resource in the whole of Bafia used for dinking, domestic, poultry and agricultural purposes, and being an area of intense agriculture, there is great necessity to do a quality assessment. Bafia is one of the main food suppliers in the Centre region of Cameroon and so to meet up with their demands; the farmers make use of fertilizers and other agrochemicals to increase their yield. Less than 20% of the population in Bafia has access to piped-borne water due to the national shortage but very limited studies have been carried out in the area to increase awareness of the groundwater resources. The aim of this study was to assess heavy metal contamination levels in ground and surface waters and to evaluate the effects of agricultural inputs on water quality in the Bafia area. 57 water samples (including 31 wells, 20 boreholes, 4 rivers and 2 springs) were analyzed for their physico-chemical parameters, while collected samples were filtered, acidified with HNO_3 and analyzed by ICP-MS for their heavy metal content (Fe, Ti, Sr, Al, Mn). Results showed that most of the water samples are acidic to slightly neutral and moderately mineralized. Ti concentration was significantly high in the area (mean value 130µg/L), suggesting another Ti source besides the natural input from Titanium oxides. The high amounts of Mn and Al in some cases also pointed to additional input, probably from fertilizers which are used in the farmlands. Most of the water samples were found to be significantly contaminated with heavy metals exceeding the WHO allowable limits (Ti-94.7%, Al-19.3%, Mn-14%, Fe-5.2% and Sr-3.5% above limits), especially around farmlands and topographic low areas. The heavy metal concentration was evaluated using: heavy metal pollution index (HPI), heavy metal evaluation index (HEI) and degree of contamination (Cd), while the Ficklin diagram was used to the water based on changes in metal content and pH. The high mean values of HPI and Cd (741 and 5 respectively), which exceeded the critical limit, indicate that the water samples are highly contaminated, with intense pollution from Ti, Al and Mn. Based on the HPI and Cd, 93% and 35% of the samples respectively are unacceptable for drinking purposes. The lowest HPI value point also had the lowest EC (50 µS/cm), indicating lower mineralization and less anthropogenic influence. According to the Ficklin diagram, 89% of the samples fell within the near neutral low-metal domain while 9% fell in the near neutral extreme-metal domain. Two significant factors were extracted from the PCA explaining 70.6% of the total variance. The first factor revealed intense anthropogenic activity (especially from fertilizers) while the second factor revealed water-rock interactions. Agricultural activities thus have an impact on the heavy metal content of groundwater in the area hence much attention should be given to the affected areas in order to protect human health/life and thus sustainably manage this precious resource.

***Keywords*—**Bafia, Contamination, Degree of contamination, Groundwater, Heavy metal pollution index.

Carine E. Tarkang is a PhD student at the University of Yaounde I Cameroon/University of Florence Italy (tel: +39 327 247 4077, email: tarkangc@yahoo.com).

Victorine N. Akenji is a Research Officer at the Ministry of Scientific Research and Innovation in Cameroon (tel: +237 674 622 127).

Dmitri R. is a Researcher at the National Institute of Geophisics and volcanology in Bologna, Italy (tel: +39 334 505 7948).

Josephine N. is a Research Master Ministry of Scientific Research and Innovation, Cameroon (tel: +237 677 83 81 02).

Andrew A.A. is is a Research Master Ministry of Scientific Research and Innovation, Cameroon (tel: +237 675 768 471).

Franco T. is a professor at the University of Florence, Italy (tel: +39 346 352 1379).

Ngoupayou J.R.N. is a professor at the University of Yaoude I, Cameroon (tel: +237 679 28 76 25).

Chemically Treated Cactus *Opuntia* as Sustainable Biosorbent for the Removal of Heavy Metals from Aqueous Solution

Yirga Weldu Abrha[*], *Fre Gebresslassie*[*], *Yongtae Ahn*[*], *Homin Kye*[*] *and Joon-Wun Kang**

[*]*Department of Land Resources Management and Environmental Protection, Mekelle University, Ethiopia*

Email: Presenter (yirga.weldu@mu.edu.et)

Abstract

Zinc and manganese are well known toxic metals, resulting a number of environmental problems. The major sources of zinc and manganese include mining, metallurgical, chemical manufacturing industries, the modern chemical industry and in commonly used goods. In our previous study with virgin cactus, we found a promising removal efficiency of metal ions (Pb^{2+} and Zn^{2+}). However, virgin cactus showed relatively less removal efficiency of Zn^{2+} compared to Pb^{2+}. Thus, the purpose of this study was to evaluate the efficiency and mechanism of chemically modified dried *Opuntia* powder adsorbent for the removal of metal ions ($Zn^{2+}$and Mn^{2+}) from aqueous solution. The characteristics of the adsorbents were studied using Brunauer–Emmett–Teller (BET), Fourier transform infrared spectroscopy (FTIR), and energy dispersive X-ray (EDX) analyses. In addition, the effect of dose, initial metal ion concentration, contact time, initial solution pH, and temperature were investigated. FTIR Adsorption kinetics, equilibrium and isotherm studies were also conducted.

The highest removal efficiencies of Zn^{2+} and Mn^{2+} was found to be with NaOH treated Opuntia followed by HCl treated *Opuntia*. The biosorption efficiency of Zn (II) enhanced from 36.0 to 95.9% and from 36.0 to 84.6% at 4 g/L when the raw biosorbent was treated by NaOH-*Opuntia*, and HCl-*Opuntia*, respectively (Fig.1a). For Mn (II), the biosorption increased from 36.0 to 88.6 % and from 33.1 to 71.0% at 4 g when the raw biosorbent was treated by NaOH-*Opuntia*, and HCl-*Opuntia*, respectively (Fig.1b). Rapid rise binding efficiency was also observed with pH up to 5 (Fig.2, a and b) and the result also showed that Zn^{+2} ion preferably adsorbed than Mn^{2+}. Metal ion adsorption increased with increasing the contact time and initial metal ion concentration. Thus, the optimal conditions for high biosorption of Zinc (II) and Manganese (II) were achieved at pH = 5, biosorbent dosage of 4 g/L, initial metal concentration of 10 mg/L for NaOH treated cactus *Opuntia*. Pseudo second-order is more appropriate to explain the adsorption process of Zn^{2+} and Mn^{2+} onto cactus than Pseudo first-order due to higher R^2. From this studies it is possible to conclude that chemical pretreatment of the raw cactus *Opuntia* with NaOH strongly enhances its biosorption potential for the selected metals.

.**Keywords:** biosorption, Cactus *Opuntia*; heavy metals, removal.

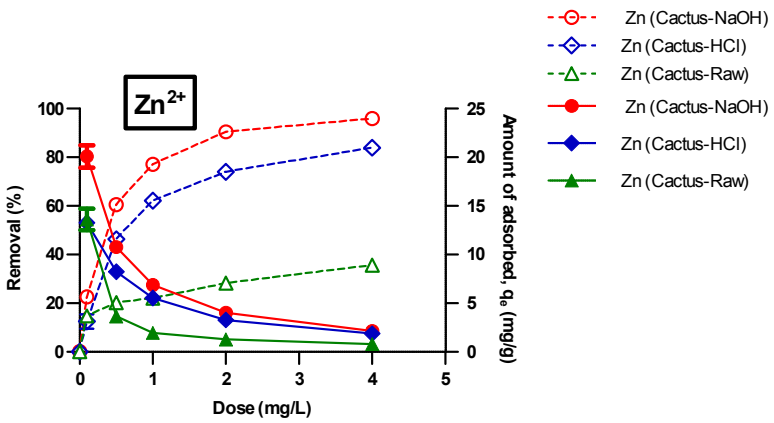

Fig 1a. Effect of dose on Zn adsorption capacity

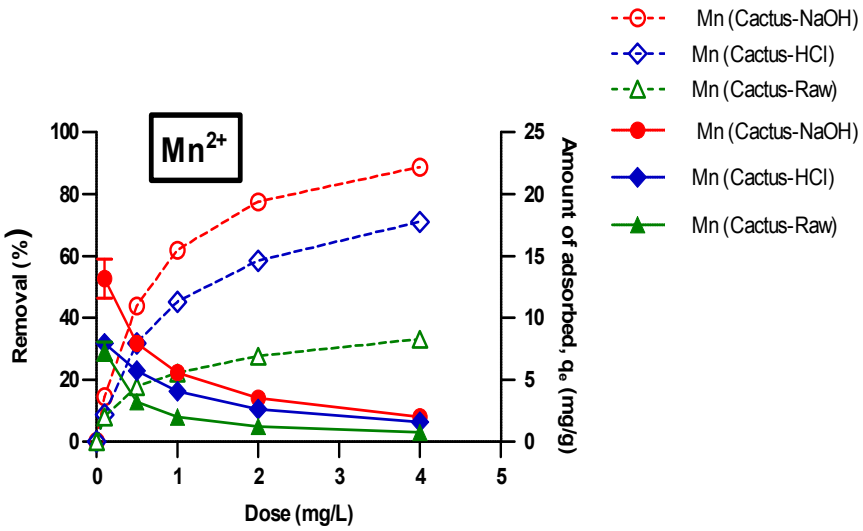

Fig 1b Effect of dose on Mn adsorption capacity

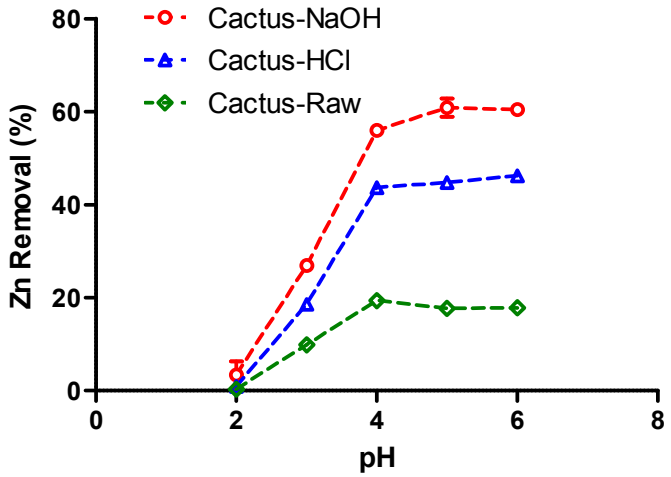

Fig 2a. Effect of pH on Zn adsorption capacity

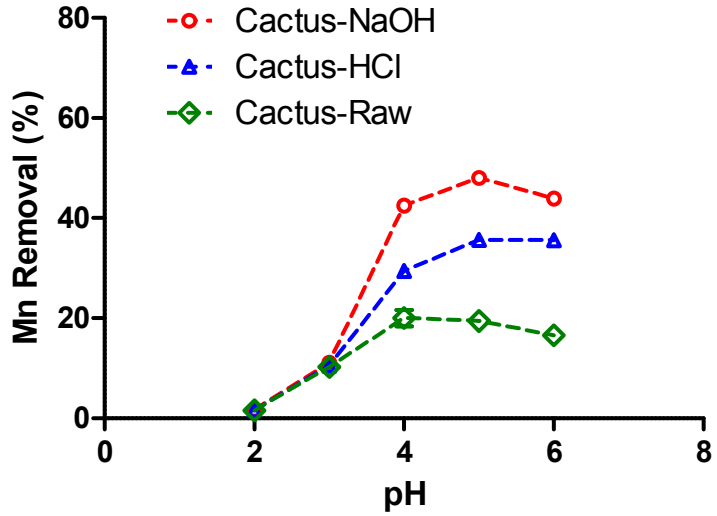

Fig 2b. Effect of pH on Zn adsorption capacity

Do Women Entrepreneurs Exit or Keep Ownership of Their Start-Ups?

Eliran Solodoha, Stav Rosenzweig

***Abstract*—** The present research offers predictions regarding the representation of women entrepreneurs and the probability of their start-ups undergoing exit. Combining two streams of literature: women's sense of ownership and women's social support at the workplace, we argue that the representation of women entrepreneurs would decrease the probability of the start-up undergoing exit because of the increased sense of ownership but that women's peer support will alleviate the sense of ownership and increase tendency toward exit. We use data on 3,743 technology start-ups in seven high-tech industries. For those start-ups that survive, we examine the association between women and their start-ups' probability of undergoing an exit and find that when women entrepreneurs are represented, entrepreneurs tend to maintain ownership of their start-ups. However, when these start-ups have women managers, they tend to undergo an exit rather than remaining at the ownership of the entrepreneurial team. We discuss theoretical contributions and offer policy implications.

***Keywords*—** women entrepreneur, sense of ownership, peer support, exit, IPO, M&A.

Eliran Solodoha is with the Peres Academic Center, Israel (e-mail: solodoha10@gmail.com).

Countering the Bullwhip Effect by Absorbing It Downstream in the Supply Chain

Geng Cui[1], Naoto Imura[1], Katsuhiro Nishinari[1,2,3], Takahiro Ezaki[1]

Research Center for Advanced Science and Technology, The University of Tokyo, 4-6-1, Komaba, Meguro-ku, Tokyo, 153-8904, Japan
Department of Aeronautics and Astronautics, School of Engineering, The University of Tokyo, 7-3-1, Hongo, Bunkyo-ku, Tokyo, 113-8656, Japan
Mobility Innovation Collaborative Research Organization, The University of Tokyo, 5-1-5, Kashiwanoha, Kashiwa-shi, Chiba, 244-8574, Japan

Abstract: The bullwhip effect, which refers to the amplification of demand variance as one moves up the supply chain, has been observed in various industries and extensively studied through analytic approaches. Existing methods to mitigate the bullwhip effect, such as decentralized demand information, vendor-managed inventory, and the Collaborative Planning, Forecasting, and Replenishment System, rely on the willingness and ability of supply chain participants to share their information. However, in practice, information sharing is often difficult to realize due to privacy concerns.

The purpose of this study is to explore new ways to mitigate the bullwhip effect without the need for information sharing. This paper proposes a 'bullwhip absorption strategy' (BAS) to alleviate the bullwhip effect by absorbing it downstream in the supply chain. To achieve this, a two-stage supply chain system was employed, consisting of a single retailer and a single manufacturer. In each time period, the retailer receives an order generated according to an autoregressive process. Upon receiving the order, the retailer depletes the ordered amount, forecasts future demand based on past records, and places an order with the manufacturer using the order-up-to replenishment policy. The manufacturer follows a similar process.

In essence, the mechanism of the model is similar to that of the beer game. The BAS is implemented at the retailer's level to counteract the bullwhip effect. This strategy requires the retailer to reduce the uncertainty in its orders, thereby absorbing the bullwhip effect downstream in the supply chain. The advantage of the BAS is that upstream participants can benefit from a reduced bullwhip effect. Although the retailer may incur additional costs, if the gain in the upstream segment can compensate for the retailer's loss, the entire supply chain will be better off.

Two indicators, order variance and inventory variance, were used to quantify the bullwhip effect in relation to the strength of absorption. It was found that implementing the BAS at the retailer's level results in a reduction in both the retailer's and the manufacturer's order variances. However, when examining the impact on inventory variances, a trade-off relationship was observed. The manufacturer's inventory variance monotonically decreases with an increase in absorption strength, while the retailer's inventory variance does not always decrease as the absorption strength grows. This is especially true when the autoregression coefficient has a high value, causing the retailer's inventory variance to become a monotonically increasing function of the absorption strength. Finally, numerical simulations were conducted for verification, and the results were consistent with our theoretical analysis.

Keywords: Bullwhip effect; Supply chain management; Inventory management; Demand forecasting; Order-to-up policy.

The Response of the Optical Properties to Temperature in Three-Layer Micro Device Under Influence of Casimir Force

M. Aali[1], F. Tajik[1,2]

[1]Department of Condensed Matter Physics, Faculty of Physics, Alzahra University, Tehran 1993891167, Iran
[2]Zernike Institute for Advanced Materials, University of Groningen, Nijenborgh 4, 9747 AG Groningen, The Netherlands

Abstract

Here, we investigate the sensitivity the Casimir force and consequently dynamical actuation of a three-layer microswitch to some ambient conditions. In fact, we have considered the effect of optical properties on the stable operation of the microswitch for both good (e.g. metals) and poor conductors via a three layer Casimir oscillator. Indeed, gold (Au) has been chosen as a good conductor which is widely used for Casimir force measurements, and highly doped conductive silicon carbide (SiC) has been considered as a poor conductor which is a promising material for device operating under harsh environments. Also, the intervening stratum is considered ethanol or water. It is also supposed that the microswitches are frictionless and autonomous. Using reduction factor diagrams and bifurcation curves, it has been shown how performance of the microswitches is sensitive to temperature and intervening stratum, moreover it is investigated how the conductivity of the components can affect this sensitivity.

Keywords— Casimir force, optical properties, Lifshitz theory, dielectric function.

Recognizing the Emergent and Submerged Iceberg of the Celiac Disease: ITAMA Project - Global Strategy Protocol

Giuseppe Magazzù, Samuel Aquilina, Christopher Barbara, Ramon Bondin, Ignazio Brusca, Jacqueline Bugeja, Mark Camilleri, Donato Cascio, Stefano Costa, Chiara Cuzzupè, Annalise Duca, Maria Fregapane, Vito Gentile, Angele Giuliano, Alessia Grifò, Anne-Marie Grima, Antonio Ieni, Giada Li Calzi, Fabiana Maisano, Giuseppinella Melita, Socrate Pallio, Ilenia Panasiti, Salvatore Pellegrino, Claudio Romano, Salvatore Sorce, Marco Elio Tabacchi, Vincenzo Taormina, Domenico Tegolo, Andrea Tortora, Cesare Valenti, Cecil Vella, Giuseppe Raso

***Abstract*—** Coeliac disease (CD) is frequently underdiagnosed with a consequent heavy burden in terms of morbidity and health care costs. Diagnosis of CD is based on the evaluation of symptoms and anti-transglutaminase antibodies IgA (TGA-IgA) levels, with values above a tenfold increase being the basis of the biopsy-free diagnostic approach suggested by present guidelines. This study showcased the largest screening project for CD carried out to date in school children (n=20,000) aimed at assessing the diagnostic accuracy of minimally invasive finger prick point-of-care tests (POCT) which, combined with conventional celiac serology and the aid of an artificial intelligence-based system, may eliminate the need for intestinal biopsy. Moreover, this study delves deeper into the "coeliac iceberg" in an attempt to identify people with disorders who may benefit from a gluten-free diet, even in the absence of gastrointestinal symptoms, abnormal serology and histology. This was achieved by looking for TGA-IgA mucosal deposits in duodenal biopsy. This large European multidisciplinary health project paves the way to an improved quality of life for patients by reducing the costs for diagnosis due to delayed findings of CD and offering business opportunities in terms of diagnostic tools and support.

***Keywords*—** coeliac disease, anti-transglutaminase, mucosal deposits, point-of-care test, negative predictive value, artificial intelligence, intestinal biopsy, ESPGHAN, guidelines.

Mark Camilleri is with the ITAMA, Malta (e-mail: mark.g.camilleri@gov.mt).

A New Design of Vacuum Membrane Distillation Module for Water Desalination

Adnan Alhathal Alanezi*
Department of Chemical Engineering Technology, College of Technological Studies, The Public Authority for Applied Education and Training (PAAET), P.O. Box 42325, Shuwaikh 70654, Kuwait; aa.alanezi@paaet.edu.kw
*Corresponding Author, Tel: +96555509994, Fax: +96522314430, Email: aa.alanezi@paaet.edu.kw

Abstract

The performance of vacuum membrane distillation (VMD) process for water desalination was investigated utilizing a new design membrane module using two commercial polytetrafluoroethylene (PTFE) and polyvinylidene fluoride (PVDF) flat sheet hydrophobic membranes. The membrane module's design demonstrated its suitability for achieving a high heat transfer coefficient of the order of 103 (W/m^2K) and a high Reynolds number (Re). The heat and mass transport coefficients within the membrane module were measured using VMD experiments. The permeate flux has been examined in relation to process parameters such as feed temperature, feed flow rate, vacuum degree, and feed concentration. Because the feed temperature, feed flow rate, and vacuum degree all play a role in improving the performance of the VMD process, optimizing all of these parameters is the best method to achieve a high permeate flux. In VMD desalination, the PTFE membrane outperformed the PVDF membrane. When compared to previous studies, the obtained water flux is relatively high, reaching 43.8 and 52.6 (kg/m^2h) for PVDF and PTFE, respectively. For both membranes, the salt rejection of NaCl was greater than 99%.

Keywords: Desalination, Vacuum membrane distillation, PTFE and PVDF, hydrophobic membranes, O-ring membrane module.

Developing Adaptive Thermal Comfort Model for Naturally Ventilated Houses in Kerala, India

Adhul S Jabir, Manju G Nair

***Abstract*—** As thermal comfort research continues to evolve, there is a growing recognition of the need for region-specific models that account for the unique climatic conditions and adaptive behaviors of diverse populations. In contrast to early global models (Fanger's PMV/PPD, ASHRAE Standard 55), this study focuses on the warm-humid climate of Kerala, India, where inhabitants exhibit distinct thermal comfort adaptations.

This paper presents a novel adaptive thermal comfort model tailored to the environmental and cultural nuances of Kerala (10.8505° N, 76.2711° E) located in the southwestern part of India. The model is developed based on comprehensive field surveys conducted in 30 different houses (121 samples) across three distinct climatic zones within the region, Lowland, Mid-land & Highland respectively. These zones were identified to capture the variations in climate that impact thermal comfort preferences.

The study emphasizes the significance of naturally ventilated houses, a prevalent architectural feature in Kerala. By analyzing occupants' responses and behaviors in diverse climatic conditions, the proposed model challenges the conventional thermal comfort ranges prescribed by international standards such as ASHRAE and EN. The results reveal a unique adaptive thermal comfort range that better aligns with the preferences and behaviors observed in the warm-humid context of Kerala.

This research not only contributes to the localized understanding of thermal comfort but also provides valuable insights for architects, designers, and policymakers involved in building design and environmental regulations in the region. The findings underscore the importance of tailoring thermal comfort standards to specific climates and cultural contexts, promoting more sustainable and occupant-centric design practices.

***Keywords*—** Adaptive Thermal Comfort Model, Region-Specific Models, Warm-Humid Climate, Field Surveys.

Adhul S Jabir is with the Department of Architecture & Planning, College of Engineering Trivandrum. Kerala, India.
Manju G Nair, is with the Department of Architecture & Planning, College of Engineering Trivandrum. Kerala , India.

Impact of Popular Passive Physiological Diversity Drivers on Thermo-Physiology and Thermal Comfort

Ilango Thiagalingam, Erwann Yvin, Gabriel Crehan, Roch El Khoury

***Abstract*—**An experimental investigation is carried out in order to evaluate the relevance of a customization approach of the passive thermal mannikin. The promise of this approach consists in the following assumption: physiological differences lead to distinct thermo-physiological responses that explain a part of the thermal appraisal differences between people. Categorizing people and developing an appropriate thermal mannikin for each group would help to reduce the actual dispersion on the subjective thermal comfort perception. The present investigation indicates that popular passive physiological diversity drivers such as sex, age and BMI are not the correct parameters to consider. Indeed, very little or no discriminated global thermo-physiological responses arise from the physiological classification of the population using these parameters.

***Keywords*—**Customization, thermal comfort, thermal Mannikin, thermo-physiology.

I. Introduction

HUMAN physiology has been studied for decades, in an attempt to properly understand how human body operates. Indeed, thanks to that knowledge, proper assumptions could be made regarding human populations, may it be for medical purposes or thermal comfort predictions.

Basal metabolic rate (BMR) was one of the parameters that was widely studied, as it describes well what are the energetic needs and consumptions of a human body and as it is also a key physiological parameter that influences the perceived thermal comfort. Harris and al. determined a model to calculate it in 1918 [1], which paved a way to other BMR models [2]-[6].

Already, sex, weight, height and age were considered as determining parameters in calculating BMR. Parameters that would be used later on to develop other models or discriminate populations when studying thermo-physiology and thermal comfort.

On Another note, Fiala's work [7] in 1998 was paramount in properly understanding thermo-physiology and human thermal regulation system. Still today, it is a major reference model in human thermoregulation and thermal comfort models [8], [9]. However, as powerful as Fiala's theory is, it lacks diversity in its human construction, considering a reference body that is a 30-year-old healthy white man.

Zhang's later works [9], published in 2003, attempted to model thermal perception based on the thermo-physiological model of Fiala. She constructed her local and global thermal sensation and thermal comfort models thanks to tests she realised with human subjects, gathering data on their direct thermal appraisal when experiencing different thermal environment. She then linked votes of people to thermo-physiological responses such as skin and hypothalamus temperatures and its derivatives. However, it should be noticed that her sample group was still biased, as it was constituted mainly by students.

Many works, like the one of Zhou et al. [10], tried to adapt the reference model of Fiala to a specific population. They focused on building a proper mannikin reproducing a Chinese adult physiology. By modifying Fiala's basic mannikin through skin layers thickness, amongst other parameters, and by adopting an individualization approach, they managed to reduce prediction bias for mean skin temperature from 0.79 °C to 0.38 °C in worst cases, and for local skin temperatures from 2.11 °C to less than 1 °C in most cases.

El Kadri et al. [11] also explored individuals' thermo-physiological characteristics. His model, called Neuro Human Thermo Model (NHTM), uses singularities and unique properties of people to rebuild an adapted thermoregulation. This goes from thermoreceptors to thermal appraisal, with the help of different models integrated in NHTM, from Fiala to Zhang, and promises to adapt to multiple populations.

An important paper written by Schweiker et al. [12] gives an extensive review on findings and results that were made around human thermal appraisal and customization. It tried to highlight physiological, psychological and context-related parameters of diversity that enable to explain thermal appraisal differences between human subjects. Regarding physiological parameters, the literature review has shown ambiguous results for age- and sex-related differences, but a clear trend for body composition (weight and BMI) and metabolic rate. Kingma et al. [13] developed a simple heat balance model that can translate physiological parameters such as body composition in terms of material layer thickness for muscle and fat to better represent the passive body insulation and metabolic rate.

Another important work is the one of Rupp et al. regarding thermal appraisal of specific populations inside a building [14], [15]. With an extremely large panel group (2094 and 5470 for HVAC and mixed-mode ventilation types of building respectively), they gathered people physiological parameters, as well as their thermal appraisal of environment, in order to build a new predictive model of thermal discomfort, that was

Ilango Thiagalingam is the responsible of research activities on thermal comfort at Vedecom, 23 bis allée des Marronniers, 78000 Versailles, France (phone: +33622247032, e-mail: ilango.thiagalingam@vedecom.fr).

Erwann Yvin was the test and data analysis engineer at Vedecom. He is now working for RATP.

Gabriel Chrean is the lead Engineer on Physiological sensing at Stellantis Group, Technical center of Vélizy A, Route de Gisy, 78140 Vélizy-Villacoublay, France

Roch El Khoury is the Head of Electrification Department at Vedecom.

based on sex, age and BMI, among other parameters. The regression model based on experimental observation was conclusive about effect of gender and BMI parameters on dissatisfied human subjects. Dissatisfied males and over-weighted subjects have a tendency to feel warmer whereas dissatisfied females have tendency to feel cooler. But as thorough as all those works are, they mainly aim for minimal discomfort for a majority of people, in spaces where cohabitation in mandatory and personal preferences are erased for greater good. They still lack insight about populations behaviours in a small, enclosed place, such as a car, where thermal comfort is sought for an individual.

The dispersion on the appraisal of the thermal environment has been observed to be quite huge in building, offices or car environments. Customization approach is seen as one of the promising ways to reduce this dispersion. It is expected that developing a set of thermal mannikins would predict thermo-physiological responses and thermal appraisal of each category of population, separated according to key parameters, with better accuracy than the default Fiala model. Two main questionings arise about this approach that need to be cleared before any modelling attempt: what are the key physiological parameters that would enable to classify population and are those population categories, based on physiological distinct parameters, would give differentiated thermal responses and thermal appraisal.

In this study, we investigate experimentally if customization of the thermal mannikin using macroscopic parameters such as gender, age and BMI is relevant. First, the experimental set-up is described, then the data are analysed using independent approaches and compared to findings presented in literature. Finally, conclusions are drawn.

II. Experimental Set-up

As an attempt to reduce dispersions in people vote about their thermal appraisal, our approach consists in studying experimentally specific populations thermal comfort perceptions in specific thermal situations, in a car-like environment. For that, a thermal test bench that represents a B-segment car cabin is used [16]. The cabin interior volume is 2.9 m^3. The internal walls of the test cell are covered with 42 independent flat stainless steel heat exchangers reproducing the car cabin geometry. Their temperatures can be controlled from 5 to 45 °C using ten independent water-glycol circulation circuits. An air handling unit provides control over the mass flow rate, temperature, and humidity of the air that is injected into the cabin. Several temperature probes monitor surface as well as air temperatures throughout the test. Other environmental parameters such as black globe temperature, air humidity, and airflow velocities are also measured around the tester. The human test subjects that underwent thermal exposures are provided with identical and thermally characterized clothes for the experiment. Indeed, before entering in the test bench, testers had to wear specific, normative clothes, in order to minimize clothing insulation influence during tests. Those were a cotton white t-shirt, black leggings, calf-length socks and trainers. Testers kept their own briefs. According to ASHRAE Handbook regarding Thermal Comfort [17], effective clothing insulation of this outfit is close to 0.39 Clo (1 Clo = 0.155 m^2K/W).

Each tester went through the following exposure:

- 30 min of sedentary preconditioning at 25 °C in a separate room
- 150 min of test with the tester seated in the driver seat inside the test bench experiencing a quasi-homogeneous scenario.

Throughout the test, airflow and humidity from the air handling unit are fixed to 200 m^3/h and 40% respectively. Air is injected into the cabin through aerators. There are three aerators at the centre of the dashboard, one on left and right-side corners, two others are below the wind shield and two below the dashboard near the driver and front passenger feet. All temperature sensors are calibrated using a standard Pt100 thermometer with an accuracy of 0.2 °C. During tests, the environmental conditions are continuously recorded at an interval of 10 s. Thermal sensation and comfort votes are collected at a five-minute interval and the Zhang nine-point scale is used for the votes.

Based on literature study, testers were classified following three major parameters: sex, age and BMI.

Multiple parameters were measured and recorded before and during tests, to help regroup testers into definite categories. Those parameters included physiological measurements (gender, age, height, weight), thermo-physiological measurements (local skin temperatures) and thermal appraisal votes (local and global sensations and comforts).

Each test is considered to be 3-hour long. The bench is preconditioned at 25 °C. First 30 minutes are generally dedicated to tester preconditioning and preparations, with hygrobuttons positioning and physiological measurements in a separate room set at 25 °C. It is then followed by a test in the bench carried out in two steps:

- 90 minutes of thermoneutrality search: the tester enters in THE BENCH AND GIVES ITS VOTE ON THE GLOBAL THERMAL sensation. If the vote is not the neutral sensation on the Zhang scale, the bench temperature (airflow and panels) is increased or decreased by 0.5°C depending on the vote (cooler or warmer global sensation vote respectively). When the tester votes the neutral sensation the temperature is not changed. Generally, testers reach the neutral state in the first 30-45 min and maintain the same temperature setpoint afterwards. However, particular testers are not able to reach and maintain the neutral state.
- 60 minutes of thermal stress test: the temperature setpoint is set to 10, 20, 30 or 40°C.

Groups		Thermoneutrality phase
Sex	**Male**	53 *(34)*
	Female	39 *(29)*
Age	**Young (< 30)**	37 *(23)*

	Adult (30 – 50)	28 *(21)*	
	Older (> 50)	27 *(19)*	
BMI	**Thin (< 20)**	4 *(3)*	
	Normal (20 – 25)	56 *(38)*	
	Stout (> 25)	32 *(22)*	
Groups		**10 °C test phase**	**20 °C test phase**
Sex	**Male**	17 *(17)*	8 *(8)*
	Female	14 *(13)*	6 *(5)*
Age	**Young (< 30)**	9 *(8)*	4 *(4)*
	Adult (30 – 50)	12 *(12)*	5 *(5)*
	Older (> 50)	10 *(10)*	5 *(4)*
BMI	**Thin (< 20)**	2 *(1)*	1 *(1)*
	Normal (20 – 25)	20 *(20)*	9 *(8)*
	Stout (> 25)	9 *(9)*	4 *(4)*
Groups		**30 °C test phase**	**40 °C test phase**
Sex	**Male**	8 *(8)*	8 *(8)*
	Female	4 *(4)*	10 *(10)*
Age	**Young (< 30)**	3 *(3)*	5 *(5)*
	Adult (30 – 50)	4 *(4)*	7 *(7)*
	Older (> 50)	5 *(5)*	6 *(6)*
BMI	**Thin (< 20)**	1 *(1)*	0 *(0)*
	Normal (20 – 25)	6 *(6)*	12 *(12)*
	Stout (> 25)	5 *(5)*	6 *(6)*

Table 1: Number of tests, distributed by scenarios and by groups; in brackets, number of individuals who partook in matching tests

In total, 63 testers realized 92 tests (the same tester is allowed to do different stress test). Testers are represented on Fig. 1, with their sex, age and BMI. All tests are gathered in Table 1, where three discriminations are presented : based on sex, age, and BMI. For the following analyses, the group BMI < 20 will not be included in data visualizations and conclusions, as its population and results are not large enough to be relevant.

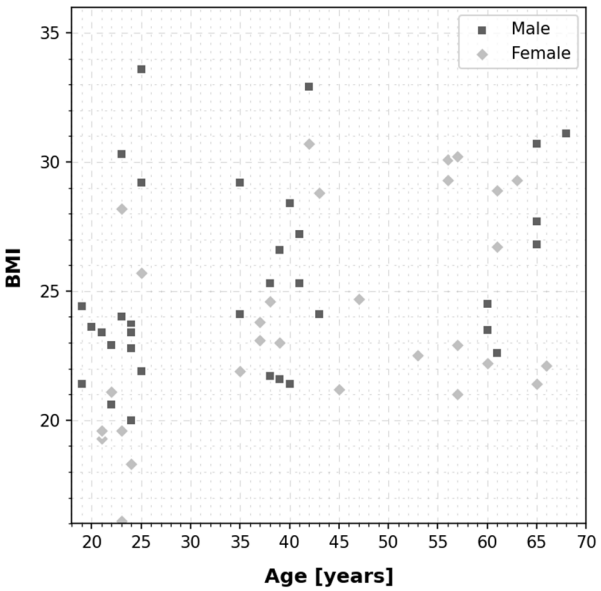

Fig. 1 Testers matrix based on sex, age and BMI

III. Data analysis and discussion

Different types of analysis are presented. First, temporal analyses are shown, where mean skin temperatures based on Hardy and Dubois' seven-point method [19] were calculated for all testers, then gathered in means and dispersals around it. Second, probability density functions are calculated to seek the optimal thermal comfort ambient temperature for each population group. Clustering algorithms are then used to identify distinct populations based on thermo-physiological responses and finally odds ratio is used to compare population trend according to discrimination parameters.

Only thermoneutrality and extreme conditions (10°C and 40°C) are shown in this paper, as phenomena were particularly visible during those phases while conclusions were also valid for other phases.

A. Mean skin temperature and its deviation

For thermoneutrality phase, all mean skin temperatures discriminated according gender is presented in Fig. 2. One can observe that a clear distinction between male and female mean skin temperatures is not seen at thermo-neutrality. The same phenomenon is observed when the discrimination is carried out with the BMI or age parameters. The statistical description of the last fifteen minutes, considered as the most stable part of this phase, is shown in Fig. 3 with boxplots.

One can observe that a clear distinct thermo-physiological response is not seen on the mean skin temperature. Likewise, those data are represented on Fig. 4 and Fig. 5 for 10°C and on Fig. 6 and Fig. 7 for 40°C scenario. One can once again observe that physiological discrimination over age or BMI is not clearly discernible on the thermo-physiological response when looking at the mean skin temperature.

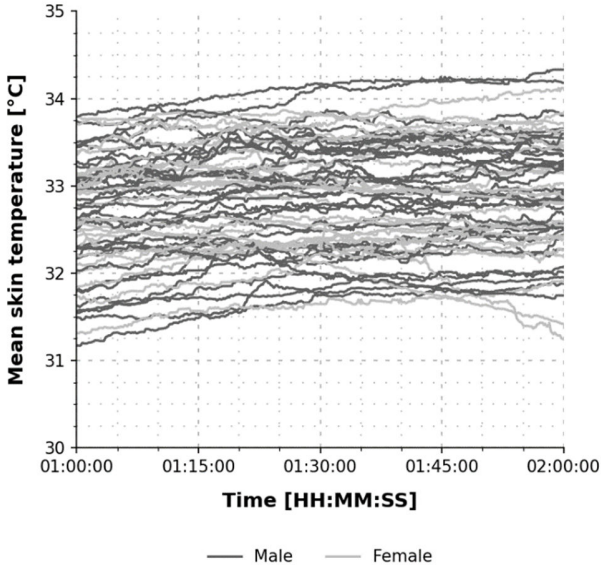

Fig. 2 Mean skin temperature for man and woman during the last 60 mins of the thermoneutrality phase

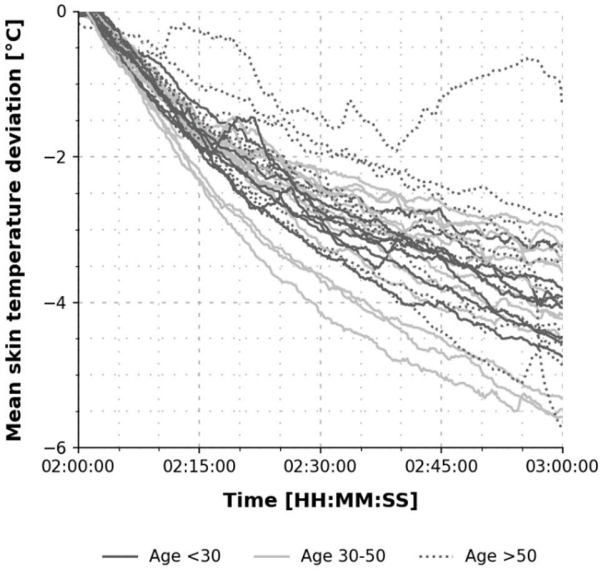

Fig. 4 Mean skin temperature deviation (tskin – tskin at thermoneutrality) for young, middle age and old age groups, during the cold phase (10°C)

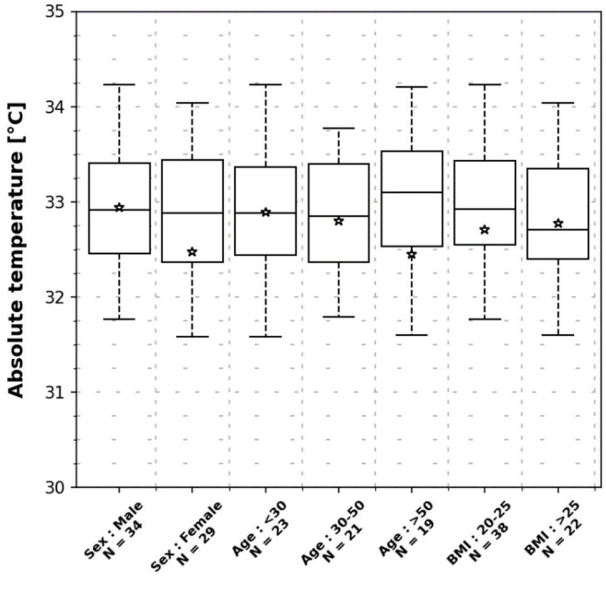

Fig. 3 Statistical description of tester groups (mean values are represented with a star) during the last 15 min of the thermo-neutrality phase

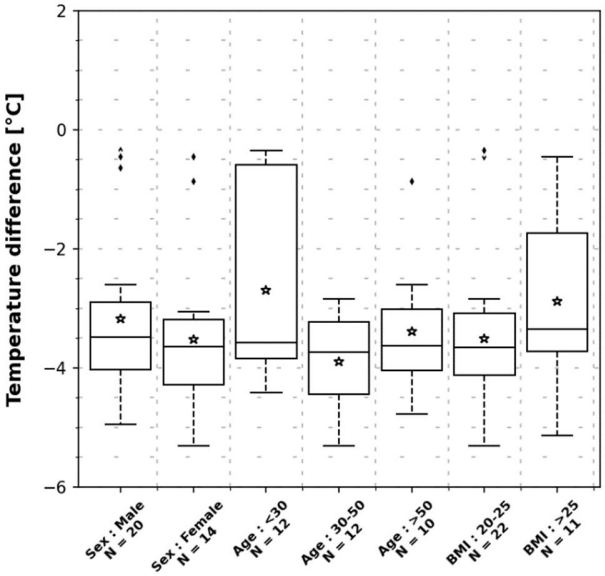

Fig. 5 Statistical description of tester groups (mean values are represented with a star) during the last 15 min of the cold phase (10°C). Temperature difference represents the difference between the absolute temperature and the mean skin temperature at thermoneutrality

One of the most striking phenomenon that can be observed in these results is how intertwined our populations are. It is particularly marked in boxplots, where data distribution is very alike from one population to another. They all seem to pack around the same value, and very few specific features stand out, if none at all. In other words, it means that, for unknown testers for which we only have their mean skin temperatures in a stabilized thermal environment, we are unable to associate their responses to a particular population, and thus, we cannot determine what are their physiological characteristics.

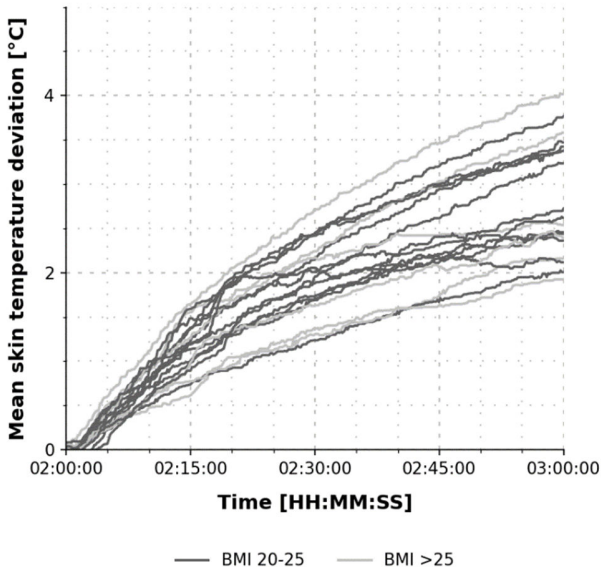

Fig. 6 Mean skin temperature deviation (tskin – tskin at thermoneutrality) for normal and high BMI groups, during the hot phase (40°C)

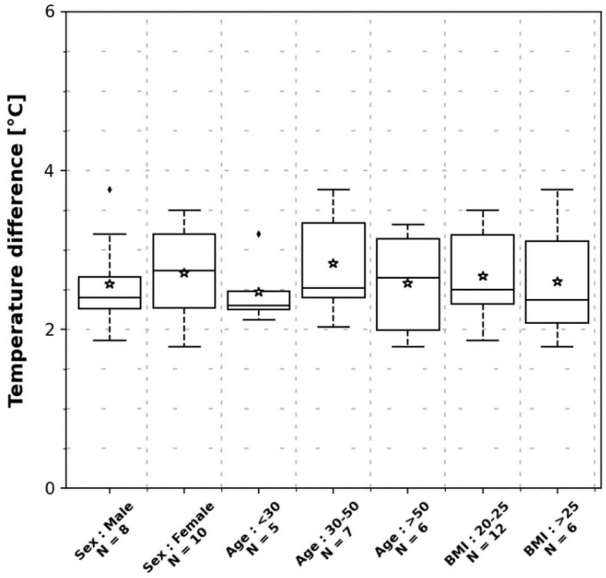

Fig. 7 Statistical description of tester groups (mean values are represented with a star) during the last 15 min of the hot phase (40°C). Temperature difference represents the difference between the absolute temperature and the mean skin temperature at thermoneutrality

Even after thermal transition to cooler or warmer thermal environments, temperature deviations from thermoneutrality seem to be identical between individuals, with a decrease of 3 to 4 °C in a 10°C environment, and an increase of 2 to 3 °C in a 40°C environment.

Cold conditions seem to bear the most visible differences between populations, and yet, they are too tenuous to properly discriminate testers between each other.

B. Probability density function (pdf)

M. Schweiker et al. [12] developed a new concept called "Probability Density Function of Thermo-Neutral Zone", shortened to pdfTNZ, that echoes Rupp et al. mentioned works [15] about predicting percentage of people dissatisfied at different ambient temperatures. Here, the idea is to determine for which ambient temperature people tend to be mostly satisfied.

Probability density function of people voting for neutral sensation at given ambient temperatures drown for different populations can be found in Fig. 8, with, as usual, a sex/age/BMI classification. It can be observed, once again, that no clear distinctions can be made on the thermal preferences for the chosen classification parameters.

C. Clustering populations with K-means algorithm

To go beyond, K-means algorithm is applied to testers' mean skin temperatures in order to determine whether a coherent and consistent clusters can be found. Clusters are determined by mean values found during the last 15 minutes of each phase (thermo-neutrality, cold or hot phase). For the thermo-neutrality phase, results are illustrated in Fig. 9 and Fig. 10, with time-related mean skin temperatures and visual representation of clusters with tester characteristics, and cluster characteristics are given in.

It is observed that clusters found by the algorithm and based on thermo-physiological responses, do not match at all with the clusters we expected using physiological parameters. Moreover, cluster populations are very close to each other, in terms of sex, age or BMI, and parameters standard deviations are extremely large. A conclusion that is also noticed for other phases. This highlights even more that mixing phenomenon we observed in analysis presented above.

Furthermore, clusters seem to have no coherence between each other. Sex, age or BMI arrangement do not match to any clear pattern, and seem to be of little importance in cluster creation. For instance, when looking at the population characteristics, we notice that cluster 3 has the higher skin temperature and corresponds to the lower BMI (22.55) whereas cluster 4 has the lower skin temperature with a higher BMI (26.74). However, this rule is invalidated by cluster 1 and 2 that have lower skin temperatures and BMI than cluster 0.

Besides, clusters are inconsistent from one phase to another, with testers switching from one cluster to another depending on studied phase. In order to underline this phenomenon, Fig. 11 shows clusters found during thermoneutrality and applied to 10°C scenario mean skin temperatures. If clusters were stable, mean skin temperatures should be organized similarly to the thermo-neutrality phase. But as highlighted here, responses are mixed, and should be attributed to new clusters.

These observations reinforce the idea that the resultant thermo-physiological responses have little dependency with physiological parameters considered in this study i.e. gender, age and BMI, as human body seems to adapt extremely well to its environment, thanks to internal physiological mechanisms that seem to find new setpoints (blood perfusion for instance) helping to the rebalance of the heat imbalance induced by body

composition differences (fat proportion for instance).

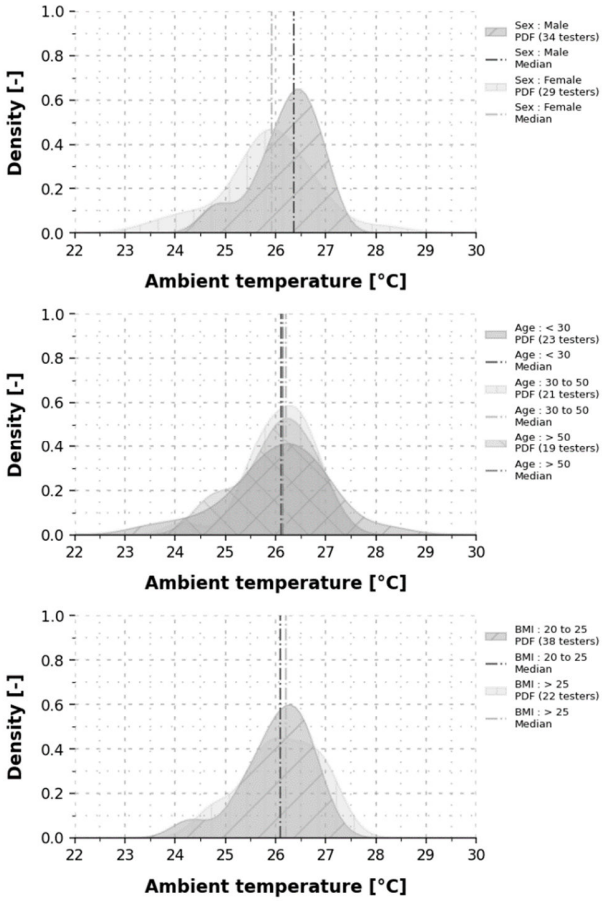

Fig. 8 PDF of thermoneutrality temperatures classified by sex, age and BMI

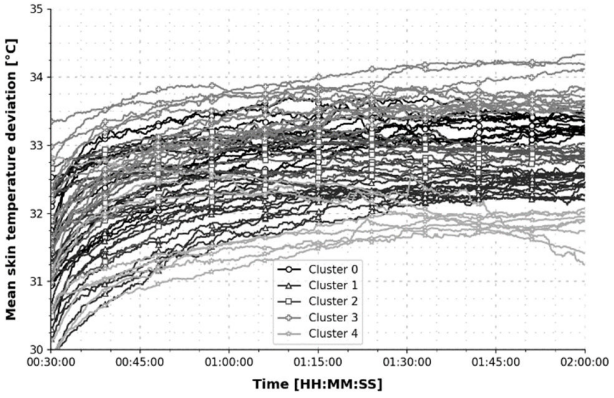

Fig. 9 K-Means clustering applied on mean skin temperatures at thermoneutrality (N. clusters : 5)

D. Odds ratio

For this part, populations will be more simply defined than previously, and a single criterion is chosen for each. That way, people are either male or female, Younger or Older than 50, and have a BMI above or below 25.

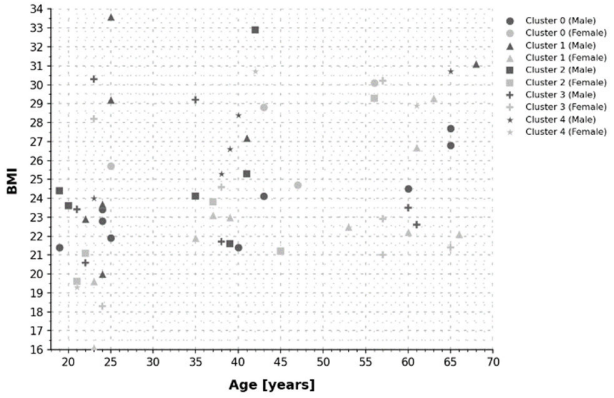

Fig. 10 Visual representation of clusters based on sex, age, BMI

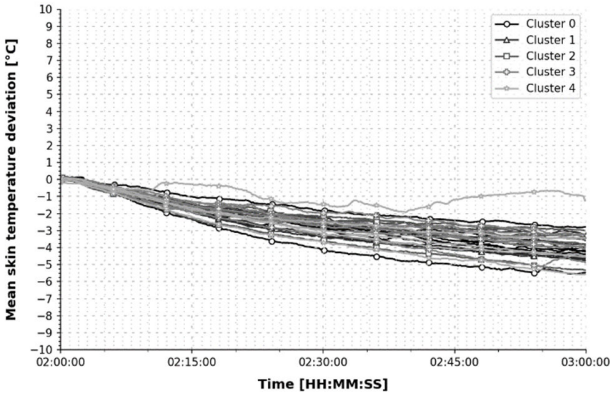

Fig. 11 Thermoneutrality K-means clusters applied to 10°C scenario mean skin temperatures

Cluster ID	Sex	Age (years)	BMI
Cluster 0	12 M 8 F	Mean : 39.70 Std. : 16.34	Mean : 24.95 Std. : 3.03
Cluster 1	7 M 10 F	Mean : 40.53 Std. : 17.49	Mean : 24.36 Std. : 4.52
Cluster 2	7 M 5 F	Mean : 36.83 Std. : 14.62	Mean : 24.48 Std. : 3.76
Cluster 3	3 M 3 F	Mean : 43.00 Std. : 17.37	Mean : 22.55 Std. : 4.11
Cluster 4	5 M 3 F	Mean : 41.12 Std. : 15.65	Mean : 26.74 Std. : 3.85

Table 2 Thermoneutrality clusters characteristics, based on sex, age and BMI

M. Schweiker et al. [12] and R. F. Rupp et al. [15] present studies about thermal appraisal of an environment, where varying parameters are sex, age and BMI. However, it should be noticed that they do have a lot more data than what has been used in this investigation, and all studies were driven in buildings or building-like configurations, which differ from car-like environment that we consider.

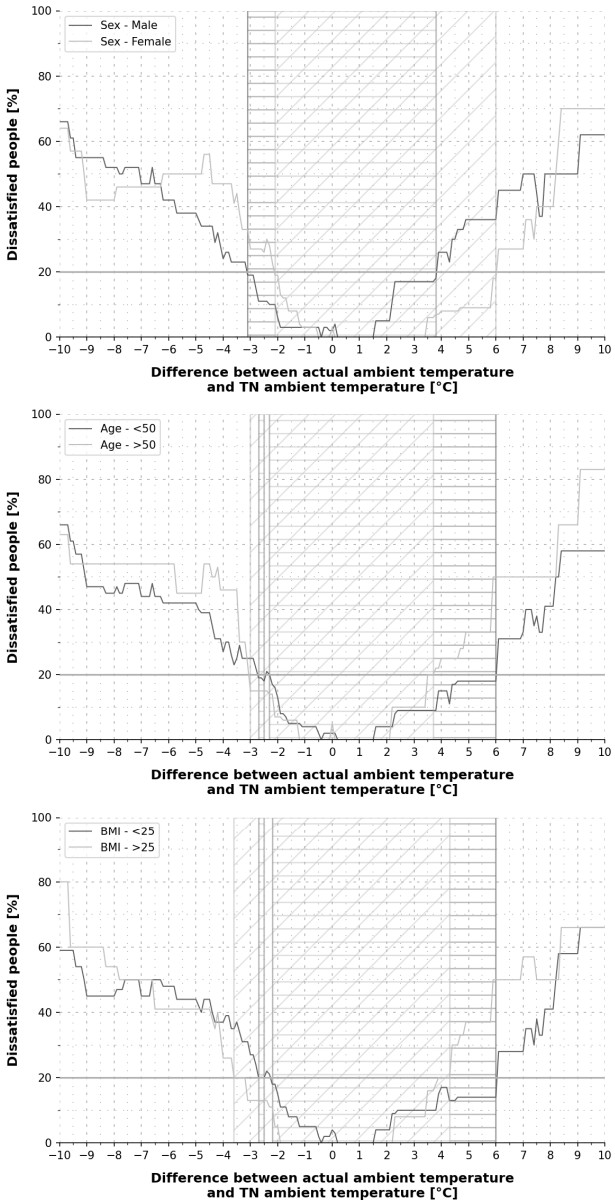

Fig. 12 Proportion of dissatisfied people calculated for Male and Female populations, Younger and Older than 50 populations and BMI Above or Below 25 populations

As mentioned, R. F. Rupp et al. results are based on the idea of finding percentage of dissatisfied people depending on ambient temperatures. They show relationship between deviation from thermoneutrality temperature and proportion of satisfied people, as well as population tendencies compared to another. For the latter, they used odds ratio, to determine whether a population was more sensitive to discomfort depending on thermal environment. Besides, a new predictive model is developed, whose parameters are current difference with thermoneutrality ambient temperature, sex, age, BMI, air conditioning solicitation and building ventilation type.

Following this idea, results for percentage of dissatisfied people are shown in Fig. 12. PPD is determined using the definition given by the ASHRAE Handbook [18], to which people comfort votes are applied. People who voted differently than -1, 0 or 1 for their global thermal sensation and who voted a negative score for global thermal comfort were considered truly dissatisfied.

It can be observed a large overlap zone between male and female, young and old as well as for normal and high BMI population groups. However, it seems that women tends to be more dissatisfied by cooler environments than men and men more dissatisfied by warmer environments than women (horizontal dashed zone for men and diagonal dashed zone for women). Likewise, youngers seem to tolerate a wider range of warm temperatures than older people and low BMI population seems to better tolerate warmer temperatures than high BMI one which better puts up with cooler environments than low BMI population.

Odd ratios are also calculated for each discrimination parameter, as shown in Figure 13. For each tenth of deviation from thermoneutrality ambient temperature, the tendency of a population compared to another to undergo a specific phenomenon, i.e. either cold discomfort or hot discomfort, is determined and applied for classifications based on sex, age and BMI. Total number individuals for each population is also represented, again for each tenth of deviation from thermoneutrality ambient temperature.

Overall, and qualitatively, results match literature conclusions, by showing that indeed, some differences do exist between populations. Specifically, when looking at dissatisfaction zones and conditions, we do find similarities between present results and Rupp et al. [15] findings, notably, with asymmetries between studied populations.

More specifically, male and female populations have same tendencies as observed with the PPD approach and, to some extent, echoes Rupp et al. results [15]. Male population tends to have a cooler comfort zone than female population, or rather, male population tends to be more susceptible to discomfort in hotter situations than female population, and conversely.

This is particularly remarkable in proportion of dissatisfied people, where male population has a satisfaction zone as defined by Rupp et al., i.e. a maximum of 20% of dissatisfied people, in cooler temperatures, compared to female population. Odds ratio gives similar conclusions, where they tend to be superior to 1 in cooler temperatures, indicating female population is more likely to feel discomfort in such conditions, and inferior to 1 in hotter temperatures, indicating that male population is more likely to feel discomfort for those cases.

Similarly, regarding differences in body composition, people with a higher BMI tend to be more easily dissatisfied in warmer conditions than people with lower BMI. Indeed, as shown in Fig. 12 and Fig. 13, satisfaction zone of population with BMI < 25 is located in warmer temperatures than its counterpart, and is particularly visible in the odds ratio approach. Indeed, for cooler conditions, odds ratios are inferior to 1, indicating that people with a BMI below 25 are more inclined to discomfort than people with BMI above 25, and for warmer conditions, this trend is reversed.

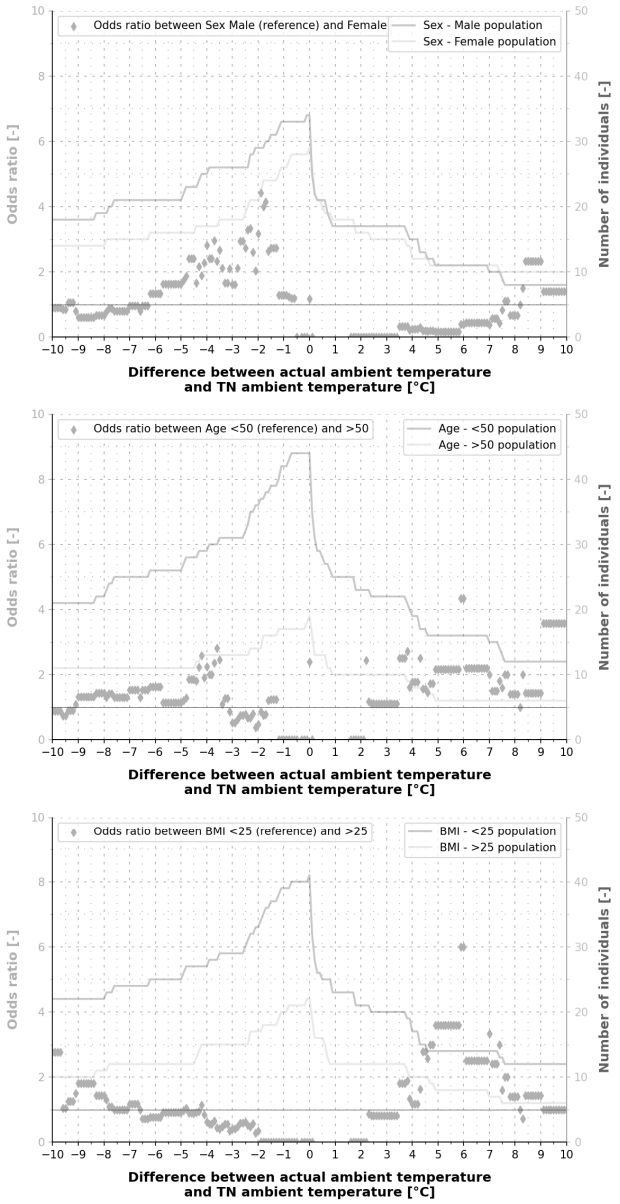

Fig. 13 Odds ratio calculated between Male (reference) and Female, Younger than 50 (reference) and Older than 50, BMI Below 25 (reference) and BMI Above 25 populations

Finally, age-discriminated populations have a different behaviour in the present study, with older people being more easily inconvenienced by thermal conditions deviations, be it cool or warm.

Odds ratio is also a point of contention for extreme conditions. While we do follow Rupp et al. conclusions for most cases, typically from a -7 °C/+7 °C offset from thermoneutrality, we do observe a trend reversal for more extreme offsets. For example, between -10 °C and -7 °C, female population tends to be less often dissatisfied than male population, while the opposite trend is observed between -7°C and 0°C. This switch can also be observed between male and female populations in extreme hot conditions, and between BMI < 25 and BMI > 25 populations in extreme cold conditions. More investigations are required to confirm this observation, as in the present investigation, the number of individuals was low in those extreme conditions to be conclusive.

IV. Conclusion

Despite many attempts to find clear patterns between populations based on objective criteria such as sex, age and BMI, it seems evident that thermo-physiological responses are not as simple as just a combination of easily accessible parameters. More than that, thermal appraisal does not seem to be only a question of physiological characteristics and external thermal parameters.

It is true indeed that tendencies can be found for specific populations. But they mainly point out a general consensus about a minimum amount of dissatisfied people, rather than describing situations where most people are truly comfortable. They aim for minimal loss rather than true benefit for all, which may be a reachable goal for buildings and large shared places, but not really interesting in small places like passenger compartments with few individuals.

In the end, works presented in this study show distinctly that customization approach in thermal comfort may not be the best way to properly define populations responses in small, enclosed thermal environments. They actually even challenged the concept of populations, and brought forth a new one : individualization.

Indeed, population responses are so mixed that it is hard to distinguish one person from another. It suggests that the population of human beings react more or less identically in strict similar conditions. It also suggests that if customized models based on passive parameters (thickness of fat, muscle layers, ration between the skin surface and body volume, …) predict differentiated thermo-physiological responses for populations classified according to BMI, age or gender, it is not observed on measured mean data. It should then exist internal auto-adaptation mechanisms (such as modified blood perfusion, or vasodilatation and vasoconstriction setpoints) that counteracts the heat imbalances induced by passive parameters. Works that consist in developing customized thermal mannikins based on passive physiological parameters will probably not help to reduce the large dispersion observed in thermal appraisal votes as classification carried out on these physiological parameters do not induce distinct mean thermo-physiological response characterizing each population group.

However, the large dispersion observed around the mean value suggests to consider an individual and characterize all the parameters (environmental, physiological, contextual, psychological, …) that are involved on the final subjective thermal comfort appraisal. This is the promise of the individualization approach: thanks to a complete set of data defined beforehand or monitored in real time (heart rate, blood pressure, …), a new individualized model could be generated for each individual, based on a general algorithm, and could maximize its precision and accuracy, much more than what a

customized population model could do.

REFERENCES

[1] J. Arthur Harris, Francis G. Benedict, "A biometric study of human basal metabolism," *Proceedings of the National Academy of Sciences of the United States of America*, vol. 4, no. 12, pp. 370-373, Dec. 1918.

[2] A. M. Roza, H. M. Shizgal, "The Harris Benedict equation reevaluated: resting energy requirements and the body cell mass," *The American Journal of Clinical Nutrition*, vol. 40, no. 1, 1984.

[3] W. N. Schofield, "Predicting basal metabolic rate, new standards and review of previous work," *Human Nutrition Clinical Nutrition*, vol. 39, 1985.

[4] D. Mark Muffin, T. Sachiko St Jeor, A. Lisa Hill, J. Barbara Scott, A. Sandra Daugherty, O. Young Koh, "A new predictive equation for resting energy expenditure in healthy individuals," *The American Journal of Clinical Nutrition*, vol. 51 no. 2, 1990.

[5] C. J. K. Henry, "Basal metabolic rate studies in humans: measurement and development of new equations," *Public Health Nutrition*, vol. 8, 2005.

[6] A. E. Black, W. A. Coward, T. J. Cole, A. M. Prentice, "Human energy expenditure in affluent societies: an analysis of 574 doubly-labelled water measurements," *European journal of Clinical nutrition*, vol. 50, 1996.

[7] D. Fiala, *Dynamic simulation of human heat transfer and thermal comfor*t, Institute of Energy and Sustainable Development, Leicester, 1998.

[8] A. Psikuta, D. Fiala, G. Laschewski, G. Jendritzky, M. Richads, K. Blazejczyk, I. Mekjavic, H. Rintamäki, R. de Dear, G. Havenith, "Validation of the Fiala multi-node thermophysiological model for UTCI application," *Int. J. Biometeoril*., vol. 56, pp. 443-460, 2012.

[9] Hui Zhang*, Human Thermal Sensation and Comfort in Transient and Non-Uniform Thermal Environments*, University of California, Berkeley, 2003.

[10] Xin Zhou, Zhiwei Lian, Li Lan, "An individualized human thermoregulation model for Chinese adults," *Building and Environment*, vol. 70, pp. 257-265, 2013.

[11] Mohamad El Kadri, *Modèle thermo-neurophysiologique du corps humain pour l'étude du confort thermique en conditions climatiques hétérogènes et instationnaires*, La Rochelle: LaSIE – Laboratoire des Sciences de l'Ingénieur pour l'Environnement, 2020.

[12] Marcel Schweiker, Gesche M. Huebner, Boris R. M. Kingma, Rick Kramer, Hannah Pallubinsky, "Drivers of diversity in human thermal perception- A Review for holistic comfort models," *Temperature,* vol. 5, no. 4, 2018.

[13] Boris R. M. Kingma, Arjan J. H. Frijns, Lisje Schellen, Wouter D. van Marken Lichtenbelt, "Beyond the classic thermoneutral zone – Including thermal comfort," *Temperature,* vol. 1, 2014.

[14] Ricardo Forgiarini Rupp, Enedir Ghisi, "Predicting thermal comfort in office buildings in a Brazilian temperature and humid climate," *Energy and Buildings,* vol. 144, 2017.

[15] Ricardo Forgiarini Rupp, Jungsoo Kimb, Richard de Dearb, Enedir Ghisia, "Associations of occupant demographics, thermal history and obesity variables with their thermal comfort in air-conditioned and mixed-mode ventilation office buildings,"*Building and Environment,* vol. 135, 2018.

[16] Ilango Thiagalingam, Sidali Mokdad, Roch El Khoury, Thomas Tanguy, "Confrontation of thermal sensation and comfort models to votes in a transient thermal exposure, *12th International Manikin and Modelling Meeting (12i3m),* St Gallen, Switzerland, 2018.

[17] Rachelle Abou Jaoude, Ilango Thiagalingam, Roch El Khoury, Gabriel Crehan, "Berkely thermal comfort models: Comparison to people votes ans indications for user-centric HVAC strategies in car cabins,"*Building and Environment,* vol. 180, 2020.

[18] ASHRAE Handbook, Atlanta: ASHRAE, 2012, chapter. 9- Thermal Comfort.

[19] James D. Hardy, Eugene F. Du Bois, G. F. Soderstrom, "The Technic of Measuring Radiation and Convection: One Figure," *The Journal of Nutrition,* vol. 15, 1938.

Navigating the Future: Evaluating the Market Potential and Drivers for High-Definition Mapping in the Autonomous Vehicle Era

Loha Hashimy, Isabella Castillo

***Abstract*—** In today's rapidly evolving technological landscape, the importance of precise navigation and mapping systems cannot be understated. As various sectors undergo transformative changes, the market potential for Advanced Mapping and Management Systems (AMMS) emerges as a critical focus area. The Galileo/GNSS-Based Autonomous Mobile Mapping System (GAMMS) project, specifically targeted toward high-definition mapping (HDM), endeavours to provide insights into this market within the broader context of the geomatics and navigation fields. With the growing integration of Autonomous Vehicles (AVs) into our transportation systems, the relevance and demand for sophisticated mapping solutions like HDM have become increasingly pertinent. The research employed a meticulous, lean, stepwise, and interconnected methodology to ensure a comprehensive assessment. Beginning with the identification of pivotal project results, the study progressed into a systematic market screening. This was complemented by an exhaustive desk research phase that delved into existing literature, data, and trends. To ensure the holistic validity of the findings, extensive consultations were conducted. Academia and industry experts provided invaluable insights through interviews, questionnaires, and surveys. This multi-faceted approach facilitated a layered analysis, juxtaposing secondary data with primary inputs, ensuring that the conclusions were both accurate and actionable. Our investigation unearthed a plethora of drivers steering the HD maps landscape. These ranged from technological leaps, nuanced market demands, and influential economic factors to overarching socio-political shifts. The meteoric rise of Autonomous Vehicles (AVs) and the shift towards app-based transportation solutions, such as Uber, stood out as significant market pull factors. A nuanced PESTEL analysis further enriched our understanding, shedding light on political, economic, social, technological, environmental, and legal facets influencing the HD maps market trajectory. Simultaneously, potential roadblocks were identified. Notable among these were barriers related to high initial costs, concerns around data quality, and the challenges posed by a fragmented and evolving regulatory landscape. The GAMMS project serves as a beacon, illuminating the vast opportunities that lie ahead for the HD mapping sector. It underscores the indispensable role of HDM in enhancing navigation, ensuring safety, and providing pinpoint, accurate location services. As our world becomes more interconnected and reliant on technology, HD maps emerge as a linchpin, bridging gaps and enabling seamless experiences. The research findings accentuate the imperative for stakeholders across industries to recognize and harness the potential of HD mapping, especially as we stand on the cusp of a transportation revolution heralded by Autonomous Vehicles and advanced geomatic solutions.

***Keywords*—** high-definition mapping (HDM), autonomous vehicles, PESTEL analysis, market drivers.

Loha Hashimy is with the Autonomous University of Barcelona, Spain (e-mail: loha.hashimy@gmail.com).

Analysis of High-Velocity Impacts on Concrete

Conceição, J. F. M.[1]; Rebelo, H.[2]; Corneliu, C.[3]; Pereira, L.[4]

***Abstract*—**This research analyses the response of two distinct types of concrete blocks, each possessing an approximate unconfined compressive strength of 30MPa, when exposed to high-velocity impacts produced by an Explosively Formed Penetrator (EFP) traveling at an initial velocity of 1200 m/s. Given the scarcity of studies exploring high-velocity impacts on concrete, the primary aim of this research is to scrutinize how concrete behaves under high-speed impacts, ultimately contributing valuable insights to the development of protective structures. To achieve this objective, a comprehensive numerical analysis was carried out in LS-DYNA to delve into the fracture mechanisms inherent in concrete under such extreme conditions. Subsequently, the obtained numerical outcomes were compared and validated through eight experimental field tests. The methodology employed involved a robust combination of numerical simulations and real-world experiments, ensuring a comprehensive understanding of concrete behavior in scenarios involving rapid, high-energy impacts.

***Keywords*:** High-velocity; Impact, Numerical analysis; Experimental tests; Concrete.

1. Introduction

With the rise of terrorist attacks, war and advanced weaponry, the need to protect critical structures and human lives is crucial. Concrete, widely used for its structural capacity and cost-effectiveness, plays a significant role in construction. Although there are several studies on the behavior of concrete against impacts and explosions, it is still an open area of knowledge due to the difficulty of characterizing it facing these extreme actions, namely high-velocity impacts [1, 2]. High-velocity impact (HVI) involves significant forces and energy transfer, leading to highly localized damage to concrete [3], and can be produced by missile or fragments impacts. This study used an Explosively Formed Penetrator (EFP) to create a HVI impacting on concrete blocks.

2. Experimental tests

A two-dimensional (2D) axisymmetric numerical model of an EFP (Fig. 1) was developed to capture its fundamental characteristics and achieve the desired velocity. EFPs were built using Computer Numerical Control (CNC) machining techniques (liner), an original Prusa i3 MK3A (casing) (**Error! Reference source not found.**) and a plastic explosive.

Fig. 1 Schematic of 2D numerical model

Fig. 2 EFP samples

[1,2] Military Academy Research Center (CINAMIL) and NOVA School of Science and Technology, Lisbon, Portugal (phone: +351 914485180; e-mail: joaofilipemelro@gmail.com).

[3]Civil Engineering Research and Innovation for Sustainability (CERIS NOVA and NOVA School of Science and Technology, Lisbon, Portugal.

[4]Air Force Research Center (CIAFA), Air Force Academy, Lisbon, Portugal.

After that, an experimental campaign was conducted using two types of concrete blocks, one with basalt aggregate and the other with limestone aggregate (Fig. 3).

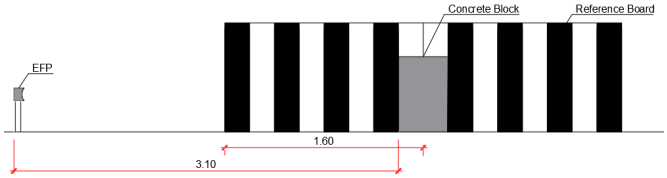

Fig. 3 - Side view of the set-up

Subsequently, a three-dimensional (3D) model was created to validate the experimental campaign and obtain deeper insights into the behavior of concrete after impact. This model enabled a more precise assessment of the EFP's performance and its interaction with the concrete block. Fig. 4 and Fig. 5 illustrate aspects from the experimental tests and the 3D numerical simulation, respectively.

Fig. 4 Concrete block after impact

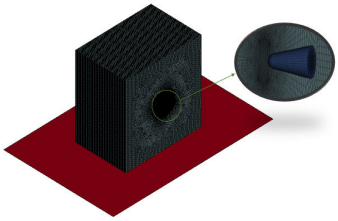

Fig. 5 Overview of the 3D numeric model

Finally, penetration depth, fragmentation, crater dimension and overall impact dynamics were analyzed and compared with the experimental results. Additionally, the experimental projectile´s velocity captured by high-velocity cameras was compared with a numerical model and with analytical formulas according to the literature review.

3. Conclusions

Through this study, it was possible to observe that harder aggregates demonstrated improved energy dissipation capabilities, as evidenced by reduced penetration. Furthermore, the existence of various fracture mechanisms were confirmed, as described in the literature. The study aims of contributing to the future development of protective solutions. Notably, the importance of numerical modelling was highlighted, as the results closely approximated real-world values.

References

[1]A. N. Dancygier, "High-performance concrete engineered for protective barriers," *Philos. Trans. R. Soc. A Math. Phys. Eng. Sci.*, vol. 375, no. 2085, 2017, doi: 10.1098/rsta.2016.0180.

[2]B. Erzar, C. Pontiroli, and E. Buzaud, "Ultra-high performance fibre-reinforced concrete under impact: Experimental analysis of the mechanical response in extreme conditions and modelling using the Pontiroli, Rouquand and Mazars model," Philos. Trans. R. Soc. A Math. Phys. Eng. Sci., vol. 375, no. 2085, 2017, doi: 10.1098/rsta.2016.0173. [3] Q. M. Li, S. R. Reid, H. M. Wen, and A. R. Telford, "Local impact effects of hard missiles on concrete targets," Int. J. Impact Eng., vol. 32, no. 1–4, pp. 224–284, 2005, doi: 10.1016/j.ijimpeng.2005.04.005.

Q-BI – Purple Yams Waste (*Ipomoea Batatas)* as Organic Corrosion Inhibitors for Carbon Steel in Oil

Gede Putra, Ambar Dwi Sustomo, Hasbi Fahada, Arif Amrullah

Abstract: The majority of research on the effectiveness of organic molecules and (nano) materials at inhibiting corrosion focuses on the discovery of compounds rather than the long-term viability of the material. As a result, the product was discovered but has not been widely used to replace chemical products that harm the environment, notably in the oil and gas industry, where sustainability and environmental issues are two primary considerations in every decision. Chemical products that could inevitably end up becoming a complete waste in the construction of oil and gas facilities (fuel tanks, pipelines, and other equipment) require special consideration. To prevent corrosion of the carbon steel material during construction, the hydro test process with fresh water or seawater requires a particular chemical compound treatment. However, the subsequent effects of the disposal treatment on chemical corrosion inhibitors before it released to the sea or ground caused a significant environmental problem. The efficiency of organic materials in preventing corrosion was evaluated using a thermodynamic corrosion test on high-quality ASTM A 283 Grade C plates by projecting the observed pH with a potential difference (volts) into the Pourbaix Fe diagram. The comparison below demonstrates the effectiveness of using Q-BI as an organic corrosion inhibitor for carbon steel in place of chemical inhibitors. We discovered that the corrosion rate of the plate with Q-BI was better than the other plate with chemical inhibitor, accounting for 3,35 mm/y compared to 6,21 mm/y from the immersion test of the identical sample of the plate. Anthocyanin concentrations of up to 700–800 mg/L were found in the extract of Ipomoea batatas waste in 600 g/L of tap water. The amount of chemical waste produced by hydro tests utilizing Q-Bi was less than the EPA's criterion, accounting for only 0.005 mg/L of the MCL of 0.1 mg/l. Finally, statistical research demonstrates that applying Q-BI to the oil and gas industry will enable us to save at least $10,000 on each hydro test, translating into cost savings of over $1 billion annually. Q-BI product, specifically when used in the oil and gas industry, is the safest Hydrotest solution, which leads to various implications that may have an impact on the environment. We believe the industry performs numerous hydro tests, treats water and finds how to stop corrosion in carbon steel. This alternative is our suggestion for the best course of action.

Keywords: nondestructive test, hydrostatic test, organic inhibitor corrosion, ipomoea batatas

All the author is part of Pertamina Oil and Gas Corporation. Gede Putra is with the Columbia University SPS, Construction Administration (phone: 646-515-8641; e-mail: gw2440@columbia.edu).

I. INTRODUCTION

Key Performance Indicators (KPIs) are instrumental in assessing the outcomes of projects and initiatives. Within the scope of Pertamina Energy Company, two KPIs, "investment realization (finance)" and "investment realization (physical)," bear significant weight and impact on overall performance. Despite their importance, reaching the desired realization targets can be a complex endeavor, hampered by various obstacles. This journal entry delves into these pivotal KPIs and delves into the challenges encountered through the lens of a Pareto analysis.

Pareto analysis, a powerful tool for prioritization, is used to identify the most substantial hindrances to achieving the KPIs' objectives. By isolating and addressing these critical obstacles, Pertamina Energy Company can enhance its ability to meet financial and physical investment realization targets. This strategic approach ensures that the company's resources are efficiently allocated and its projects and initiatives are set on a path to success.

The "Buildup of Storage Tank" project presents a substantial financial challenge, with an impact of IDR 342,143,363,000. This issue warrants a comprehensive assessment, especially during the construction phase. Within this phase, the Inspection & Testing tasks have assumed critical importance as they dictate the project's timeline. Among these tasks, the hydrotest emerges as the most financially demanding component, with a projected cost of IDR 1,593,504,478.

Addressing challenges linked to the hydrotest process is imperative to tackle the overarching financial concerns associated with the "Buildup of Storage Tank" project. By focusing on optimizing the hydrotest phase, the project can potentially achieve significant cost reductions, contributing to improved overall financial efficiency and the successful realization of this vital project.

When applying a cause and effect analysis to the issue at hand, we have identified three potential root causes: The High Cost of Freshwater (A), High Cost Overloads of Workers' Man-days for Water Tank Truck discharges (B), and High Cost of Certified Hydrostatic Test Personnel (C). To determine the most significant root cause, we have conducted a Benefit-Cost (B/C) comparison (as depicted in Figure 3).

Upon analysis, it is evident that point A, which relates to the high cost of freshwater, emerges as the primary root cause with

the highest B/C value. This finding suggests that addressing the issue of costly freshwater is likely to yield the most substantial benefits in relation to the incurred costs. Therefore, prioritizing solutions to mitigate the expense of freshwater is crucial in our efforts to optimize the "Buildup of Storage Tank" project.

II. ANALYSIS

In light of the freshwater cost issue, an effective alternative solution is to utilize abundant seawater while implementing a protective system to counter the threat of corrosion. The choice of alternative solutions is presented in Table 1. Among the available options, the "Hydrotest Using Seawater and Organic Inhibitor for Corrosion Protection" has been selected as the optimal choice. This preference is based on its notably lower expenses when compared to the other three alternatives. By adopting this method, we mitigate the freshwater cost concern and ensure adequate corrosion protection, aligning with our cost-saving objectives for the "Buildup of Storage Tank" project.

Table 1 . Choosing an Alternative Solution

Root Cause	Alternative Solutions	Cost	Time	Chosen Solution
The High Cost of Freshwater	Hydrotest Using Seawater and Cathodic Protection for Corrosion Protection	IDR 23.100/Liter	45 HK	Hydrotest Using Seawater and Organic Inhibitor for Corrosion Protection
	Hydrotest Using Seawater and Internal Coating for Corrosion Protection	IDR 26.800/Liter	40 HK	
	Hydrotest Using Seawater and Chemical Inhibitor for Corrosion Protection	IDR 17.000/Liter	35 HK	
	Hydrotest Using Seawater and Organic Inhibitor for Corrosion Protection	IDR 5.452/Liter	30 HK	

Before this research was undertaken, Pertamina had traditionally relied on synthetic corrosion inhibitors derived from chemicals for their hydrotest processes using seawater. However, a notable shift occurred with the introduction of organic corrosion inhibitors, specifically those based on purple yam waste. This innovation was first implemented in the Marketing Operation Region (MOR) V of Pertamina, as it was not available on the KOMET portal for similar innovations.

What makes this development particularly unique is the use of organic corrosion inhibitor Q-Bi, which leverages locally sourced raw materials. This approach not only fosters collaboration with micro-enterprises in the region but also promotes the sustainable use of purple yam waste. This waste material is both abundant in Indonesia and environmentally friendly, offering the added benefit of replicability, thus potentially setting a precedent for similar innovations in the future. This transition showcases a commitment to cost-effectiveness and ecological responsibility within the context of the "Buildup of Storage Tank" project.

A. Trial and Error

The trial-and-error system has been instrumental in determining the most efficient method for producing organic corrosion inhibitors from purple yam waste, as revealed by the results presented in Table 2. Among the various trials, Trial 3 has emerged as the most effective process for generating these inhibitors. This outcome emphasizes the pivotal role that Trial 3 plays in achieving the intended results and underscores its potential as a successful approach for producing these valuable inhibitors. The choice of Trial 3 as the most effective process marks a critical milestone in optimizing this innovative solution for the "Buildup of Storage Tank" project.

Table 2. Trial and Error

No	Trial & Error	Trial 1	Trial 2	Trial 3
1	Storage Method	Dry waste (slow dry)	Liquid waste (The problem of Q-Bi inhibitors is fast decaying)	Pollen form (successful, easy to store, last longer, anaerob)
2	Water mixture composition and purple yam waste extract	0,3 kg/liter (too much water and less effective)	0,9 kg/liter (not homogen, many residue)	0,6 kg/liter Large milling (effective)
3	Processing Method	Tumbuk manual (takes longer and exhausting)	Small milling (takes longer)	Large milling (effective)
4	Drying Temperature	ambient temperature (slow dry)	90 ^{0}C (broken anthocyanin content)	75-80 ^{0}C (effective)

No	Trial & Error	Trial 1	Trial 2	Trial 3
5	Corrosion Inhibitor Dosage	2% volume (less effective)	4% volume (less effective)	100 ppm (effective)

B. Result and Discussion

The data provided in Table 3 serves as a window into the outcomes achieved subsequent to the implementation of the chosen solution. This dataset pertains specifically to the "News on the Field of Hydrotest" and is centered around a storage tank with a substantial capacity of 1500 KL, situated at the Fuel Terminal in Atapupu. These insights are of immense value as they shed light on the real-world application of the hydro test process utilizing seawater coupled with the organic corrosion inhibitor derived from purple yam waste. This practical data is instrumental in grasping the tangible implications of this approach within the broader context of the "Buildup of Storage Tank" project.

Table 3. Before After Implementation Comparison

Root Cause		Rank	Existing			After the Implementation		
			B/C	%	% Cum	Sum	%	% Cum
A	High Cost of Freshwater	1	1,4041	37%	37%	0	0	0
B	High Cost Overloads of Workers' Man-days for tanker discharges	2	1,2285	33%	70%	0	0	0
C	High Cost of Certified Hydrostatic Test Personnel	3	1,1168	30%	100%	0	0	0
Total			3,7495	100%		0	0	

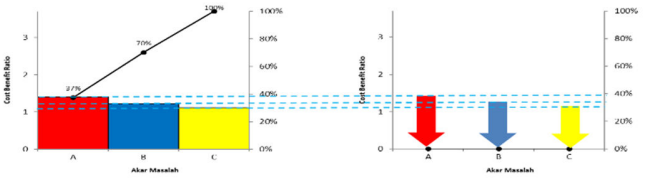

Fig. 1. Pareto for Root Cause Benefit Cost Ratio 2

The thermodynamic corrosion assessment of qualitative ASTM A 283 Grade C plates involved collecting data that established correlations between measured pH values and corresponding potential differences in volts. This data was then used to create visual representations through Pourbaix Fe (Iron) diagrams, enabling in-depth analysis. Figure 5 and Figure 6 provide clear and insightful illustrations of the thermodynamic corrosion behavior exhibited by the ASTM A 283 Grade C plates under examination.

These Pourbaix Fe diagrams hold immense importance in understanding the material's susceptibility to various corrosion mechanisms. They serve as invaluable tools for making informed decisions regarding strategies for corrosion prevention and control. By offering a visual overview of the material's behavior across diverse environmental conditions, these diagrams facilitate the development of effective corrosion mitigation techniques. Ultimately, they play a vital role in contributing to the success of projects involving ASTM A 283 Grade C plates.

Before Using Q-Bi

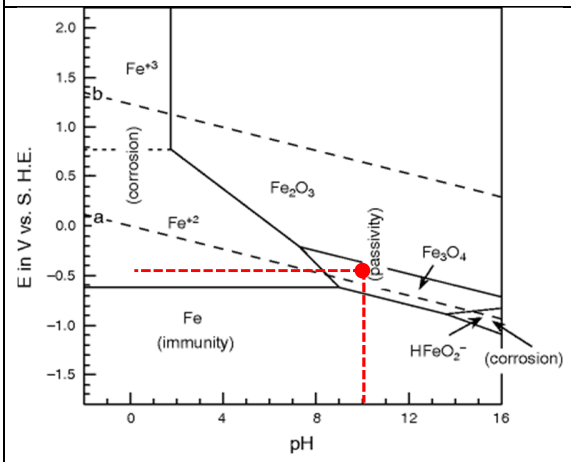

Fig. 2. Pourbaix Fe diagram Before Using Q-Bi

The intersection of pH 8 and the average voltage -0.45 is on the corrosion zone. These conditions describe the plate exposed to seawater in corroded conditions.

After Using Q-Bi

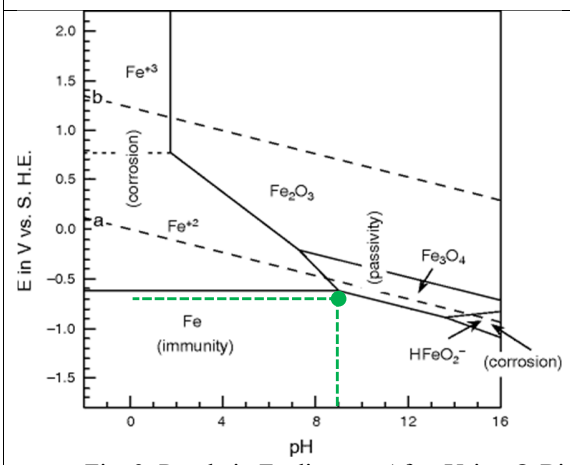

Fig. 3. Pourbaix Fe diagram After Using Q-Bi

The intersection of pH 6.9 and the average voltage of -0.62 is in the immunity zone. These conditions describe the plate exposed to seawater in immune / corrosion-resistant conditions.

The corrosion rate data for ASTM A283 Grade C [3][5][6][7], acquired through immersion testing, is comprehensively presented in Table 4. This data is complemented by a graphical representation found in Figure 7. An analysis of the results demonstrates that the application of Q-Bi, an organic corrosion inhibitor sourced from purple yam waste, has significantly outperformed the predefined target. In particular, the corrosion rate observed with the use of Q-Bi has reached 185.37%, surpassing the initial target of 100%.

These findings underscore the remarkable effectiveness of Q-Bi in mitigating corrosion, offering a considerable margin of safety beyond the expected level of corrosion prevention. This exceptional performance enhances the viability of Q-Bi as a valuable solution for corrosion control, especially within projects involving ASTM A283 Grade C materials [5][7][8].

Table 4. Immersion Test Result

Parameter	Chemical Inhibitor	Organic Inhibitor (Q-Bi)	Attainment
Corrosion rate ASTM A 283 Grade C	6,21 mm/y	3,35 mm/y	185,37 %

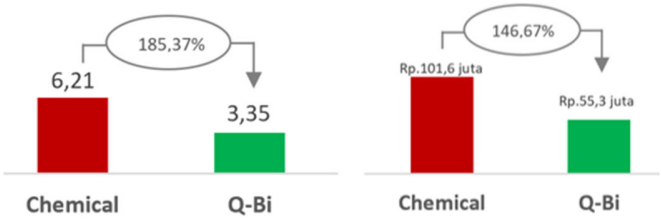

Fig. 4. Chemical and Organic Inhibitor Comparison, rate (left); cost (right)

The conducted test had the primary objective of detecting the presence of anthocyanin compounds within the extract derived from Ipomoea batatas waste. The results of this assessment indicate that the prepared extract, generated by mixing 600 grams of waste with 1 liter of tap water, contains a concentration of anthocyanins within the range of 700-800 milligrams per liter (mg/L). This conclusive finding serves to confirm the existence of anthocyanins in the extract and offers essential quantitative data regarding their concentration.

Anthocyanins are widely recognized for their antioxidant properties, making them a valuable component in various applications. Depending on the source and quality of the anthocyanin extract, these compounds can find utility in diverse fields, including the food industry, cosmetics, and pharmaceuticals. This revelation underscores the potential for utilizing anthocyanins extracted from Ipomoea batatas waste in various products and processes, capitalizing on their beneficial characteristics.

Table 5. Efficiency from Chemical Inhibitor Removal

Parameter	Chemical Inhibitor Cost	Cost (Q-Bi)	Efficiency
150 L	IDR 24,075,000	IDR 817,800	Rp23,257,200
Chemical inhibitor		Q-Bi	
Cost per liter : IDR 160,500		Cost per liter : IDR 5,452	

Table 6. Efficiency from Certified Man Poer Removal

Parameter	Exceed Cost Certified Man Power	Efficiency
1,500 KL	IDR 21,505,498	IDR 21,505,498

The calculated results clearly demonstrate that the utilization of Q-Bi as a substitute for chemical inhibitors in the hydrotest process significantly reduces the cost associated with the construction of a 1,500 KL storage tank. The cost reduction amounts to IDR 44,762,698, down from the original cost of IDR

101,578,106. This cost-saving measure translates to a commendable efficiency gain of 44%, surpassing the predefined target of 30% efficiency improvement.

Moreover, when considering the implementation of Q-Bi for the 2018 carry-over (CO) storage tank construction project and the proposed 2020 new tank project, the potential benefits are substantial. These cost reductions, if applied to these projects, could result in a total cost savings of Rp7,476,519,130. This financial benefit underscores the practical and cost-effective advantages of incorporating Q-Bi into the construction and maintenance of storage tanks, reinforcing its potential for wider adoption in similar projects.

The environmental impact of chemical waste generated by the hydrotest process using Q-Bi is notably positive. The test results indicate that the chemical waste levels are well below the threshold mandated by the Ministry of Environment, achieving a remarkable 100% compliance with the set standards. This outcome reflects a commitment to environmental responsibility and sustainability.

Furthermore, the Risk Priority Number (RPN) reduction has been exceptionally effective, surpassing the target with a reduction of 115% compared to the expected 100%. This demonstrates that the implementation of Q-Bi not only delivers on cost savings but also significantly mitigates potential risks associated with the hydrotest process. The combined benefits of reduced chemical waste and enhanced safety make Q-Bi a highly advantageous choice for this application.

Table 7. HSSE Value Creation

Parameter	Chemical Inhibitor	Organic Inhibitor (Q-Bi)	Kepmen LH	Attainment
Chromate Toxicity	0,005 mg/l	0,001 mg/l	0,005 mg/l	100%

Table 8. Morale Value Creation

Location	Chemical Inhibitor	Organic Inhibitor (Q-Bi)	Attainment	Vs 30% Target
MOR V	68,2%	87,5%	28,3%	94,3%
	Hesitated	Very Satisfied		

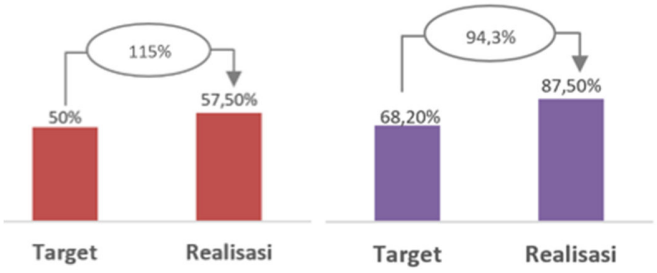

Fig. 5. Target and Realization Comparison, HSSE (left); Morale (right)

The innovation involving the use of organic corrosion inhibitors (Q-Bi) has had a notable positive impact on employee satisfaction, as revealed through data collected over a two-month period. In this assessment, 66.67% of the sampled employees expressed their satisfaction using a Likert scale. While the achievement stands at 94.3%, it slightly falls short of the targeted 100%.

Nonetheless, the significant improvement in employee satisfaction indicates that the implementation of Q-Bi has been well-received by a substantial portion of the workforce. This not only enhances the overall work environment but can also contribute to increased morale and productivity, underscoring the positive influence of this innovation on employee well-being.

C. Conclusion

In summary, the adoption of Q-Bi organic corrosion inhibitors presents a highly promising alternative to traditional chemical inhibitors, successfully aligning with the Quality, Cost, Delivery, Safety, and Morale targets established for this innovative solution. The outcomes of this study underscore the efficacy of Q-Bi organic corrosion inhibitors in enhancing the efficiency of storage tank construction, particularly during the critical hydrotest phase involving seawater.

Notably, this innovative approach has garnered support and endorsement from internal management, underlining its practical benefits and its potential for broader implementation in similar projects. Q-Bi's multifaceted advantages extend to improving cost-effectiveness, promoting environmental responsibility, and contributing to enhanced employee satisfaction within the construction and maintenance of storage tanks. It serves as a valuable and progressive solution for addressing various challenges and optimizing project performance.

REFERENCES

[1] Fontana, G. (1986). "Corrosion Engineering." New York: McGraw-Hill Book Company.

[2] Giuseppe Mazza, E. Miniati (1993). "Anthocyanins in Fruits, Vegetable, and Grains." London: CRC Press.

[3] Luke R. Howard & Zhimin Xu (2012). "Analysis of Antioxidant-Rich Phytochemicals." UK: John Wiley & Sons Ltd.

[4] Hermawan, Beni. "Ekstrak Bahan Alam sebagai Alternatif Inhibitor Korosi." (Publication Date: April 22, 2007).

[5] ASM Handbook Volume 13B, Corrosion: Materials (USA: ASM International, 2005).

[6] American Standard Testing & Material G31-72 - "Standard Practice for Laboratory Immersion Corrosion Testing of Metals."

[7] American Standard Testing & Material G102-89 - "Standard Practice for Calculation of Corrosion rates and Related Information from Electrochemical Measurements."

[8] API Standard 650 - "Welded Tanks for Oil Storage."

Book Exchange System with a Hybrid Recommendation Engine

Nilki Upathissa, Torin Wirasinghe

***Abstract*—** This solution addresses the challenges faced by traditional bookstores and the limitations of digital media, striking a balance between the tactile experience of printed books and the convenience of modern technology. The book exchange system offers a sustainable alternative, empowering users to access a diverse range of books while promoting community engagement.

The user-friendly interfaces incorporated into the book exchange system ensure a seamless and enjoyable experience for users. Intuitive features for book management, search, and messaging facilitate effortless exchanges and interactions between users. By streamlining the process, the system encourages readers to explore new books aligned with their interests, enhancing the overall reading experience.

Central to the system's success is the hybrid recommendation engine, which leverages advanced technologies such as Long Short-Term Memory (LSTM) models. By analyzing user input, the engine accurately predicts genre preferences, enabling personalized book recommendations. The hybrid approach integrates multiple technologies, including user interfaces, machine learning models, and recommendation algorithms, to ensure the accuracy and diversity of the recommendations.

The evaluation of the book exchange system with the hybrid recommendation engine demonstrated exceptional performance across key metrics. The high accuracy score of 0.97 highlights the system's ability to provide relevant recommendations, enhancing users' chances of discovering books that resonate with their interests. The commendable precision, recall, and F1-score scores further validate the system's efficacy in offering appropriate book suggestions.

Additionally, the curve classifications substantiate the system's effectiveness in distinguishing positive and negative recommendations. This metric provides confidence in the system's ability to navigate the vast landscape of book choices and deliver recommendations that align with users' preferences.

Furthermore, the implementation of this book exchange system with a hybrid recommendation engine has the potential to revolutionize the way readers interact with printed books. By facilitating book exchanges and providing personalized recommendations, the system encourages a sense of community and exploration within the reading community. Moreover, the emphasis on sustainability aligns with the growing global consciousness towards eco-friendly practices. With its robust technical approach and promising evaluation results, this solution paves the way for a more inclusive, accessible, and enjoyable reading experience for book lovers worldwide.

In conclusion, the developed book exchange system with a hybrid recommendation engine represents a progressive solution to the challenges faced by traditional bookstores and the limitations of digital media. By promoting sustainability, widening access to printed books, and fostering engagement with reading, this system addresses the evolving needs of book enthusiasts. The integration of user-friendly interfaces, advanced machine learning models, and recommendation algorithms ensure accurate and diverse book recommendations, enriching the reading experience for users.

***Keywords*—** Recommendation Systems, Hybrid Recommendation Systems, Machine Learning, Data Science, Long Short-Term Memory, Recurrent Neural Network.

Nilki Nawanjna Upathissa is with the University of Westminster, Sri Lanka (e-mail: nilki.upathissa@gmail.com).

Reverence Posture at Darius' Relief in Persepolis

Behzad Moeini Sam, Sara Mohammadi Avendi

***Abstract*—**The beliefs of the ancient peoples about gods and kings and how to perform rituals played an active part in the ancient civilizations. One of them in the ancient Near East civilizations, which were accomplished, was paying homage to the gods and kings. The reverence posture during the Achaemenid period consisted of raising one right hand with the palm and the extended fingers facing the mouth. It is worth paying attention to that the ancient empires such as Akkadian, Assyrian, Babylonian, and Persian should be regarded as a successive version of the same multinational power structure, each resulting from an internal power struggle within this structure. This article tries to show the reverence gesture with those of the ancient Near East. The working method is to study Darius one in Persepolis and pay homage to him and his similarities to those of the ancient Near East. Thus, it is logical to assume that the Reverence gesture follows the Sumerian and Akkadian ones.

***Keywords*—**Darius, Persepolis, Achaemenid, Proskynesis.

I. INTRODUCTION

One of the most important rituals was the reverence of gods and kings among ancient peoples. Those were performed with little difference in ancient civilizations. Verbs relating to worship commonly connect with verbs used for prayer based on some gesture of homage (kiss or bow) or are verbs for honor [1, p.1468]. The performance of religious rituals for gods and kings among the civilizations of the ancient Near East has been accompanied by some symbols and gestures [2, p. 85]. It is only very recently that historians have started to become interested in gestures as a key to the cultural codes and sensibilities of the past [3, p. 10]. One of the terms that have widely been discussed among historians on this subject is the Greek word *Proskynesis*, which means to worship [4, p.577],[1.p.1496]. The term is referred to as the act of strain on a higher authority and was a common practice in the ancient East [5, p.228].

One of the most significant actions is the bending down in homage to Zoroastrianism. This action has a two-pronged symbol. It aims at reproducing the bending of the fire and the movement of the earth bulging and bending, thereby expanding to provide more living space. What kind of movement does this term express; it is not evident whether the body bends forward and down or the whole body bends, including the knees. In any case, the bent position of the knees is probably a remnant of the Indo-European era [6.p24]. Regarding the last word (humility and bowing), we can mention the English words humble = close to the earth, as well as human derives from the Latin humus = earth (equivalent to Persian zam= earth), and Indo-European **dhghom*. Given the many similarities between the Semitic and Indo-European peoples, this idea is tantamount to the Semitic notion that man was made of earth or soil [7, p.150],[8, p.174]. A kind of reverence has long been done by hand. The hand can have multiple meanings: the gesture of taking hold or pushing away [9, p.162]. It has been a symbol of the monarchy, an instrument of rule, and a symbol of power and authority. The Hebrew word lad means hand and power [10, p.200]. In Semitic cultures, hand and might are one concept referring to a ruler's power; thus, it is a royal symbol [9, p.162]. Another hint of our topic is kissing. This practice presents mutual unity and membership, which in ancient times also had a spiritual meaning. Kissing a simple gesture is a complete reference to the physical expression of social relations, which is also a cultural practice. As a cultural one, kissing involves sign language and a series of concepts. Every kiss that is made contains some situations and relationships and is not always limited to love and passion and is also used in the social and cultural context; three types of kisses were common among the Romans: *Oscula* (the kiss of friendship and affection), *Basia* (the kiss of love) and *Suavia* (passionate kiss) [3, p.311].

It is necessary to compare the cultural, social, and political process with the ancient Near East in all respects. Some essays and books have compared the old Iranian pictographic materials with the Mesopotamian ones, but there is not essay about Darius' relief in Persepolis with those of the ancient Near East. What is recoverable from the *Persepolitan* evidence is the existence of visual imagery involving the Achaemenid king and the divine with deep ties to long-standing traditions of the exposition of kingship and the prophecy from Assyria and Babylonia [11, p.26].

This essay also searches for these questions: Is the reverence posture in Persepolis' inscription of Darius an Iranian ritual, or has it been borrowed? If so, from which ancient Near Eastern civilizations did it borrow?

II: THE REVERENCE GESTURE (PROSKYNESIS) IN DARIUS' RELIEF AND THE OPINIONS OF THE GREEKS

There is a relief in Persepolis palace, which shows the reverence posture and the practice of the homage gesture in the Achaemenid period.

Behzad Moeini Sam is Associate professor of Ancient Iranian Languages, and Sara Mohammadi Avendi is Master of Persian Literature, Faculty of Humanities, Islamic Azad University, Izeh Branch, Iran (e-mail: Behzadms44@gmail.com & bmssma60@gmail.com).

It displays an official with a raised hand in front of his mouth [12, p.107]. The king is sitting on a throne with his feet on the foot of the throne. His multi-layered royal gown is his royal emblem, and he holds a crown of lotus flowers and a cane on his head. The crown prince stands behind the king and the throne, with two high-ranking officials, and separates the king's two incense burners from the audience. The Iranian aristocrats, wearing round hats, robes, and trousers, respectfully bowed slightly to the king and kept their hands in front of his mouth. A similar scene is depicted in the doorways of the audience hall of Artaxerxes I, the One-Hundred-Column-Hall [13, p.142]. The raised hand in front of the mouth was probably to express fear and respect. In Assyrian culture, the symbol of the Assyrian god is a winged person placed in a wreath and holding one of his hands out of the wreath. This hand gesture was probably a sign of peace and prosperity that could have been borrowed from Egyptian civilization [14, p.12]. Of course, sitting on the throne of gods and kings and respecting them is a remnant of Sumerian times [15, p.4]. A similar image is seen at the entrance of Ardeshir I Hall, the Hundred Columns Hall. This image shows the king sitting on a throne with two court officials or two servants behind [13, p.142].

There is another cylinder seal from the Achaemenid Period (6th- 5th) that shows a winged person with two men in royal dress, one raised hand in front of their mouth, worshiping a deity emerging from a sun disk supported by two sphinxes[16, p,74].

On the social relations of the Iranians, Herodotus points out that the social hierarchy in Iran could not be the same for the rich and the poor. Among the symbolic social elements of the Persians, there was special attention to the method of greeting each other according to their social status. If they were the nobles (gnorimoi) or of equal dignity (isotimoi), they would kiss their lips; If one of them had a lower class (hypodeesteros, tapeinoteros), they kissed the cheek, and finally, if one of them had a much lower rank than the other, he had to perform Proskynesis in front of the higher-ranked person. Hence, this religion can be divided into three categories the noble aristocracy, the lower aristocracy, and the inferior people [17, p.134-5],[18, p.184]. Xenophon describes this ritual in the time of Cyrus, with his hands protruding from his sleeves and with him, a spinning wheel Cyrus looked very tall, and when the crowd saw him, everyone prostrated before him (Kiss or Proskonesis), Either because some of them started this act or because they were fascinated by his majesty or greatness [19, p.27]. Strabo (XI.13.9) tells us about the tribute that the Persians inherited ritual of respect that the subjects performed to their rulers from the Medes. Undoubtedly, the Achaemenid kings inherited many royal symbols from their ancestors [20, p.266].

The essential point is that the ritual of Proskynesis is not invented by the Persians and is taken from the court customs of the ancient East, and the Medes took this ritual and passed it to the Achaemenids [21, p.184]. It was a tradition in the ancient Middle East that was a greeting to the official in the form of bending, bending the knees, or prostrating on the ground [22, p.156].

By comparing ancient texts and common reliefs, there are several interpretations of *Proskynesis*. Indeed, what should one do in the presence of the king? In other words, what does the word *Proskynesis* mean? [23, p.224]. The act of reverence is thought to be a particular sign of *Proskynesis* to the king, and kissing one's hand is a confirmation of the etymology of the Greek word [12, p.107]. Bow or *Proskynesis* is a term used by Greek writers on two very different subjects (the Greeks later denied it). First, it referred to the reverence (or hierarchy) performed by idols or statues of gods. Second, it was a form of Iranian homage that differed in their degree of kinship. In this case, the Greeks considered the word in the whole bow of the subjects to the king [24, p.13]. This ritual was a tradition in the ancient East, and it was a greeting toward the official by bending the knees or prostrating on the ground [24, P.1560. In classical sources, the word means kissing as a gesture of respect. According to Richard Fry, the meaning of this word has changed from the Achaemenid to the Sassanid period. Frye considered *Proskynesis* as the divine attribute of the Persian kings in the Achaemenid period, but it seems that this act did not indicate the spiritual status of the Achaemenid rulers [12, P.103].

Brosius has insisted that *proskynesis* or reverence was performed by the ruler to receive the audience [25, p.35]. It should be remembered that *Proskynesis* was particularly common in the royal court, where subjects bowed to their kings. Most Greeks who witnessed this religion denounced it and believed such an act should be against only one God [21, p.182]. As Greek historians have noted, the Macedonians and Greeks became troubled by Alexander's close relations with the Persians. The Macedonians were very upset that Alexander had a favorable view of material clothes, and in Susa, they did not welcome the wedding ceremony according to Persian customs; according to Arian and other historians in the IRGC, disorder prevailed; the reason was wearing Persian clothes. To accept humility and sternness towards a great king, Alexander tried to implement the tradition of Proskynesis for the Macedonians and Greeks [26, p.15].

In any case, Alexander was accepted as the manifestation of God when he conquered Egypt. Alexander, who was Zeus-*Amun*, was recognized as their son and was considered a god by his people, not to make it a formal ritual but as a political means to empower him and the Greek cities. He introduced *Proskynesis*, bowing to the kings in the Achaemenid court [27. P.217]. The Iranians must have performed this ritual first in honor of Alexander since the Battle of Issus, and among them, the first captive family of Darius III performed it [28, p.289]. We see that after the conquest of Iran, the captives were taken personally to Alexander, and in the performance of this Persian tradition, the women performed the traditional prostration or prostration in the presence of the new subordinate. Unfortunately, they were wrong about the new ruler, because they had strained in front of Hephastion, who

was standing next to Alexander and seemed taller than him. When the harem eunuchs explained the mistake to the women, Sisigambis shouted at them, for this insulting mistake to Alexander, you must fall at his feet [28, p.175]. At a court party in the spring of 327 BCE, Alexander performed this Persian rite of passage for the Macedonian, Greek, and Persian courtiers in sympathy with his companions. Greek sources later reported that Alexander attempted to bow down as a command to worship as a god as if he had done the proskynesis. But he did nothing to embarrass the Greeks. Callisthenes, the great historian of Alexander, also refused to bow, and there are reasons why we think his refusal was for religious reasons. Alexander the Great sought to establish a qualitative balance between Iranian and Western nobles to appease the Persians. Even if Alexander was aware of the religious significance of the bow to the Greeks (as opposed to the Macedonians), it is hard to accept that the Greeks were the first to perform it in 327 BCE. [24, p.13]. On the contrary, if Alexander sought to unite his entire court and ruling class according to these traditions, it would be difficult to refuse to implement them [28, p.289]. Undoubtedly, the general meaning of this ritual was to recognize the superiority of the ruler. This ritual could have been accomplished without the presence of the physical aspect of the king; we see that Satrap Datames performed the proskynesis in front of a letter he received from Alexander [23, p.224].

Maria Brosius traces the origins of court rituals to establish family institutions in Egypt. Brosius also researched the social roots of the authorities in the Achaemenid court and found a connection between the early classes of ancient Egyptian society and the court of the Pharaohs [25, p.89]. Spawforth realized that the Egyptian court was culturally the founder of royal ceremonies performed by courtiers and that the reign of Akhnaton was a turning point. Falling to the ground was part of the Shah's ritual of honor in Egypt and later in Achaemenid Iran. Egypt, like Iran, probably traces the cultural customs of the court to older court traditions; That is, it borrowed from the ancient Near East. In the time of Philip and Alexander, this court method penetrated the West and was performed in the previous style and then held in ancient Rome [24, p.14]. This state of reverence may have been established by the late Babylonian kings for the worshipers to appear on their seals and was then taken in Achaemenid texts as a salutation or a state of sacred allusion and seeking happiness [29, p.107].

III. The REVERENCE POSTURE IN THE ANCIENT EGYPT

In the ancient East, one of the most important rituals was the worship and respect of a single group of people for a particular belief or deity. To this end, there have been terms related to a system that unifies people in their beliefs. The ceremony was crystallized in rituals and prayers that included prayers, worshipers, the praise of statues, a state of reverence, and sacrifice [30, p.17]. The pharaohs of ancient Egypt were god-kings on earth who had life and death in their hands [31, p.6]. In Egypt, as in Mesopotamia, the relationship between God and the king was based on reciprocity [32, p.482]. The relationship between God and the king was based on the principle of exchange: the government offered, and God restored his blessing. Each building built in Karnak refers to the son's gratitude to his divine father. The presence of giving was more valuable than doing something, and for a long time, the Egyptian kings followed the tradition of their ancestors. Hence, many buildings are dedicated to the gods [32, p.481]. Thus, we find similarities in the cultures of the ancient East concerning a god or a king with slight differences. An issue should be noted about paying homage to the king; the king was God's successor on earth and the manifestation of God, and there was a reciprocal relationship between them [32, p.482]. The images are magnificent and impressive and show men and women dancing with their hands raised above their heads, a gesture that could have been a sign of a cow's horn. One of the most important relations of the pre-Egyptian people was with the herding people in the valley, and the small statues were a manifestation to them [33, p.25].

Egyptian composers developed their ideal art forms and became customary for them, becoming a way of conveying the meanings of their ideals. These shapes were higher than the actual size and showed them standing, sitting, women walking, and kneeling. Hand and arm postures were used to describe their work in these pictures when, praying, both arms were facing forward, and the hands were facing up. When offering, both arms extended forward with an object held in one or both palms.

When ready to receive an offering, seated with one or both arms resting on one's lap, palms down. When summoning, one arm extended forward with the palm open. When protecting, both arms extended out to the sides with the palms facing forward. When rejoicing, both arms reached out to the sides with palms turned away from the body. When praising, crouched on one knee, one arm raised and the other held against the chest with a clenched fist. During mourning, arms were lifted with palms and turned toward the face. [34, p.37].

In ancient Egypt, however, the hands or arms outstretched, kneeling, or standing, seem to have been a traditional symbol of reverence for a god. According to Frye, this kind of respect is a style that we have found in a small number of Achaemenid reliefs and in which the king did it before *Ahuramazda* [12, p.103]. In most Egyptian paintings, the hand of kings and officials to pay homage to the gods is depicted [32, p.505]. In the Egyptian language, the hand gesture was related to a pillar (support or power) or a palm tree. In the hieroglyphic system, hand means appearance, action, offering, and agriculture, and open hand means human duty and the force of gravity [35, p.1233-4]. Moreover, in Egyptian art, the left hand is the receiver, and the right hand is the giver. In palmistry, the left hand contains fate and destiny, and the right hand justifies destiny. This symbolism of hands shows some inequalities in Egyptian paintings [35, p.125]. Aside from pointing with the hand, evidence suggests that prostrating

(kissing the ground in Egyptian etymology) to the king was a common practice. The letters of Amarna are documents sent by the tyrants and subordinate states and indicate that they fell to the ground at the feet of the king: Rib-hadda says to the king, his Lord, the sun of all countries, I will follow the Lord, the sun of my time [24, p.239].The scene of the tomb of Amarna and other objects of this place shows that the royal family embraces, kisses, rests, and eats in the same way that these rites of respect are seen in the art of the Egyptian rulers [36, p.324]. In Egyptian paintings and sculptures, we see various signs and poses. In these paintings, mourners are crying, a woman is spreading dough and baking bread, and worshipers are standing and sitting with their legs together and apart. In most of these paintings, the hands are facing up, and the palms are facing God or the [37, p.213].

In the surviving works of art from the burial rite of the ancient kingdom onwards, the deceased is placed with his hand on his knee, palm facing up, and extensive food placed on the table to keep him alive after death [35, p.124]. In Egyptian mythology, *Shu* is the god of air and sunshine. He was portrayed in human form as a kneeling man with his hands raised and sunscreen on his head. [38, p.217]. In the relief that belongs to Pianch, the great holy shrine, and he is in the service of the god *Amun* in the time of Ramses VI of the twenty-first dynasty, the state of respect is in the form of kneeling and pointing hands in the temple of *Amun* [39, p.93],[40, p.30].

We know that the Persians and the nations of the ancient East were indebted to Egypt. For example, the Zoroastrian calendar may have been taken from Masroum around 441 BCE. Frye believes that pointing to praise to a deity could be such borrowing or inherited from the Indo-Iranian period before the Iranians entered the Iran plateau; however, we have no evidence from ancient India in this regard. The rulers raised their hands to honor the gods [12, p.104].

The history of Egypt is divided from the beginning to the end of the Achaemenid rule as follows: Ancient period 3100-2600 BC; Ancient kingdom 2680-2160 B.C; Middle kingdom 2060-1780 B.C; New kingdom 1570- 1086; Late dynastic period 650- 332 B.C. [41, p.99]. In the following, it is brought some samples from the Old Kingdom to the late dynastic period to find out the reverence posture:

An ivory statue of Khufu from the Fourth dynasty of the Old Kingdom 2589-2566 BCE, found in Abydos, shows the king sitting on a throne, holding a mortar in his right hand in front of his shoulder, and holding the red crown of lower Egypt [31, p.42].

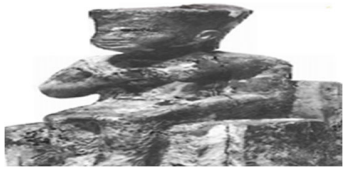

An obelisk from Karnak found in the temple of Amun shows Hatshepsut (1472- 1458 BC) from the New Kingdom as a male, kneeling and supported by Amun's gesture [31, p.105].

Amarna bas-reliefs from Karnak show the king on the occasion of the annual celebration in the palace, where the curtains were bowed before him. Reverence was performed only before the gods, and even Akhenaten (1352- 1336 BC) himself and his family prostrated before the god of Athens [24, p.239].

Tutankhamun was the pharaoh of the 18th dynasty of ancient Egypt of the New Kingdom (1336- 1327 BC), and Kheperkheprure Ay (1325- 1321 BC) was the penultimate pharaoh of Ancient Egypt's 18th dynasty. A fragment of gold foil shows Tutankhamun smiting an enemy while Ay and Ankhesenamun raise their hands in praise [42, p.67].

Merneptah 1213- 1203 BC was the successor of Ramesses II, whose portrait has been painted in the entrance corridor of his tomb in the Valley of the Kings. He has dressed in an elaborate royal custom that extending his hand to the sun god, Re-Harakhti [43, p.129].

The surviving image of the Temple of Ramesses IX shows him praying with his hands raised in prayer [31, p.169].

Nakhthorheb (Nectanebo II) (reigned 359/358–342/341BC), Pharaoh of the 30th Dynasty, whom we have a Metternich Stele, a magical text designed to secure dominion over the powers of anarchy and evil. In this stele, the hand posture of prayers is just like in earlier periods [44, p.124].

In the Ptolemaic Period, we see the goddess Isis and a figure of Osiris, who stands a man between them with curly black hair and a beard, wearing another Egyptian version of the tunic and mantle. The posture of reverence in this image is like most Egyptian paintings, raising hands [42, p.92].

We know that, like other ancient Near Eastern nations, the Persians borrowed from Egypt, and for example, the Zoroastrian calendar was probably borrowed from Egypt around 441 BCE. In other cases, it may have been a sign of respect and admiration for a king. Richard Frye believes it may have been a tribute to the Indo-Iranian era before the Iranians entered the Iranian plateau; however, there is no evidence of this in Indian works [12, p.104].

IV. THE REVERENCE POSTURE IN MESOPOTAMIA

A. Sumer

In the ancient Near East, kingship was the principal condition of civilization, and only primitive societies could live without a king. Security, peace, and justice would not have been possible for the people without a ruler. Also, in Egypt and Mesopotamia, religion was the basis of life [45, p.3]. An issue to be noted about paying homage to kings in these civilizations was that the king was God's successor on earth and the manifestation of God, and there was a reciprocal relationship between the two. In Egypt, like in Mesopotamia, the relationship between God and the king was based on exchange. The king offered it, and God, Amen, renewed his grace and mercy. The aim of offering has been fundamentally more important than the king's principle work [32, p.482]. For example, according to the Babylonian kings, Cyrus took the hand of the god Bel, and with this move, he legalized his kingdom [27, p.132]. In Mesopotamian civilizations, despite similarities, there is a difference in paying homage. The posture of the worshiper was the raising of the hand to the mouth (inim-inim-ma šu-il-la-kam). They combined a form of word reading with the act of worship in prayers [46, p.237]. In the Mesopotamian civilizations, we see many resemblances in the reverence practice, although there are a few differences. Clasped hands are typical of Mesopotamian worshippers from the late 4th to early 3rd mill. B.C, onwards. This situation is seen in a votive scene from Ur-Nanshe (ca. 2550). They are almost invariably on votive statuettes pic 6/7 [35, p.135].

A seal dedicated to Urnammu, King of Ur, shows the founder of the Third Dynasty of Ur (2113–2096) [47, p.181]. He first ruled as governor of Ur. This seal displays the defied king, seated on a throne, and is approached by a goddess leading Hashhamer, governor of the province of Ishkun-Sinn, by the hand, followed by another goddess. The three approaching figures have their hands raised in supplication [48, p.22],[49, p.24].

A limestone panel sculpture in relief, with a scene representing Gudea (Sumerian ruler of Lagash, 2141- 2122 BC) being led by Ningishzida and another god into the presence of a deity who is seated on a throne (Fig.2). Most of retain seals of Gudae show the worshipers with the lifted hand or hands [50, p.47]

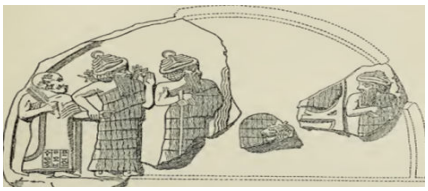

A cylinder of Šulgi, king of Ur (formerly read as Dungi), who was the second king of the third dynasty of Ur from c. 2049- 2046BC. It presents a standing god before an altar, form which has raised a flame, with two figures in the attitude of adoration with lifted hands in front of their mouths: To Meslamtaea, the right arm of Lagash, for the life of Dungi, the strong hero [48, p.22].

Amar-Sin was initially misread as Bur-sin (2046- 2038 BC), son of Šulgi. He was the third ruler of the Ur III dynasty. His cylinder shows a seated god with a worshiper and the flounced goddess following him with lifted hands. The inscription reads; Bur-sin mighty king, king of Sumer and Akkad [48, p.22].

Ibbi-sin (Suen), fifth and last king of the third dynasty of Ur, Son of F=Shu-Sin (2026- 2004?). His reign is well documented since the standard forms of historical information in Mesopotamia, date formulae, votive inscriptions, and omen texts with historical allusions, are supplemented by letters that consider the volatile situation in Ibbi-Sin's time. The style of the worshiper is the same as previous Sumerian seals with lifted hands or hands before mouth [47, p.74].

A cylinder seal refers to the Ur III, ca. 2112- 2004 B.C, its figure shows a man wearing a flounced rob and a brimmed cap and holding a hat in his extended right hand sitting on a padded stool beneath a sun disk in a moon crescent. Two worshipers against him raised their hands to their mouths [51, p.56].

B. Akkad

The iconography of the Mesopotamian gods, such as Šamaš, first took place in Akkadian times. The astronomical Semitic gods and the first ancient Sumerian gods were equated in this period. The ritual of the sun god, Šamaš, may have taken place in Agade. The image of the god of the sun sitting and holding a rod or ring may be specific to Sipar, which came from one place to another as a sculpture, and the version of the ancient Babylonian god was the sitting god of the sun: He holds a knife and sits on a chair, often adorned like a mountain with seals from the early Babylonian period. This version of the sun-god is probably a reflection of a ritual from the city of Sipar or other temples, similar to the Akkadian seals of Tal al-Rimah, where God sits on a chair [52, p.60].

A seal from Lugalushumgal, a vassal of Shargalisharri of Akkad, shows Shamash with others, the god standing on the level ground. The tree, which occasionally appears on seals, is a mere filling motive or a connection between the sun god and the life of plants on Earth [45, p.99].

A cylinder seal from late Akkadian, ca. 2254- 2154 B.C. that shows a figure wearing a long robe and with right arm extended sits before a laden table on a box stool beneath a sun disk in moon crescent. Approaching are two robed figures, each with the left hand raised [45, p.116].

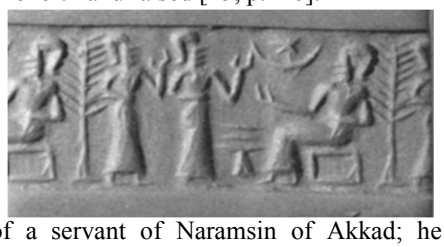

A seal of a servant of Naramsin of Akkad; he was the Akkadian king, son of Manish-Tusu (2260- 2223 BC) [47, p.117]. The Goddess of vegetation is seated before her statue, she carries a bowl from which water streams. The hand situation of the worshiper is in front of his mouth [45, p.117].

A cylinder seal from the Akkadian period (ca. 2350- 2220 BCE) shows a water god, a two-faced god, and two minor gods carrying a plant and birdman with a raised hand [53, p.95].

The scene takes place in front of a deity seated on a throne. Another deity and an attendant are behind the figure performing the libation. There was an inscription of two lines, which had been erased. The posture of the hands of the worshipper is the same as in previous periods [54, p.130].

C. Babylon

In the written tradition, the royal inscriptions of the late Babylonian period and the Achaemenid kings also go back to the first royal writings in Mesopotamia. In terms of the use of titles, Achaemenid inscriptions are very similar to the Assyrian-New Age. Gray and Garelli comment on the similarities between the Assyrian / Babylonian inscriptions and the Achaemenid royal inscriptions [29, p.104].

Indeed, the iconography of Mesopotamian deities, including Shamsh, was first standardized in the Akkadian period, when the Semitic astral gods and the earlier Sumerian – and predominantly agrarian- gods were assimilated. Shamash is

shown holding his saw-toothed knife, with rays rising from his shoulders, and placing his foot on a mountain in what is known as the ascending posture. This version of the god's iconography survives on numerous seals of the Old Babylonian period. Given the persistence of this iconography during at least half a millennium, it is probable that there was a famous cult statue of the standing sun god, perhaps set up in the Akkadian capital, Agade. It is, however, probable that the image of Shamash, seated and holding a rod and ring, was specific to Sippar, as glyptic from other sites shows another, possibly earlier Old Babylonian version of the seated sun god: he holds his knife, and his seat is a chair, often high-backed and decorated like a mountain and coming on other earlier Old Babylonian seals [52, p.61]. The seating of gods and kings, of course, facing other gods and attendants originated in the Sumerian time [55, p.40].

There is better evidence from the kings of the ancient Babylonian period about the Reverence, especially Hammurabi. There have been recent studies on this famous historical figure to show the relationship between the king and the gods. An image found in a bronze donation in Larsa is dedicated to the god Marduk and the actions of Hammurabi. This image (Sumerian word alam ša-ne-ša = statue of supplication) shows the king kneeling with his right hand raised before his face or nose, praying. The same gesture can be seen in a stela in the British Museum dedicated to a goddess and the actions of Hammurabi. The upper part of the stone pillar is about the law of Hammurabi and shows the king sitting next to the sun god.

The same features can be seen in other royal inscriptions of Hammurabi and his successor, Samsu-iluna, which emphasize the position of the king as the beloved of the god Enlil or the beloved Nin-lil [29, p.83].

Also, a cylindrical seal of the soft white stone shows the image of a worshiper sitting before a deity. The style of the seal is older than the Kossaen period. This seal probably dates back to the first Babylonian dynasty, perhaps the Isin and Larsa dynasties. In any case, its date should not be later than the beginning of the second millennium [56, p.91].

There is a seal inscription of Annum-pī-Šamaš Son of Warad-Sîn (1890- 1878 BC) from Old Babylonian king: dingir-pi-^{d}utu Dumu ir-EN.ZU sanga-^{d}utu [57, p.21].

Seal dedicated to samsu-iluna (1904- 1876 B.C), the seventh king of the first dynasty of Babylon, by the owner, Dakiya, son of Damiq-illishu. Damiq-illishu was the last king of the Isin dynasty. A god wearing a turban-like cap, a short skirt, and a mantle and clasping a mace to his chest is approached by a goddess wearing an elaborate horned headdress and a long, flounced garment. Both her hands are raised in supplication [49, p.26].

The impression of the Old Babylonian cylinder seal (*c*.1850–1720 BCE) depicts a suppliant goddess and king facing Ishtar in her guise as a warrior goddess with her right foot resting on a lion's neck and beneath a six-pointed star-disc (her symbol) and crescent (symbol of her father, Sin, the moon-god) [58, p.337].

A seal has been shown the image of Shamash on a cylinder-seal impression in an ascending posture, approached by a king offering a goat. The hand posture of the worshiper is up to his mouth. This image refers to the Old Babylonian Period 1827-1725 B.C. [16, p.27].

A seal dedicated to the goddess Kubaba shows the mother-goddess of north Syria, by Matrunna, the daughter of Aplahanda (early 18th century B.C) and the king of Carchemish. Two figures, a god and a goddess, stand facing each other. The god wears a short undergarment, a long, fringed coat, and a helmet, and the goddess puts on a flounced dress. This seal is a Phoenician adaptation of the first Babylonian dynasty [49, p.36].

A cylinder seal refers to the old Babylonian (1800-1625 B.C) that shows the weather god brandishing a scimitar and a lightning fork standing on the back of a winged fire-breathing

dragon. Approaching is a worshiper holding an animal offering. A goddess stands frontally, clasping both hands at her waist [16, p.59].

A seal dedicated to Burnaburiash II (1359-1330 B.C) shows the Kassite King of Babylon. A god is seated on a throne, clad in a loosely draped gown and a turban-like cap, with a bracelet on his extended arm. Before him, a nude man is kneeling, and below the man, a dog sits in adoration of the god. In the field are a Kassite cross, a characteristic symbol of the period; a rosette; two lozenges, two unknown symbols. The hand posture of the worshiper is up to his mouth [49, p.30].

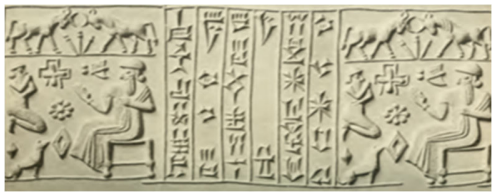

D. Assyria

In Assyrian culture, the relationship between king and deity has been reciprocal. Brisch considers the role of the king the representative of the gods. As the Assyrian rulers, as fathers and nobles, often embodied themselves as gods; a text from Adad-Nirari II, the Assyrian king in 911-891, declares that the gods have perfected his face and body and have seen him as a suitable king. Such references are also seen throughout the neo-Assyrian period, indicating that the king was quite like God [29, p.86].

A cult pedestal of Tukulti-Ninurta I (1243- 1207 BCE) shows an adoration gesture in the Assyrian period [53, p.295].

A cylinder seal refers to the Neo-Assyrian (9th- 8th), which shows an armed male deity (Adad?) between stars and Ishtar in nimbus approached by a worshiper with raised hands [16, p.69].

There is a relief from the throne room that shows a king and winged genii performing a rite at the sacred tree in the presence of an Assyrian god in the winged disk. This relief refers to the reign of Ashurnasirpal II (883- 859 B.C) in the Neo-Assyrian period. The Posture of the worshipper in relief is in the shape of a bent finger [16, p.44].

The image left on the seal of Asarhadun (669-680 BCE) shows the God standing on the left side of the stage with a ring in one hand and an ax in the other. Opposite him stands a mediating deity who introduces a kneeling king (his crooked hands and fingers are visible). In this scene, the image of a man is another god who has been equated with Ninurtu [52, p.57].

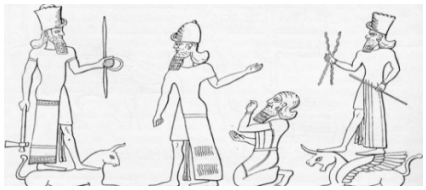

A cylinder seal from the Assyrian period shows Ishtar standing on a lion with a quiver with a bow in hand and a suppliant with index finger to venerate (meissner.1925.2: 28).

A seal refers to a ceremonial scene. A worshiper (center) is facing Marduk, god of Babylon, with Nabu, god of Borisppa and patron of writing, behind him. The worshiper is beardless; he is dressed in a turban and a long, fringed garment and wears a bracelet on the left arm. The position of the fingers indicates adoration [49, p.40].

A cylinder seal refers to the Assyrian period that shows a fighting between a deity and a dragon, and a person behind a dragon with index finger to venerate [59, P.264].

In most Assyrian seals and reliefs presented above, the reverence posture is with the curved index finger.

V. The REVERENCE POSTURE IN ELAM

Since the Achaemenids borrowed from the Elamites on many subjects, it is essential to examine the Elamite paintings. A general look at the Elamite inscriptions and seals shows that the posture of homage in the Elamite period was in the Mesopotamian style, and the mode of the hands was lifting or holding hands [60, p.149].

A cylinder from southwestern Iran refers to the Old Elamite (18th- 17th century B.C.) that shows a god wearing a fringed robe and a square-topped miter with turned-out horns and holding a curved palm frond standing before a worshiper with outstretched arms.[16, p.57].

A cylinder seal from the Elamite period shows this seal inscribed for Ginadu, an official of King Inshushinakshailani of Susa. The hands of the worshipper are similar to the posture of Mesopotamian ones [53, p.427].

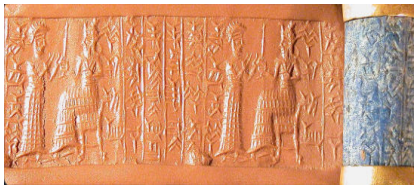

Elamite Seals and reliefs inscriptions at Kol Farah and elsewhere show the reverence posture [60, p.149].

A comparison can be made with the Achaemenid and Sassanid styles [60, p.182]. Root attributes the upper hand to the image of Queen Napirasu and Queen Untash-Gal of Susa and the reliefs of the local kings Hani Hanni and her queen in Salman's cave in Malmir (Izeh), which were adopted by the Persian in art and used in their court [13, p.149].

V. Conclusion

The ancient empires such as Akkadian, Assyrian, Babylonian, and Persian are a successive version of the same multinational power structure, each resulting from an internal power struggle within this structure. In other words, the empire was each time reborn under new leadership, with political power shifting from one nation to another. Of course, the empire changed with each change of power. However the changes were relatively slight. Once the Achaemenids were the first great empire of the ancient world, they were influenced by the previous empires and peoples who lived in their kingdom and influenced them in different fields. It is clear that reverence during the Achaemenids was neither Indo-European nor Aryan, but its roots might have been in ancient Middle Eastern empires. It can be said that there have been some customs about paying homage to gods based on existing words and reconstructing them. But how they were performed is a question because of the lack of works of art.

By comparing the Egyptian and Achaemenian reliefs, even though there are some similarities, and the act of "raising hand" by paying attention to the posture of the hand gesture before the god or the king, it is clear that this reverence posture has so much similar with the seals and reliefs from the late Sumerian till Babylonian Periods and the Achaemenids were influenced by the Mesopotamian Rituals and customs.

REFERENCES

[1] Carl Darling. Buck: A Dictionary of Selected Synonyms in the Principal Indo-Europan Languages. Chicago and London. The Uinversity of Chucago Press. 1940

[2] R.A.S Lubicz: Symbol and the Symbolic, Ancient Egypt, Science, and the Evolution of Consciousness. London. 2004

[3] S.K. Thomas: A Cultural history of Gesture, from Antiquity to present time. UK. Polity press in association with Blackwell publisher. 1991

[4] J.M Whiton: Abriged from Liddell and Scotts Greek-English Lexicon. New York. American Book Company. 1871

[5] Don Nardo. Ancient Mesopotamia. London. Christine Nasso publisher. Greenhaven press. 2007

[6] ProdesOktor Skjærvø.: Introduction to Zoroastrian. Harvard University. New York. 2005

[7] D.B Givens: Nonverbai Dictionary of Gestures, Signs and Body Language Cues. Washington. 2002

[8] J.P Mallory. & Adams.D.Q: Encyclopedia of Indo-European culture. London and Chicago. Fitzry Dear Born Publisher. 1997

[9] Hans Biederman: Dictionary of Symbolism. Translated by James Hulbert. New York. Oxford. Facts On File

[10] J Chevalier. & Gheerbrant. A: Dictionnaire des Symbols. Paris. Editions Robert Leffont Jupiter. 1982

[11] P. Panagiotis Iossif. & Chankowski. Andrej S: More Men, Less Than Gods, Studies on Royal Cult and Imperial Worship. 2011

[12] Richard Nelson Frye: Gestures of Deference to Royalty in Ancient Iran. Iranica Antiqua, 9. 1972

[13] J Curtis. & Simpson. J: The World of Achaemenid Persia. London. Published by I. B.Tauris & Co Ltd. 2005

[14] A. Z. Razgozin: Assyria from the Rise of the Empire to the Fall of Neineveh. New York. 1905

[15] S. N. Kramer: Sumerian Mythology, a Study of Spiritual and Literary Achievement in the third millennium B.C. New York. University Pennsylvanian press. 1977

[16] Pittman. H & Aruz. J: Ancient Art in Miniature: Near East Seals from the Collection of Martin and Sarah Cherkasky. New York. Published by the Metropolitan Museum of Art. 1987
[17] Herodotus: Histories. Vol 1. Translated by A. D. Godley. London. Willam Heiemann LTD and Harvard University Press. 1920
[18] M. Drury: Achaemenid Empire. Sydney. 1999
[19] Xenophon: Cyropaedia. Translated by Walter Miller. Cambridge. Harvard University Press. 1914
[20] Strabo: The Geography of Strabo. Translated by Leonardo Jones. Cambridge. Harvard University Press
[21] G. Ahn: Religiouse Herscher Legitimation im Achamenidischen Iran. Acta Iranica XVII. Leiden. 1922
[22] A.B Basworth. & Baynham. E. J: Alexander the Great in Fact and Fiction. Oxford University Press. 2000
[23] Piere Briant: From Cyrus to Alexander. A History of the Persian Empire. Translated by peter Daniels. Indiana. 2002
[24] A. J. S. Spawforth: The Court and Court Society in Ancient Monarchies. London. Cambridge University Press. 2007
[25] Maria Brosius: The Persian an Introduction. London Routledge Publisher. 2006.
[26] D. Rostam-Afshar. (2005). Alexander der Grosse und Iran: Freie Universität Berlin Institute für Iranistik. 2005
[27] Roman Ghirshman: Iran from the Earliest Times to the Islamic Conquest. New York. 1954
[28] K. Nawotka: Alexander the Great. London. Cambridge Scholars Publishing. 2010
[29] N. Brisch. N: Religion and Power, Divine Kingship in the Ancient World and Beyond. Chicago. The oriental institute. 2008
[30] R. Wallenfels: The ancient Near east encyclopedia. New York. Charles Scribner's Sons. 2000
[31] P. A Clayton: The Reign-by-Reign Record of the Rulers and Dynasties of Ancient Egypt. New York. Thames and Hudson. 1994
[32] K. A. Bard: Encyclopedia of the Archaeology of ancient Egypt. London and New York. Routledge Taylor and Francis Group. 1999
[33] M. Rice: Egypt's Making, the Origins of Ancient Egypt 5000- 2000 BC. London and New York. Routledge Taylor and Francis Group. 2003
[34] P. Montebello: The Art of Ancient Egypt, a Resource for Educators. London and New York. Routledge Taylor and Francis Group. 2009
[35] J. Hall, J: Illustrated Dictionary of Symbols in Eastern and Western Art. London. Westview Press. 1994
[36] A.B. Liyod: A Compendium to Ancient Egypt. United Kingdom. Blackwell publishing Ltd.
[37] G Maspero: Manual of Egyptian Archaeology and Guide to the Study of Antiquities in Egypt. New York. Published by EBD. 1895
[38] M.L, Bierbrier: Historical Dictionary of Ancient Egypt. Maryland. Toronto. The Scarecrow Press, Inc.
[39] H. K. Klinkott & R. Müller-Wollwemann: Geschenk und Steuern, Zölle und Tribute. Leiden and Boston. 2007
[40] M. R. Bunson: Encyclopedia of Ancient Egypt. Library of Congress Cataloging-Publication Data. New York. 2002
[41] H. Rogers. Writing Systems, a Linguistic Approach. Usa and Oxford. Blackwell Publishing. 1977
[42] A. Dodson: Amarna Sunset, Nefertiti, Tutankhamun, Ay, Horemheb, and the Egyptian Counter-reformation. New York. The American University in Cairo Press. 2004
[43] M. J. Raven: Prisse D'Avennes Atlas of Egyptian Art. Egypt. The American University in Cairo Press. 2000
[44] J. Ray: Reflections of Osiris, Lives from Ancient Egypt. Oxford and New York. Oxford University press. 2002
[45] H. Frankfort: Kingship and the Gods, a Study of Ancient Near Eastern Religion as the Integration of Society and Nature. Chicago. The University of Chicago Press. 1978
[46] W.W. Hallo: Origins the Ancient Near East Background of Some Modern Western Institutions. New York. 1999
[47] G Leick: Historical Dictionaries of Ancient Civilizations and Historical Eras. Lanham & Toronto. The Scarecrow Press Inc. 2010
[48] William Hayes Ward: The Seal Cylinders of Western Asia. Washington. Carengie Institute of Washington. 1910
[49] R. A Martin: Ancient Seals of the Near East. Chicago. Field Museum of Natural History. 1940
[50] Leonard W King: A History of Sumer and Akkad, an Account of the Early Races of Babylonia from Prehistoric. New York. Frederick A Stokes Company. 1988
[51] Holly Pittman. Ancient Art in Miniature, Near Eastern Seals from the Collection of Martin and Sara Cherkasky. New York. The Metropolitan Museum Art. 1987
[52] B Groneberg & H. Spieckermann: Die Welt der Götterbilder. Berlin. New York. Walter de Gruyter. 2007
[53] Ann. C. Gunter: A Companion to Ancient Near Eastern Art. New York. John Wiley & Sons, Inc. 2019
[54] Palazzo Loredan: Signs before the Alphabet, Journey to Mesopotamia at the Origins of Writing. New York. Giunti. 2017
[55] S. N. Kramer: Sumerian Mythology. A Study of Spiritual and Literary Achievement in the third millennium B.C. New York. University Pennsylvanian press
[56] E. E. Herzfeld. Iran in the Ancient East. Oxford University Press. London. 1941
[57] M Tanret: The Seal of the Sanga, on the Old Babylonian Sangas of samas of Sippar-jahurum and Sippar-Amnaum. Leiden and Boston. Brill Publishing. 2010
[58] Gwendolyn Leick. The Babylonian World. New York and London. Routledge Taylor & Francis Groups. 2007
[59] B Meissner: Babylonien und Assyrien. Erster Band. Heidelberg. Carl Winters Universität Buchhandlung. 1920
[60] D.T. Potts: The Archaeology of Elam. London. Cambridge University Press. 2004

Spectrum Allocation in Cognitive Radio Using Monarch Butterfly Optimization

Avantika Vats, Kushal Thakur

Avantika Vats is with the Chandigarh University, India (e-mail: vats0avantika@gmail.com).

Abstract

This paper displays the point at issue, improvement, and utilization of a Monarch Butterfly Optimization (MBO) rather than a Genetic Algorithm (GA) in cognitive radio for the channel portion. This approach offers a satisfactory approach to get the accessible range of both the users, i.e., primary users (PUs) and secondary users (SUs). The proposed enhancement procedure depends on a nature-inspired metaheuristic algorithm. In MBO, all the monarch butterfly individuals are located in two distinct lands, viz. Southern Canada and the northern USA (land 1), and Mexico (Land 2). The positions of the monarch butterflies are modernizing in two ways. At first, the offsprings are generated (position updating) by the migration operator and can be adjusted by the migration ratio. It is trailed by tuning the positions for different butterflies by the methods for the butterfly adjusting operator. To keep the population unaltered and minimize fitness evaluations, the aggregate of the recently produced butterflies in these two ways stays equivalent to the first population. The outcomes obviously display the capacity of the MBO technique towards finding the upgraded work values on issues regarding the genetic algorithm.

Index terms- *Cognitive radio, Channel allocation, Monarch Butterfly Optimization, Evolutionary computation.*

1. INTRODUCTION

With the current developing increments of wireless devices, radio range shortage happens and commands the foundation of strategies for creating specialized depictions to get the effectively accessible radio range. For this, COGNITIVE RADIO (CR) methods [1] can be utilized to give a promising answer for the increment of the range usage. The rule of the CR, incorporated into the IEEE 802.22 and IEEE 802.16h standards, needs an option range administration when every secondary/unlicensed user (SU) is allowed to detect and get to the range when the range is empty by primary/authorized users (PUs) [2]. At the point when a PU solicitations to get to its own particular range, the SUs utilizing a similar range craftily ought to mutation to other empty spectra to ensure the transmission of the PU and proceed with their own particular information conveyance [3]. In any case, serious throughput degradation may happen in this circumstance . In the writing, a few calculations have been proposed for direct portion in cognitive radio, regardless of whether they are neighborhood or disseminated look strategies. In this unique circumstance, our work comprises of showing a powerful optimization technique to take care of the direct task issue in Cognitive radio frameworks. The goal of this issue concerns limiting the channel obstruction to the essential radio users meeting those prerequisites for pioneering range usage. The calculation of MBO is very fitting with regards to cognitive radio to control and keep away from impedance in the channel task issue.

Avantika Vats is with the Chandigarh University, India (e-mail: vats0avantika@gmail.com).

1.1 Approaches for Cognitive Radio

COGNITIVE RADIO offers a promising answer for a productive and full utilization of radio channel assets. It has pulled in much research consideration, and both distributed and centralized plans have been proposed to encourage the range sharing amongst SUs and PUs . At that point, the idea of machine learning was connected to boost limit and dynamic range get to access the spectrum. Diverse learning calculations can be utilized as a part of CR systems, for example, Fuzzy Logic, Neural Networks, Genetic Algorithms, [4]. The multilayered neural systems were utilized to model and gauge the exhibitions of IEEE 802.11 systems. They come as an arrangement of interconnected rudimentary processors that can play out the whole handling data chain. Every neuron adjusts its parameters with its neighbors to accomplish the goal for which they have been composed. Along these lines, the neural systems can be considered as a reasonable model for a cognitive radio system, and where an incite reaction to the changing radio condition is required from an unlicensed user. Fuzzy logic is regularly joined with neural systems that can adjust to the earth amid the advancement of a CR framework. It can be connected to acquire the answer for an issue having uncertain, loud, and fragmented info data. Rather than convoluted numerical plans, the Fuzzy logic utilizes human reasonable Fuzzy sets and deduction principles to acquire the arrangement that fulfills the coveted framework goals. The fundamental favorable position of Fuzzy logic is its straight forwardness. It is more reasonable for continuous subjective radio applications in which the reaction time is basic to framework execution [5]. A genetic calculation is a powerful developmental calculation that models organic procedures to take care of an exceedingly complex computational issue to discover ideal arrangements. Crossover and transformation are two fundamental operators of GA. Execution of GA depends

firmly on these operators, and new arrangements are discovered in light of old arrangements using crossover and mutation forms. Crossover and transformation perform two unique parts. Crossover is a meeting operation; it is proposed to pull the population toward a nearby least/most extreme. Transformation is a uniqueness operation; it is proposed to once in a while break at least one individuals from a population out of a nearby least/most extreme space and conceivably find a superior least/greatest space. GA has been connected to range improvement in intellectual radio systems. For instance, genetic calculations have been explored through CR test-beds under certain controlled radio environment [6-8]. In [9], a genetic calculation has been utilized to upgrade the Bit Error Rate (BER) execution in intellectual radio. Dissimilar to the customary GA, Kaur et al.,[10] in, proposed an Adaptive Genetic Algorithm (AGA) to upgrade QoS parameters in an intellectual radio framework. The calculation utilizes a distinctive crossover and transformation rates [11]. In the genetic calculation is utilized with two criteria: (1) amplifying the likelihood of discovery (i.e., the capacity of a SU to decide whether a PU is utilizing a specific part of range) and (2) limiting the likelihood of false alert (i.e., detecting the nearness of a PU while it is not), for an ideal space designation. An enhanced genetic range task show with the thought of obstruction imperatives is proposed in , keeping in mind the end goal to decrease computational intricacy, where the number of inhabitants in genetic calculation is isolated into two sets: the possible range task and the haphazardly refreshed range task. In , the genetic calculation is contrasted with a Particle Swarm Optimization (PSO) calculation, and writers infer that in a dynamic domain, the GA requires a greater number of operations to perform than PSO and subsequently takes longer time. In [11-13] a Chaotic Genetic Algorithm (CGA) was produced, where a confused grouping is utilized to create the underlying population and join the tumult through the crossover and mutation forms. Fuzzy rationale is a far intense and adaptive strategy, in view of learning in transmission rate and expectation. It has potential in either particular critical thinking territories or as a piece of subjective radio framework, to lessen its multifaceted nature. Fuzzy rationale can rough the arrangements autonomously for certain information, yet it doesn't give exact arrangements. Different parameters could be incorporated to foresee the best radio arrangement; it ought to build up a lead identified with the particular circumstance in which it is utilized, and these tenets may include a few confinements in programming. Neural systems have a lesser requirement for early learning; they can be utilized as a part of any period of comprehension. They incorporate broad preparing to produce watched conduct, however, they end up noticeably temperamental when limitations are important to represent. Their application to various situations should be broken down for a CR; every individual node must be given a pre-prepared system or an arrangement of preparing cases mapping perceptions of right activities. For the last case, every CR additionally needs to know the parameters utilized in preparing the neural system so that all radios can make and replicate the same neural system deterministically. GA is appropriate for multi-target execution and non-scientific advancement issues in cognitive radio but in genetic algorithm there are few main disadvantages and they are-

(1) No guarantee of finding global maxima- But then again,apart from brute force,there is rarely any guarantee for non-trivial problems. But the likelihood of getting struck in a local maxima early on is something might have to deal with, for example some kind of stimulated annealing mutation rate decay.
(2) Time taken for convergence- we usually need a decent sized population and a lot of generations before we see good results. And with a heavy simulation, we can often wait for a days for the solution.
(3) It's a black art- Fine tuning all the parameters for the GA, like mutation rate, elitism percentage, crossover parameters, fitness normalization/selection parameters, etc, is often just trial and error.
(4) Other complex aspects- Apart from the genetic parameters of the GA, other things like the fitness function, choice of genetic encoding, genotype to phenotype mapping, etc, are also important in the efficacy of the system.
(5) Incomprehensible solutions- The way we communicate our desires to the system is through the fitness function. But GAs will take it literally, with absolutely no common sense. The result could be totally different, inefficient or incomprehensible from an engineering point of view. We have to be very careful while designing the fitness function.

So, in order to avoid such kind of issues a new optimization technique commonly known as Monarch butterfly optimization (MBO) can be introduced.

2. MONARCH BUTTERFLY OPTIMIZATION

MBO is another sort of meta-heuristic calculation which is enlivened by the nature and it is proposed for persistent improvement issues. In MBO the movement conduct of monarch butterflies is contemplated and afterward summing it up to define a broadly useful metaheuristic strategy [14]. In MBO, all the ruler butterfly people are romanticized and situated in two grounds just, viz. Southern Canada and the northern USA (Land 1) and Mexico (Land 2). As needs be, the places of the ruler butterflies are refreshed in two ways. At first, the off springs are created (position refreshing) by movement administrator, which can be balanced by the relocation proportion. Hence, the places of different butterflies are tuned by butterfly changing administrator. As it were, the hunt bearing of the ruler butterfly people in MBO calculation is predominantly controlled by the movement administrator and butterfly modifying administrator. Additionally, relocation administrator and butterfly modifying administrator can be executed at the same time. Subsequently, the MBO technique is in a perfect world suited for parallel preparing and well fit for making exchange off amongst intensification and diversification, an imperative wonder in the field of metaheuristics. It is completed by first concentrate the movement conduct of ruler butterflies and after that summing it up to plan a broadly useful metaheuristic strategy. Besides, a relative investigation of the execution of MBO as for other population based optimization techniques is finished. This has been tended to by taking a gander at the shared traits and contrasts from an algorithmic perspective and in addition by looking at their exhibitions on a variety of benchmark capacities.

2.1 Monarch Butterfly Optimization

Monarch butterfly has an orange and dark example that can be effectively perceived [15]. Both female and male monarchs have diverse wings with the goal that they can be easily recognized. To

make the movement conduct of monarch butterflies address different advancement problems have been included. There are few principles by which the conduct of monarch butterflies can be idealized.

1.All the monarch butterflies are just situated in land 1 or in land 2, so that the monarch spread flies in land 1 and land 2 make up the entire monarch butterfly population.

2.Monarch butterfly individual is produced by movement administrator from monarch butterfly in land 1 or in land 2 by every child.

3.Once a child is created, an old monarch butterfly will pass away with a specific end goal to keep the population unaltered. In this MBO strategy, it can be performed by supplanting its folks with newly created one just when it has better wellness when contrasted with its parent. Then again, the recently created one is obligated to be disposed of in the event that it doesn't display better wellness when contrasted with its parent. Under this situation, the present is kept in place and undestroyed.

4.The monarch butterfly individuals which have best wellness will move consequently to the individuals to come, and after that they can't be mutationd by any operators. What's more, this can ensure that the quality or the adequacy of the monarch butterfly population will never retrograde with the increment of generation.

3. SYSTEM MODEL

We will utilize the model portrayed in where the channel (i.e., recurrence band) designation issue is figured as a chart shading issue. As in Figure 1, the system is preoccupied as an undirected diagram G=(V, E, L), where vertices (V) speak to users, edges (E) speak to obstruction, so that no channels can be relegated all the while to any adjoining nodes, and L speaks to the accessibility of channel groups at vertices of G. let K be the number of available channels in G. In spite of the fact that it is conceivable that distinctive channels have diverse transmission capacities, the model treats all channels with a similar data transmission. The accessible channel band is separated into orthogonal channels of a similar data transmission utilizing the FDMA technique. It is accepted that there is a component that empowers remote gadgets to utilize numerous channels to impart in the meantime. Let N=|V|denotes the aggregate number of optional users. Edges will be spoken to by the N×N lattice E={eij}, where eij=1 if there is an edge between vertices i and j and eij=0 infers that i and j may utilize a similar channel; take note of that since G is an undirected chart, E is symmetric. In a comparative documentation, we speak to the accessibility of channels at vertices of G by a N×K matrix L={lik}, alluded as the shading framework. Specifically, lik=1 implies that channel k is accessible at vertex i, and lik =0 something else. Figure 1 is then spoken to by the accompanying matrix.

$$E1=\begin{bmatrix}1&1&0&1&0\\1&1&1&0&0\\0&1&1&1&0\\1&0&1&1&1\\0&0&0&1&1\end{bmatrix}\quad L=\begin{bmatrix}1&1&1\\1&0&1\\0&0&1\\0&1&1\\1&0&1\end{bmatrix}$$

A channel assignment policy is denoted by an N×K matrix S = $\{sik\}$, where sik = 0 or1 and sik = 1 if channel k is assigned to the nodes i and 0 otherwise. In this system model there are four primary users and five secondary users and the totoal number of channlels are 3. The channel is allocated to the primary user and if the slot is idle then it is allocated to secondary user. The main motive is to utilize the spectrum in an efficient way. The channel accessibility seen by the optional users. These sorts of availabilities are area ward and time fluctuating additionally, which is brought about by the exercises of primary users. Figure.1 demonstrates a depiction of the quantities of nodes that are doled out with diverts so as to utilize the spectrum; however the nodes are irregular so channel will be allocated according to the necessity of theuser. Time shifting channel accessibility is presented by the portability of users (both PUs and SUs) and the movement stack a variety of primary users. For a point of reference, in the outcomes, the time-shifting channel accessibility at secondary users is introduction duced by changing the utilization of primary users. In this time-opened framework is considered. In a non exclusive schedule vacancy, if an primary user involves one of the channel, it will keep a similar direct in whenever opening, yet in the event that an primary user sits without moving on that specific channel, it will possess a divert in whenever space. At that point the availability of a channel for the optionauser mutations at each schedule opening relying upon all the primary users. Be that as it may, when the channel availabilities mutation, secondary users need to alter their channel assignment likewise. They may likewise fundamental to trade data with neighboring nodes. Be that as it may, the data traded by the secondary users may have restricted ability and experience delay amid data trade since optional users exist together in an imprompt way. It is different from cell frameworks in which committed (and private) flagging channels exist between cells. According to figure 1 every node in the system has its own, accessible channel set by the position of PUs. The parameters which are utilized to look at the performance of different calculations are

(1) The number of nodes in the system

(2) The aggregate number of channels and,

(3) Interference range of primary users.

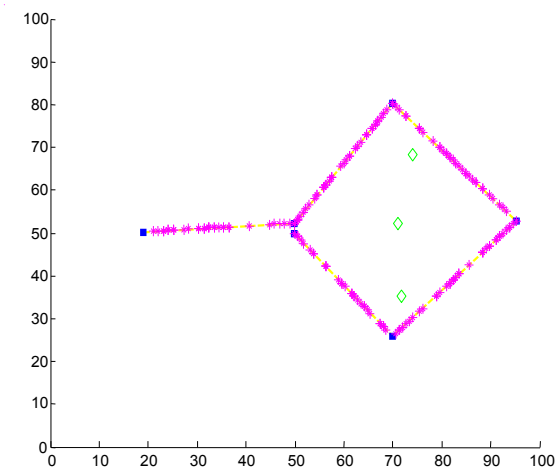

Figure 1 System Model

Nodes are haphazardly circulated and can arbitrarily create a specific number of primary users (PUs). Every primary user involves just a single, direct and every node in the system has its own, accessible channel set according to the position of PUs. There are three parameters utilized as a part of this case and that ought to be tunable with each other and they are – add up to number of nodes, aggregate number of channels, and obstruction scope of primary users. One of these three parameters will be mutations each time and afterward the calculation will be analyzed utilizing three parameters:

(1) Assigned link rate: it is characterized as the proportion of relegated connections over conceivable connections;

(2) Delivery rate: it is characterized as the proportion of greatest reachable nodes over aggregate number of nodes;

(3) Number of rounds: it is defined as the quantity of rounds that are required by channel portion.

5. Simulation results

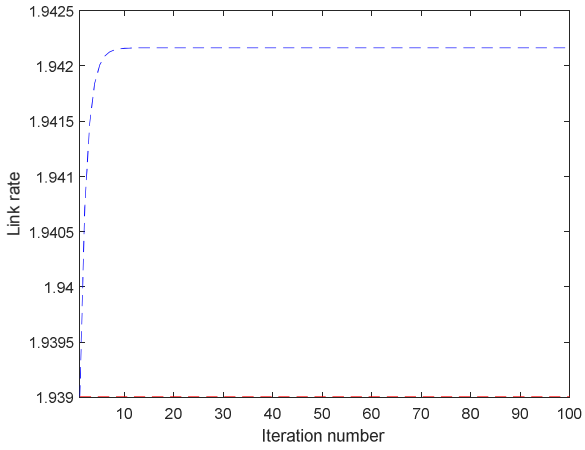

Figure 2 The plot between number of iterations and link rate

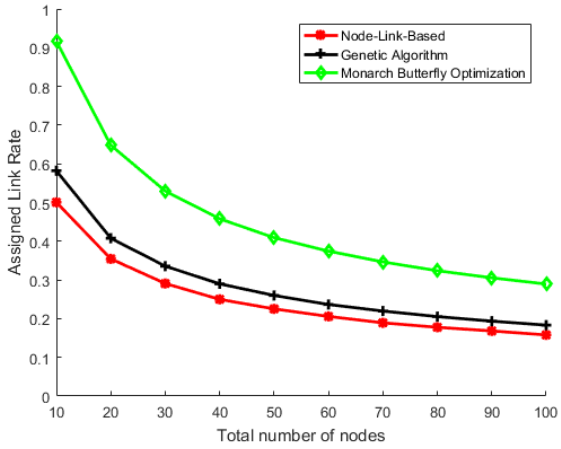

Figure 3 The plot between assigned link rate and total number of nodes based on MBO

As it is shown in Figure 3 the assigned link rate is calculated between total number of nodes using three different algorithms and they are- node link based, genetic algorithm and the last monarch butterfly optimization. The link rate calculated using monarch butterfly optimization is higher as compared to the other mentioned techniques. The higher the assigned link rate, the better the result.The number of nodes utilized are 100.

6. Conclusion

Channel allocation issue is the fundamental issue in cognitive radio system, and the deployable constant dynamic range arrangements are one of its effective intends to enhance the worldwide spectral efficiency to grow new wireless communications services. In this paper, we propose a monarch butterfly optimization for channel assignment problem in cognitive radio and we give the means of its execution. Using MBO the assigned link rate calculated is higher than the link rate calculated using Genetic Algorithm.The MBO algorithm is simple and has no confounded calculation and operators. This makes the usage of MBO algorithm simple and

quick. Regardless of different focal points of the MBO technique, the accompanying focuses ought to be clarified and centered around later on research. Right off the bat, it is outstanding that the parameters utilized as a part of a metaheuristic technique have awesome influence on its execution. In the present work, we do little push to fine-tune the parameters utilized as a part of MBO technique. The best parameter settings will be chosen through hypothetical examinations or observational tests. Furthermore, computational prerequisites are of imperative significance for any metaheuristic strategy. It is basic to enhance the pursuit speed by dissecting the MBO strategy. In future, more benchmark issues, particularly true applications, ought to be utilized for successful execution of the MBO strategy. The convergence of MBO method will be analyzed theoretically by dynamic systems and markov chain. This can ensure stable implementation of MBO method.

7. REFERENCES

[1]. Mitola, J., & Maguire, G. Q. (1999). Cogni tive radio: making software radios more person al. *IEEE personal communications*, *6*(4), 13-18.*)*.

[2]. Haykin, S. (2005). Cognitive radio: brain-empowered wireless communications. *IEEE journal on selected areas in communications*, *23*(2), 201-220.

[3]. Tseng, P. K., Chung, W. H., & Hsiu, P. C. (2013, April). Minimum interference topology construction for robust multi-hop cognitive radio networks. In *Wireless Communications and Networking Conference (WCNC), 2013 IEEE* (pp. 101-105). IEEE..

[4]. Clancy, C., Hecker, J., Stuntebeck, E., & O'Shea, T. (2007). Applications of machine learning to cognitive radio networks. *IEEE Wireless Communications*, *14*(4).

[5]. Amraoui, A., Benmammar, B., Krief, F., & Bendimerad, F. T. (2012). Intelligent wirless communication system using cognitive radio. *International Journal of Distributed and Parallel Systems*, *3*(2), 91.

[6]. Zhao, Y., Gaeddert, J., Bae, K. K., & Reed, J. H. (2006, November). Radio environment map enabled situation-aware cognitive radio learning algorithms. In *Software Defined Radio Forum (SDRF) technical conference*.

[7]. Rondeau, T. W., Le, B., Rieser, C. J., & Bostian, C. W. (2004, November). Cognitive radios with genetic algorithms: Intelligent control of software defined radios. In *Software defined radio forum technical conference* (pp. C3-C8).

[8]. Zhao, Y., Gaeddert, J., Bae, K. K., & Reed, J. H. (2006, November). Radio environment map enabled situation-aware cognitive radio learning algorithms. In *Software Defined Radio Forum (SDRF) technical conference*.

[9]. Deka, R., Chakraborty, S., & Roy, S. J. (2012). Optimization of spectrum sensing in cognitive radio using genetic algorithm. *Facta universitatis-series: Electronics and Energetics*, *25*(3), 235-243.

[10]. Kaur, M. J., Uddin, M., & Verma, H. K. (2012). Optimization of QoS parameters in cognitive radio using adaptive genetic algorithm. *International Journal of Next-Generation Networks*, *4*(2), 1.

[11]. Jegede, O. D., Ferens, K., & Kinsner, W. (2013, January). A chaotic genetic algorithm for radio spectrum allocation. In *Proceedings of the International Conference on Genetic and Evolutionary Methods (GEM)* (p. 1). The Steering Committee of The World Congress in Computer Science, Computer Engineering and Applied Computing (WorldComp).

[12]. Elhachmi, J., & Guennoun, Z. (2016). Cognitive radio spectrum allocation using genetic algorithm. *EURASIP Journal on Wireless Communications and Networking*, *2016*(1), 1-11.

[13]. Mingjun, J., & Huanwen, T. (2004). Application of chaos in simulated annealing. *Chaos, Solitons & Fractals*, *21*(4), 933-941..

[14]. Wang, G. G., Deb, S., & Cui, Z. (2015). Monarch butterfly optimization. *Neural computing and applications*, 1-20

[15]. Garber, S. D. (1998). *The urban naturalist*.

AI Applications in Accounting: Transforming Finance with Technology

Alireza Karimi

***Abstract*—** Artificial Intelligence (AI) is reshaping various industries, and accounting is no exception. With the ability to process vast amounts of data quickly and accurately, AI is revolutionizing how financial professionals manage, analyze, and report financial information. In this article, we will explore the diverse applications of AI in accounting and its profound impact on the field. Automation of Repetitive Tasks: One of the most significant contributions of AI in accounting is automating repetitive tasks. AI-powered software can handle data entry, invoice processing, and reconciliation with minimal human intervention. This not only saves time but also reduces the risk of errors, leading to more accurate financial records. Pattern Recognition and Anomaly Detection: AI algorithms excel at pattern recognition. In accounting, this capability is leveraged to identify unusual patterns in financial data that might indicate fraud or errors. AI can swiftly detect discrepancies, enabling auditors and accountants to focus on resolving issues rather than hunting for them. Real-Time Financial Insights: AI-driven tools, using natural language processing and computer vision, can process documents faster than ever. This enables organizations to have real-time insights into their financial status, empowering decision-makers with up-to-date information for strategic planning. Fraud Detection and Prevention: AI is a powerful tool in the fight against financial fraud. It can analyze vast transaction datasets, flagging suspicious activities and reducing the likelihood of financial misconduct going unnoticed. This proactive approach safeguards a company's financial integrity. Enhanced Data Analysis and Forecasting: Machine learning, a subset of AI, is used for data analysis and forecasting. By examining historical financial data, AI models can provide forecasts and insights, aiding businesses in making informed financial decisions and optimizing their financial strategies. Artificial Intelligence is fundamentally transforming the accounting profession. From automating mundane tasks to enhancing data analysis and fraud detection, AI is making financial processes more efficient, accurate, and insightful. As AI continues to evolve, its role in accounting will only become more significant, offering accountants and finance professionals powerful tools to navigate the complexities of modern finance. Embracing AI in accounting is not just a trend; it's a necessity for staying competitive in the evolving financial landscape.

***Keywords*—** artificial intelligence, accounting automation, financial analysis, fraud detection, machine learning in finance.

Alireza Karimi is with the University of Applied Science and Technology, Iran (e-mail: Alirezakarimi.acc@gmail.com).

Macroeconomic Policy Coordination and Economic Growth Uncertainty in Nigeria

Ephraim Ugwu (Corresponding author), Christopher Ehinomen

Department of Economics, Federal University, Oye -Ekiti, Nigeria

ephraim.ugwu@fuoye.edu.ng, christopher.ehinomen@fuoye.edu.ng

Abstract

Despite efforts by the Nigerian government to harmonize the macroeconomic policy implementations, by establishing various committees to resolve disputes between the fiscal and monetary authorities, it is still evident that the federal government had continued its expansionary policy, by increasing spending, thus creating huge budget deficit. This study evaluates the effect of macroeconomic policy coordination on economic growth uncertainty in Nigeria from 1980 to 2020. Employing the Auto regressive distributed lag (ARDL), bound testing procedures, the empirical results shows that the error correction term, ECM(-1) indicates a negative sign and is significant statistically with the t-statistic value of (-5.612882). Therefore, the gap between long run equilibrium value and the actual value of the dependent variable is corrected with speed of adjustment equal to 77% yearly. The long run coefficient results showed that the estimated coefficients of the intercept term indicates that other things remains the same, (ceteris paribus) the economics growth uncertainty will continue reduce by 7.32%. The coefficient of the fiscal policy variable, PUBEXP indicates a positive sign and significant statistically. This implies that as the government expenditure increases by 1%, economic growth uncertainty will increase by 1.67%. The coefficient of monetary policy variable MS also indicates a positive sign and insignificant statistically. The coefficients of merchandise trade variable, TRADE and exchange rate EXR show negative signs and significant statistically. This indicate that as the country's merchandise trade and the rate of exchange increases by 1%, the economic growth uncertainty reduces by 0.38% and 0.06% respectively. This study therefore advocate for proper coordination of monetary, fiscal and exchange rate policies in order to actualize the goal of achieving a stable economic growth.

Keywords: Macroeconomic, policy coordination, Growth uncertainty, ARDL, Nigeria.

Jel Classification: C20, D81, E02**,** E61, F41, N17

The Moderating Impacts of Government Support on The Relationship Between Patient Acceptance and Telemedicine Adoption in Malaysia

Anyia Nduka[1], Aslan Bin Amad Senin[1], Ayu Azrin Binti Abdul Aziz[2].

[1]Universiti Teknologi Malaysia, 81310, Johor Bahru, Malaysia.
Email – anyia@graduate.utm.my.

Abstract:

Telemedicine is a rapidly developing discipline with enormous promise for better healthcare results for patients. To meet the demands of patients and the healthcare sector, medical providers must be proficient in telemedicine and also need government funding for infrastructure and core competencies. In this study, we surveyed general hospitals in Kuala Lumpur and Selangor to investigate patient's impressions of both the positive and negative aspects of government funding for telemedicine and its level of acceptance. This survey was conducted in accordance with the Diffusion of Innovations (DOI) hypothesis; the survey instruments were designed through a Google Form and distributed to patients and every member of the medical team. The findings suggested a framework for categorizing patients' levels of technology use and acceptability, which provided practical consequences for healthcare. We therefore recommend the increase in technical assistance and government-backed funding of telemedicine by bolstering the entire system.

Keywords: Technology acceptance, Quality assurance, Digital transformation, Cost management.

1.0 Introduction

Telemedicine started in 1970's to reach patients in remote locations. With the rapid changes in telecommunication technology over the last few decades, telemedicine has transformed into a complex integrated service used in hospital, homes, private physician offices and other healthcare facilities [1] The technology of telemedicine evolved from telegraphy, radio and telephone since the 19th century, but the application of telecommunication technology applied to the field of medicine [2]. In 1925, Dr. Hugo Gernsback invented teledactyl, spindly robot fingers and radio technology used to remotely assess a patient and display a live video feed of the patient to the attending physician [3], [4]. Subsequently, a small number of hospital networks and academic medical centres began exploring the feasibility of telemedicine in the 1950s. One of the practices was when medical staff at two different health centers about 24 miles apart transmitted radiologic images via telephone in Pennsylvania.

In Canada, a doctor built upon this technology into a Teleradiology system that was used in and around Montreal. During the year 1959, A two-way interactive TV allowed doctors at the University of Nebraska to send neurological exams to students in the medical school across campus. Even though Norfolk State Hospital was 112 miles distant from campus, they were able to deliver health care through a telemedicine link which was constructed in 1964 [5]. After a few years of application, medical staff and the United States government realized the potential

impacts of telemedicine to reach urban populations with healthcare shortages and its convenience to respond to medical emergencies by sharing medical consults and patient health records without delay [6]. Therefore, by the 1960's, Funding for telemedicine research and innovation came from several sources within the United States government, including the Public Health Service, the National Aeronautics and Space Administration, the Department of Defence, and the Health and Human Sciences Department. [7], [8]. The utilization of telemedicine was eventually extended to space activities to monitor astronauts' health, while carrying the space mission [9].

1.1 Background of the problem

Telemedicine providers in Malaysia, have shown increase in the number of users or patients. HomeGP, Speedoc, Sunway Medical Centre Velocity (SMCV) and eHealth Video Consultation by Parkway Pantai, according to [10], [11]. However, the outbreak of Covid-19 pandemic has affected more of the elderly than the young, due to number of death cases globally involving mostly the age of 30 and above with multiple complications during infection. [12] in their study investigated the Antecedents of Wearable Healthcare Technology (WHT) adoption by the Elderly and suggested key predictors, that in order to reduce hospitalization and mortality rates, increase quality of life, provide a healthier lifestyle, and aid in the management of emergencies, it has been advocated that WHT be employed in health monitoring of the elderly [13], [14]. It analyses significant determinants that affect the adoption of WHT through Structural Equation Modelling (SEM) and neural network model was applied to validate the findings and establish the relative importance of each determinant to the adoption of WHT.

According to the results, WHT was more likely to be adopted by those who reported higher levels of the following factors: social influence, performance expectancy, functional congruence, self-actualization, and hedonic motivation. Worries about new technologies and unwillingness to change were major, unfavourable factors in people's acceptance of WHT. Consequently, the success and efficacy of the use of telemedicine in Malaysia's post-pandemic healthcare system resilience will be determined by the same factors that determined its success and effectiveness during the pandemic.

The evolution can be traced back to the dismantling of barriers caused by people's attitudes and the cost of implementing telemedicine. These limitations stymied earlier attempts to implement telemedicine more widely, According to [6]. In order for telemedicine to be recommended for adoption in the healthcare system of Malaysia, it must first be evaluated by its end-users to see if it fits their expected criteria as patients or healthcare practitioners.

1.2 Problem statement

The Covid-19 (named officially on 11 February 2020), formally known as 2019-nCoV, was a global pandemic of coronavirus disease that threatened the economy and health state of all citizens globally from an epidemic in the city of Wuhan, China to an uncontrollable pandemic worldwide. WHO China Country Office was notified of a certain pneumonia of unknown cause, detected in the city of Wuhan, China on the 31 December 2019. Subsequently, the genome sequencing of novel coronavirus was made publicly available on 11th January 2020, for other countries as reference during the development of specific diagnostic kits. On 13th January 2020, officials confirmed a case of the novel coronavirus in Thailand. Despite a few countries reported on cases in the Republic of Korea, Japan, Thailand and Singapore, the declaration of 2019-nCoV outbreak a Public Health Emergency of International Concern (PHEIC) was declared on 30 January 2020 by WHO Director-General. Hence, the only solution

to interrupt virus spread is through early detection, isolating and treating cases, contact tracing and social distancing measures [15]. Immediate investment of US$675 million Strategic Preparedness and Response Plan (SPRP) was allocated to protect states with weaker health systems on 5th February 2020, to limit transmission, provide early care, communicate key information and minimize social and economic impacts. The Crisis Management Team (CMT), led by the Executive Director of WHO Health Emergencies Programme, assembled together WHO, OCHA, IMO, UNICEF, ICAO, WFP, FAO, the World Bank and several UN Secretariat departments.

The Covid-19 outbreak instantaneously changed the behavioral and economic barriers to widespread adoption of telemedicine. Having officially and legally operated since 1997 in Malaysia through the telemedical Act of 1997 and applied by the government of Malaysia's Telemedicine Blueprint (Ministry of Health, 1997). The implementation road map for telemedicine was provided for a full nation-wide rollout of telemedicine by 2020 in which Malaysia's healthcare system was fully transformed into the information age healthcare.

1.3 Purpose of study

The purpose of this study is to examine the moderating impacts of government support on the relationship between patient acceptance and telemedicine adoption in Malaysia.

1.4 Research objective

- To analyze the impact of patients' acceptance on adoption of telemedicine by the Malaysian Healthcare System as the new norms of Covid-19 pandemic.
- To analyze the impact of healthcare providers' acceptance on adoption of telemedicine by the Malaysian Healthcare System as the new norms of Covid-19 pandemic.
- To determine the moderating effects between management support and patient's acceptance

1.5 Research questions

- What is the impact of patients' acceptance on adoption of telemedicine by the Malaysian Healthcare System as the new norms of Covid-19 pandemic?
- What is the impact of healthcare providers' acceptance on adoption of telemedicine by the Malaysian Healthcare System as the new norms of Covid-19 pandemic?
- What are the moderating effects between management support and patients' acceptance?

1.6 Scope of study

The scope of the study will be centered on analysing the moderating impacts of government support on the relationship between patient acceptance and telemedicine adoption in Malaysia. This study will investigate moderating dimensions affecting patient acceptance and telemedicine adoption. This study will be measured and tested to check their correlation.

1.7 Significant of study

1. This research will aid in the development of telemedicine and expand our current understanding of healthcare services by providing relevant information to healthcare providers in Malaysia and other associated organizations. Management can use this report to learn more about their existing telemedicine initiative.

2. As a response to the Covid-19 pandemic, this research will examine the possible advantages, acceptance, and utilization of telemedicine among Malaysian patients and the community. It's also useful for telemedicine researchers and policymakers in planning how to implement telehealth services for the demographically and socioeconomically diverse Malaysian population. Patients of various linguistic and medical cultural backgrounds should be considered in the design of telemedicine systems.

2.0 Literature review

Table 2.1. Review of previous literatures on Government Support, Patient Acceptance and Telemedicine Adoption.

No	Authors	Tittle	Findings	Limitation
1	[16]	The triple-edged sword of COVID-19: understanding the use of digital technologies and the impact of productive, disruptive, and destructive nature of the pandemic	Organizations need to equip themselves with the knowledge and tools to imagine, prototype, and evaluate the ways digital technology might change the way they handle crises like pandemics, both now and in the future.	The need for an effective virtual communication and interaction management protocols intended to fulfil the requirements to the creation of digital facilities.
2	[17]	Assessing or Predicting Adoption of Telehealth Using the Diffusion of Innovations Theory: A Practical Example from a Rural Program in New Mexico	The study proved to be helpful in terms of identifying barriers to the diffusion process and relating them to a larger body of research on effective practices and conditions to facilitate diffusion.	There is a great need for Program development of a predictive tool for assessing the likelihood of telemedicine adoption within a social system.
3	[18]	Telehealth consultations in general practice during a pandemic lockdown: survey and interviews on patient experiences and preferences	patients reported high satisfaction with telehealth in general practice during lockdown. Telehealth was convenient and allowed patients to safely access health care without having to weigh-up the fear of COVID-19 infection against the need to be seen.	The sample size was the biggest limitation with this study. It was difficult to draw any broad conclusions, especially about underrepresented groups like persons living rural areas or those who don't have access to

				computers or smartphones.
4	[19]	Assessing advantages and barriers to telemedicine adoption in the practice setting: A MyCareTeamTM exemplar	This study findings were found to be consistent with previous research on the benefits of telemedicine systems for diabetes treatment, this investigation found that patients benefited from increased access to care both in and out of the office, as well as from a reported enhancement of the effectiveness and standard of their office visits.	Although this investigation sought to solve an area-specific difficulty, it Is therefore design as a scientific proof enhanced performance initiative and limits the applicability of its results to larger groups.
5	[20]	Determinants of satisfaction among social entrepreneurs in e-Government services	The research offers those in power that establishing an e-Government delivery system isn't enough; they must also establish a network of stakeholders who can help virtual learning environments (VLEs) run smoothly and generate greater income so they can stay in business. This will improve the VLE's financial health, which in turn will make policy-makers happy.	Although this study made a lot of progress, it does have certain limits that will provide researchers new things to look into in the future. To begin, there may be psychological difficulties in assisting others, particularly if the customer is difficult to engage. It is crucial for social entrepreneurs to possess resilience since they may encounter a similar situation.

2.1 Conceptual framework

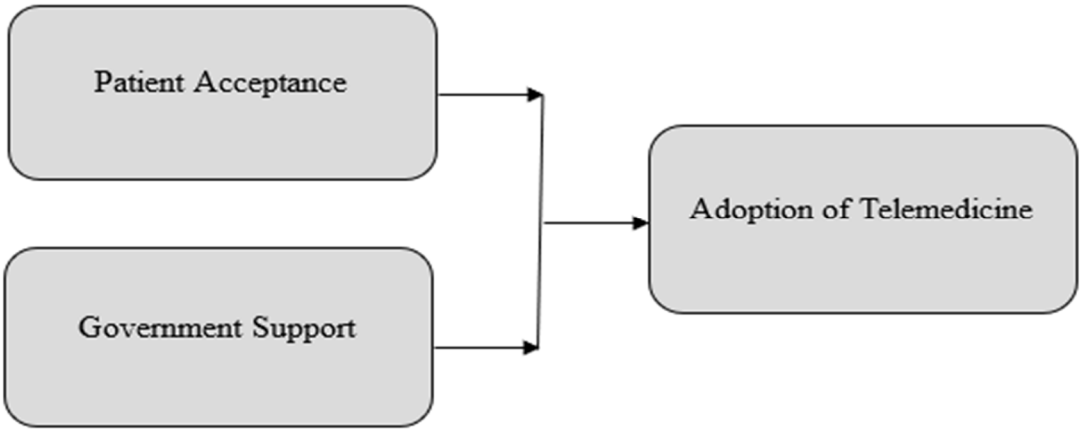

Fig. 2.1. Conceptual Framework for the Study.

3.0 Methodology

This section will cover the details about the research design, the research context, population and sampling, research instrument, the research procedure, including data collection, and data analysis process and methods. The chapter is organized into eight sub-sections including an introduction, a conclusion, and six other sub-sections addressing each of the (8) concepts listed above.

3.1 Research Process

This study research strategy is mostly quantitative, with some use of qualitative techniques to validate the numerical results. The study will employ the deductive approach to examine the moderating impacts of government support on the relationship between patient acceptance and telemedicine adoption in Malaysia. The Deductive approach involves reasoning action and planning behavior from the more general to the more specific, and its conclusion follows logically from the premise. The deductive approach was used because this study is based on existing theories including diffusion of innovation theory, and Technological acceptance Model theory as its underpinning explanations.

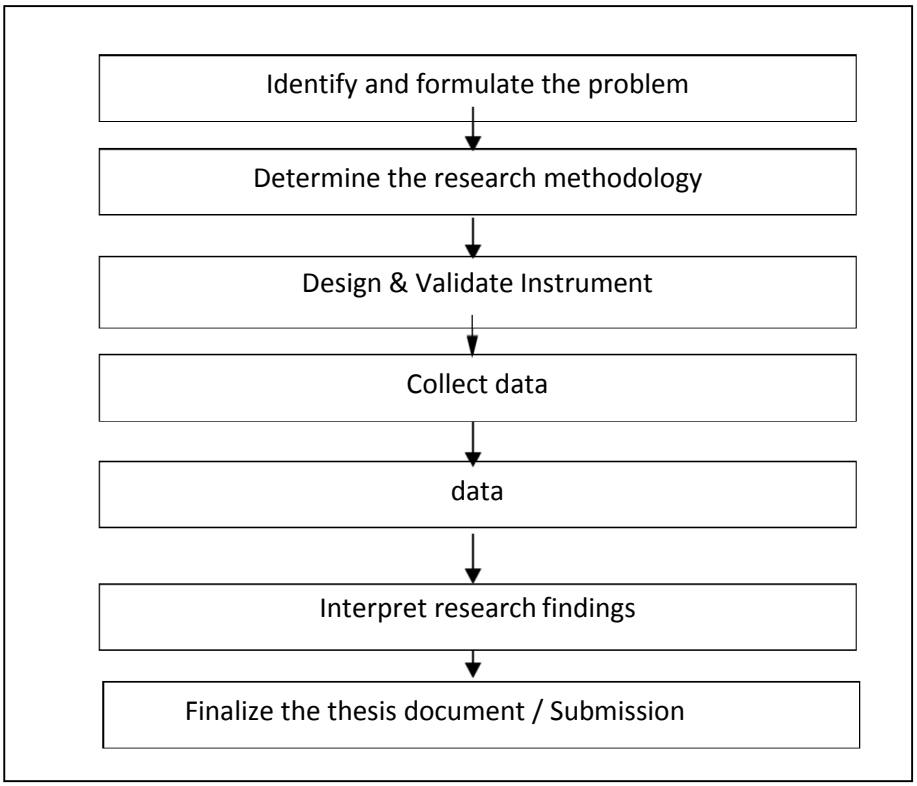

Fig 3.1 Research Process

3.2 Research Design

Table 3.1. Summary of Research Design

Approach	Philosophy	Strategy Design	Choice	Unit of Analysis	Time Dimension	Data Collection Method
Deductive	Positivist	Survey	Quantitative	Individual	Cross-Sectional	Questionnaire

3.3 Research Context

This study will be conducted within the context of public hospitals in Malaysia. In Selangor, Malaysia with participants selected from among the public hospital healthcare practitioners and administrative staff working with public hospitals. The choice of public hospitals is based on the history of the healthcare section and it a relevant sector and one of the very few organizations that can provide the type of data required in this study.

3.4 Population and Sampling

The population of this study comprises all the medical practitioners working with public hospitals that has worked with the hospital for at least two years. The limitation on two years is to ensure total population of the staff that falls in this category, based on public hospital staff

directory, acquire important knowledge about the healthcare sector norms. The medical practitioner employees at the public hospitals will be the respondents.

3.5 Research Instrument

This study will use the self-administered questionnaire as an instrument to collect data from respondents. These questionnaires will administer by the researcher with the help of the human resource department.

3.6 Measurement of Constructs

In this section, we discuss the data source that will be used for the measurements in this investigation. The measurement items for patient's acceptance, government support and adoption of telemedicine. The questionnaires will be presented in English to facilitate the answering of the question as all respondents speak English language. Table 3.4 shows the list of all the study variables on patient's acceptance and the number of items for this study. Table 3.5 shows list of study variables on government support. Table 3.6 shows list variables on adoption of telemedicine. However, the measure of this study regards to questionnaire adapt from the researcher will only focus on the concerned direction of this study, not the whole questionnaire. However, the question select will only be applicable to the use of patient's acceptance to examine the influence of government support and adoption of telemedicine, the study will select only those person logical items that are pertinent to adoption. Doing so is according to Lamiell (1981)'s, requirement for an idiographic approach rather than a nomothetic one in which all individuals are rated in terms of a given attribute.

3.7 Discussions of Variables

The questionnaire will also collect demographic information, such as the respondent's gender, age, education level, employment history, job title, and marital status. The measurement of gender will be a nominal variable, while age, and the number of years in the workforce will be treated as continuous variables.

3.8 Data Analysis

This study will employ the quantitative technique for data analysis. Data will be analyzed using the use of Nvivo 12 version to run both descriptive and inferential analyses.

The main objective of this study is to examine the moderating impacts of government support on the relationship between patient acceptance and telemedicine adoption among employees working at the public hospitals in Malaysia. Relationships between variables will be established using the Pearson correlation and additional multiple regressions.

[Reference]

[1] J. J. Brotman and R. M. Kotloff, "Providing Outpatient Telehealth Services in the United States: Before and During Coronavirus Disease 2019," *Chest*, vol. 159, no. 4, pp. 1548–1558, 2021, doi: 10.1016/j.chest.2020.11.020.

[2] N. T. Moulding, C. A. Silagy, and D. P. Weller, "A framework for effective management of change in clinical practice: Dissemination and implementation of clinical practice guidelines," *Qual. Heal. Care*, vol. 8, no. 3, pp. 177–183, 1999, doi: 10.1136/qshc.8.3.177.

[3] A. Mohammadzadeh, "Application of E-visit and E-services in Reducing the Suffering of COVID-19 (SARS-CoV-2) and Increasing the Therapeutic Adherence of High- Risk

Patients," *Multidiscip. Cancer Investig.*, vol. 4, no. 2, pp. 5–5, 2020, doi: 10.30699/mci.4.2.5.

[4] A. W. Sistrunk, "An Exploration into the Benefits, Challenges, and Potential of Telehealth in the United States: A Mississippi Case Study," *Univ. mississippi*, vol. 5, no. 9, 2019.

[5] J. M. R. A.M. House, "Telemedicine in Canada," *C. J.*, vol. 117, no. 20, pp. 1118–1119, 1977, doi: 10.1136/bmj.1.2575.1118.

[6] J. J. Brotman and R. M. Kotloff, "Providing Outpatient Telehealth Services in the United States: Before and During Coronavirus Disease 2019," *Chest*, vol. 159, no. 4, pp. 1548–1558, 2021, doi: 10.1016/j.chest.2020.11.020.

[7] R. Bashshur, G. Shannon, and H. Sapci, "Telemedicine evaluation," *Telemed. e-Health*, vol. 11, no. 3, pp. 296–316, 2005, doi: 10.1089/tmj.2005.11.296.

[8] A. C. Norris, "The strategic support of telemedicine and telecare," *Health Informatics J.*, vol. 7, no. 2, pp. 81–89, 2001, doi: 10.1177/146045820100700205.

[9] I. Perwitasari, "The Role of Space Technology to Telemedicine in Indonesia towards the Goal of Sustainable Development," *Int. J. Innov. Sci. Res. Technol.*, vol. 4, no. 12, pp. 868–879, 2019, [Online]. Available: www.ijisrt.com868

[10] H. K. Thong, D. K. C. Wong, H. S. Gendeh, L. Saim, P. P. B. S. H. Athar, and A. Saim, "Perception of telemedicine among medical practitioners in Malaysia during COVID-19," *J. Med. Life*, vol. 14, no. 4, pp. 468–480, 2021, doi: 10.25122/jml-2020-0119.

[11] S. Zailani, M. S. Gilani, D. Nikbin, and M. Iranmanesh, "Determinants of telemedicine acceptance in selected public hospitals in Malaysia: Clinical perspective," *J. Med. Syst.*, vol. 38, no. 9, 2014, doi: 10.1007/s10916-014-0111-4.

[12] M. S. Talukder, G. Sorwar, Y. Bao, J. U. Ahmed, and M. A. S. Palash, "Predicting antecedents of wearable healthcare technology acceptance by elderly: A combined SEM-Neural Network approach," *Technol. Forecast. Soc. Change*, vol. 150, 2020, doi: 10.1016/j.techfore.2019.119793.

[13] S. Kekade *et al.*, "The usefulness and actual use of wearable devices among the elderly population," *Comput. Methods Programs Biomed.*, vol. 153, pp. 137–159, 2018, doi: 10.1016/j.cmpb.2017.10.008.

[14] T. Lee and L. Kim, "Telemedicine in Gastroenterology: A Value-Added Service for Patients," *Clin. Gastroenterol. Hepatol.*, vol. 18, no. 3, pp. 530–533, 2020, doi: 10.1016/j.cgh.2019.12.005.

[15] WHO, "Naming the coronavirus disease (COVID-19) and the virus that causes it," *Brazilian J. Implantol. Heal. Sci.*, pp. 1–4, 2020, [Online]. Available: https://www.who.int/emergencies/diseases/novel-coronavirus-2019/technical-guidance/naming-the-coronavirus-disease-(covid-2019)-and-the-virus-that-causes-it

[16] M. M. Kamal, "The triple-edged sword of COVID-19 : understanding the use of digital technologies and the impact of productive , disruptive , and destructive nature of the pandemic ABSTRACT," *Inf. Syst. Manag.*, vol. 00, no. 00, pp. 1–8, 2020, doi: 10.1080/10580530.2020.1820634.

[17] D. L. Helitzer and D. Alverson, "Assessing or Predicting Adoption of Telehealth Using

the diffusion of Innovations theory: A practical example from a rural program in New Mexico.," *Telemidicine J. e-Health*, vol. 9, no. 2, p. 11, 2003, doi: 10.1089/153056203766437516.

[18] F. Imlach *et al.*, "Telehealth consultations in general practice during a pandemic lockdown : survey and interviews on patient experiences and preferences," *BMC Fam. Pract.*, vol. 21, no. 269, pp. 1–14, 2020.

[19] S. T. L'Esperance and D. J. Perry, "Assessing advantages and barriers to telemedicine adoption in the practice setting: A MyCareTeamTM exemplar," *J. Am. Assoc. Nurse Pract.*, vol. 28, no. 6, pp. 311–319, 2016, doi: 10.1002/2327-6924.12280.

[20] R. Sharma, R. Mishra, and A. Mishra, "Determinants of satisfaction among social entrepreneurs in e-Government services," *Int. J. Inf. Manage.*, vol. 60, no. July, p. 102386, 2021, doi: 10.1016/j.ijinfomgt.2021.102386.

Ready Student One! Exploring how to build a successful Game-based Higher Education Course in Virtual Reality

Dr. Robert Jesiolowski, DSW, LCSW
Monique Jesiolowski, MA

Abstract:
Today more than ever before, we have access to new technologies which provide unforeseen opportunities for educators to pursue in online education. It starts with an idea, but that needs to be coupled with the right team of experts willing to take big risks and put in the hard work to build something different. An instructional design team was empowered to reimagine an Introduction to Sociology university course as a Game-Based Learning (GBL) experience utilizing cutting edge Virtual Reality (VR) technology. The result was a collaborative process that resulted in a type of learning based in Game theory, Method of Loci, and VR Immersion Simulations to promote deeper retention of core concepts. The team deconstructed the way that university courses operated, in order to rebuild the educational process in a whole learner-centric manner. In addition to a review of the build process, this paper will explore the results of in-course surveys completed by student participants.

Keywords: *Higher Education, Innovation, Virtual Reality, Game-based Learning, Loci Method.*

Introduction

Information technology has literally changed every aspect of modern life. Higher education is no different. Game-Based Learning (GBL) research has become a key growth area in higher education over the last decade [19]. GBL is an innovative educational paradigm where learners are placed into a theme-based environment where their decisions impact the storyline [12]. The learners are drawn to the relative power of their decision-making which assigns a deeper level of meaning to information studied in the process. Students also navigate mandatory game elements such as incentive systems to motivate them to fully engage in educational tasks they might otherwise find less appealing, boring, or difficult. Instead, placed in the role of the protagonist, these students are empowered to make choices, take on challenges, and maximize rewards in the form of badges or achievements [1].

GBL is not the same as Gamification. GBL is a subset of Gamification. GBL involves an entire gamified education course with clearly defined learning outcomes for learners [19]. This is different than Gamification, which refers to a broader concept, used for learning through educational game play [19]. Therefore, if a higher educational institution adds a game element as one aspect to an academic course that is considered Gamification. If the same higher education institution builds an entire course as an immersive story where all elements are gamified to help the student achieve learning outcomes that is a specific type of Gamification called Game-Based Learning (GBL).

In the past, the positive impact of GBL in higher education has been undervalued [12]. Part of this devaluation comes from a resistance to new modalities of pedagogy by institutions and instructors who are comfortable in their current traditional form of teaching [12]. While some resistance to new innovations is understandable and expected there are advancements in technology over the last ten years specifically which has made the use of gaming in higher education courses more potentially powerful than ever [4]. One of these is the development of Virtual Reality systems.

The GBL approach is rooted in the concept that to facilitate a deeper understanding of course material, students need to be engaged in what they are learning and how to apply it [19]. It is not enough, to present the student with a reading and assess their understanding through testing or papers. GBL presents an opportunity to immerse the student in the educational experience, promoting a deeper level of learning than ever before. Indicators of the impact of GBL on higher education across multiple research studies note improvement in three key areas. These include acquisition and application of course content; motivation and interest in course tasks; and confidence and satisfaction in course completion [19].

This paper will review the literature on GBL, as a subset of Gamification, as well as examine the use of VR simulations in higher education courses. The purpose of the literature review will be to identify potential gaps in the literature where further research would be useful. Following, the literature review, the paper will explore how the instructional design team at Indiana Wesleyan University used current research to guide its current Introduction to the Sociology course build. Finally, a proposal for future research will be offered.

Literature Review

A recent study at the University of National and World Economy into utilizing GBL in higher education business courses to improve student motivation, activity, confidence, creativity, and teamwork yielded interesting results [19]. This study followed the impact of a higher education course in which used GBL elements including simulation games, interactive presentations, and interactive tests [19]. The study's conclusions found that students self-reported an increase in motivation and learning in GBL courses [19]. Students reported that the GBL system enhanced their knowledge acquisition and helped their decision-making process [19].

Another recent study which occurred at this time at the University of Extremadura in Spain compared students in a control group of traditional online education utilizing workshops, rubrics, and assignment to an experimental group in a GBL design of the same course utilizing badges, achievements, and leaderboards [11]. This study found that GBL favored an active learning environment where students performed better academically and felt a higher level of confidence in their skills [11]. This study went on to report that in this new modern digital society, students must be given the best opportunity to develop into flexible, confident professionals in their chosen field to compete in the job market [11]. The study challenged the whole academia to consider how it become the needed simulation field where the students as future professionals can learn to take ownership for their own education and carry that forward into their careers [11].

Academic performance in higher education courses is generally considered to be impacted by cognitive factors and affective-motivational factors [1]. Motivation is generally a difficult process for institutions to encourage [1]. A research study into using GBL with higher education architecture courses showed that student motivation is directly related to learning satisfaction and academic accomplishment [5]. This study found that GBL motivated students to learn and retain course content better than traditional teaching methods [5].

Motivation comes in two forms, intrinsic and extrinsic. Extrinsic motivation takes the form of being inspired to complete a task to earn a reward or avoid a punishment [14]. This may include earning a grade or completing a course seen as merely a step towards earning a degree. Learning becomes a necessary evil to push through to earn the degree for the career that one wants. Conversely Intrinsic motivation is when student's feel inspired to finish a task because it is found to be personally rewarding [14]. Research has concluded that intrinsically motivated learners demonstrate greater academic successes than learners who are extrinsically motivated. Intrinsically motivated learners have been found to be more dedicated to put in more effort into educational tasks, process more complex course material, and use more effective retention strategies [13].

GBL in higher education strives to create a story in which the course learning makes sense and is meaningful for the student, thereby increasing their intrinsic motivation [1]. Deeper learning accompanies intrinsic student motivation [4]. Keller's learning model known as the ARCS motivation model is a teaching approach that is proven to increase and maintain motivational learning in students [5]. It identifies four essential motivating factors for learning which include attention, relevance, confidence, and satisfaction [5]. GBL has been identified by research studies as a strong avenue to promote these four motivating factors [5].

One way the GBL is seen as an innovative and important new higher educational tool is because it challenges learners to be more autonomous and responsible for their learning process [1]. Recent generalized research into higher education indicated that GBL promotes an active learning environment where the students are encouraged to be independent and take ownership of their own scholarship [11].The instructor is not then seen as the purveyor of course knowledge or the authority over the student's efforts, but rather as a guide or facilitator of the student's own journey to discover the knowledge, develop the skills, and apply the learning [11]. The result is a deeper internalization of the course content and a sense of personal accomplishment in the learners [11].

One focus of a GBL course is to remove the stigma from not doing well or making a mistake on an educational task and replace this with an environment that encourages students to take risks and try their best [1]. A large-scale study of GBL at Idaho State University used GBL to create a martial arts themed higher education statistics course showed that the GBL course design lowers student anxiety levels significantly [3]. This research study also identified that students perceived the GBL method was the cause of their lowered anxiety and increased success [3].

A large-scale research study in the UK on higher education coursework that was identified to have the most significant attrition rate, yielded interesting results. The study found that all students who participated in GBL gained significant benefits [20]. A higher retention rate was found to be a result among the participants in the GBL course

[20]. This study also found that GBL courses that utilized personalization enhanced the deep learning experience of the learners [20]. The same study reported that GBL works best for students who are learning course content for the first time rather than review [20]. It may be that GBL courses work better with introductory higher education classes than upper program review courses.

According to a new research study out of Europe, GBL in higher education promotes deep learning in students, as well as a desire to share their experience with friends [1]. Results also show a correlation between student satisfaction in a higher education course experience and their willingness to engage in deep learning strategies [1]. An interesting finding of this study is the connection between the users' satisfaction and the promotion of the academic institution to others [1]. It was noted that students who had a higher degree of satisfaction in a course, were more likely to engage in word-of-mouth promotion of the higher education institution [1]. Another interesting finding arising from recent research showed that GBL designed higher educational coursework is generally well accepted by the student body and results in an enhancement in the academic reputation of the institution [1].

Current meta-analysis of the use of GBL in higher educational coursework showed it can enhance student enthusiasm and performance substantially [12]. The incorporation of GBL into higher education course appear to show a notable increase of student motivation, course movement, skill development, and information retention [2]. This analysis is based on the research of the perceptions of both the instructors and students in gamified courses [2].

Despite the many studies indicating the positive proponents of GBL, there do exists detractors in the higher educational field who would focus on more traditional, passive course constructions that place the instructor as the master authority of the course content with students following prescribed assignments to earn points towards a grade [11]. These detractors distrust the student having autonomy in the active learning environment of GBL [11]. Instructors may even fear losing their positions due to the proliferation of GBL, but this form of education still needs the competent instructor. The role of the instructor must though shift to come alongside the student as a humble leader and guide through the growth process, rather than someone dictating information.

In summary, current research has shown that GBL increases students' intrinsic motivation, deeper learning, decision-making skills, flexibility, confidence, knowledge retention, autonomy, and satisfaction. Research also illustrates how a secondary effect of GBL's positive impact on course retention rates, the institution's academic reputation, and word-of-mouth promotion of the university. There appears to be two gaps in the existing literature that this study can fulfill. First, an exhaustive search of GBL higher education studies shows a lack of application of GBL to sociology courses. Second, the same search found a lack of literature concerning using VR in GBL course design. These literature gaps combine in the current Introduction of Sociology VR GBL course build at IWU.

GBL Design Elements

Research shows that for GBL to have significant impact on student learning, the game elements must be designed with the expected learning results in mind and active promote learner involvement [7]. It appears to be very important to identify the learning outcomes of the GBL course first and work towards them through each gamified experience.

Several research studies have proven that when learners experience fun during their studies, satisfaction increases significantly [1]. It is important to keep GBL experiences engaging and entertaining. Having a strong story element that the student could lose themselves in also can aid in achieving fun. Conversely, teaching such a course may be considered fun for the instructor as well.

Perceived ease of use also positively impacts student satisfaction of the overall course [1]. It is important not to overly complicate the GBL course with difficult interactions and instructions. Keeping it simple and using repetition to encourage student mastery over the course mechanics is imperative. A tutorial may be indicated to help with this process.

Studies have found that GBL factors that enhanced student learning included competence-based learning, achievement rewards, creativity opportunities, and concept challenges [20]. In designing the GBL course, designers need to explore how to incorporate each of these elements into the flow of the class proportionately.

Research identifies that GBL elements that lower student anxiety and improve performance include storyline, achievements, personalization, segmenting, boss battles, and use of multi-media experiences [3]. All these elements are important to a GBL build, but the instructional team needs to keep an ongoing communication throughout the process to maintain balance and inclusion.

Tasks that seemed specifically impactful in GBL higher education courses include experiential web-based experiences resulting in a deliverable [1]. Research shows these experiences result in higher student motivation and deep learning benefits [1]. Effective GBL in higher educational courses incorporates cutting edge technology into the class and invites the learners to immerse themselves into the experience [1]. The cutting-edge technology for immersion today is Virtual Reality (VR). The inclusion of VR into GBL has not been significant up until now, but advances in VR are making this an active field for growth.

To be most effective, GBL of higher education courses must focus on learners working towards prizes such as leaderboards, achievements, and badges rather than grades [1]. Many GBL efforts utilize the PBL triad: Points, badges, and leaderboards [11]. As students accomplish the course objectives, studies show that receiving an educational badge increases their motivation [1]. Best practice in this field has these earned prizes in turn impact the student's final grade [1]. These GBL elements invite the student to be engaged in the story of the course and have fun with the process. This lessens anxiety over grades.

Research shows that the inclusion of a process where students complete a profile helps with commitment to the story [1]. This allows students to join into the creation process with the instructional design team and enjoy their course progress on a whole new level.

Studies show that feedback about a learner's game task performance in the form of status gains improve the student's sense of belonging in the course scenario [1]. Evaluations by the instructor should be interwoven into the course storyline to encourage learners to feel immersed fully into the storyline. Research shows that replacing traditional instructor grading with an assessment based on a rating system like one to five stars better encapsulates the game theory into the evaluation process [1].

Another GBL task that promotes learning in higher education courses is having the learner contribute something they have designed or created to a shared online platform [1]. This improves student belonging to the process and competence in the learning area.

Virtual Reality

Virtual Reality (VR) technology uses sensory devices to immerse users in 360-degree environments (Liu, 2022). VR achieves attributes of high engagement, interactivity, and creativity [9]. This technology immerses the student in a three-dimensional simulation where they are integrated directly into the experience. New studies show using VR in higher education political science courses challenges the students to move from passive acceptance of course content to an active autonomous learning [9].

The use of VR has increased dramatically over the last decade as head-mounted display (HMD) units have become more affordable and available [8]. Researcher's note that educational trends show VR use in education is becoming more prevalent [8]. Modern VR simulations allow students to take part in learning opportunities not achievable in a physical classroom or home setting [8].

VR allows education to enter the metaverse. The metaverse is currently considered a disconnected VR platform that can be accessed through different levels of immersion including full-immersion using head-mounted displays, semi-immersion using projection screens, and non-immersion using desktop-based VR [17]. Therefore, a course could be built in VR leaving it up to the student to decide which level of immersion they are comfortable with. The more immersive the experience is, the more impactful it will be to the learning that accompanies it.

A recent study at Stanford University on running a VR classroom found the benefits of VR was that it provided the learner with an immersive, interactive, experiential environment [17] Participants felt that VR made education more accessible, since people could take a university course from anywhere in the world in a constructed environment that reflected the learning outcomes [17]. A student who underwent a 10-week course in VR at Stanford University noted this, "Learning in VR is nothing like what you'd expect. Simply existing within VR cannot be described to one who has never experienced it. The metaverse and all its features force you to think about how we understand the technology and the world around us, and the way we have come to live in a society on autopilot. In a way that can't be described and can only be felt, the metaverse shows you how to disable that autopilot and be actively aware of your presence and existence within a space. It changes your perspective on how much power we have as humans not just within a society, but within ourselves." [17].

A recent study reported that use of VR for educational purposes taps into visuospatial memory states to increase active memory training and promote learned retention [10]. It posits that how a student perceives and moves within a learning environment significantly impacts how they subsequently recall and retain course material [10].

A research study done in a higher education geography course has shown that while students may have initial fear or anxiety concerning the use of VR in higher education coursework, surveys of the same students after taking part in VR experiences show an increase in positive perceptions towards the technology [8]. These study results strengthen the case for using VR technology in a GBL course build.

Method of Loci

The Method of Loci is a memory retention technique originally posited by Cicero in his *De Oratore*. It is also referred to as the journey method, or the mind palace technique. The Method of Loci involves using visualization of spatial environments to increase deeper learning [16]. This memory technique is widely used and taught to enhance retention of learned material. With the utilization of VR technology to provide immersive environments, Method of

Loci can be practiced within the confines of the online coursework proving a more intense level of learning hereto unachievable for students. Students in the GBL, VR course are challenged to seek out their learning experience in an interactive city environment called "Curios City". The act of searching through the immersive, three-dimensional, 360 degree learning environment promotes linking key concepts to their lived experience. No longer is a student tasked with imagining the experience of identifying course material and locating it in a mind's eye version of a palace, for no they can place on the VR hardware and freely explore those places pre-designed for just such a purpose.

IWU GBL VR Build

The effort of the build at Indiana Wesleyan University was not only to use a meta-analysis of Gamification research studies to identify the most impactful and positive elements of this course design to construct a GBL VR version of Introduction to Sociology. In doing this the instructional design team went through a series of critical analysis of the course build each time leaning more into the GBL concept until a point was reached where traditional education had to be sacrificed for the betterment of the student experience. The following list is what was identified from recent research studies to be core elements of a successful GBL build.

Achievement prizes rather than grades [1]
Competence-based learning [20]
Concept challenges instead of traditional assignments [20]
Creativity opportunities [20]
Cutting edge immersion technology [1]
Easy to use [1]
Educational badges that impact final grade [1]
Experiential web-based experiences with a deliverable [1]
Feedback in the form of status gains [1]
Fun [1]
Instructor Evaluations interwoven into the storyline [1]
Interactive presentations [19]
Interactive tests [19]
Learner creation contribution to a shared online platform [1]
Learning Outcome driven [7]
Multi-media experiences [3]
Opportunity for Personalization [3]
Rating system replacing traditional grading [1]
Remove stigma of failure [1]
Segmenting [3]
Boss battles [3]
Simulation games [19]
Strong storyline [3]

With these core GBL elements in mind the Instructional Design Team (IDT) for the Introduction to Sociology (SOC 150) online GBL VR build at IWU first worked on what the Course Learning Outcomes would be. Seven Course Learning Outcomes (CLOs) were developed and scaffolded in the SOC 150 build. These learning outcomes served a guide for the rest of the course build process. Each experience of the SOC 150 build had one to three CLOs grounding it in educational value. This was designed to meet the core GBL element of being Learning Outcome driven [7].

A Course Map was constructed from the initial instructional design meeting to guide the build process. The IDT would meeting weekly to advance the build. In between meetings, dozens of emails were shared back and forth serving brainstorming and critique functions. An introduction to the course was written to be delivered to the prospective student by an AI Chatbot persona that would serve as a job coach and tour guide to the learners throughout the course. We focused on making the story and resulting course flow meet the GBL element of fun and engaging.

After several sessions of the IDT, a story concept was settled on for SOC 150. Since the course was an introductory study of sociology, it was believed that the story should be grounded in the student taking part in building a community of people. That way, the sociological concepts could be learned and then applied to the community. The story evolved into a new community called Curios City that was created by the Curios City Council. The Council then hires a Community Builder (played by the student) to learn sociological concepts and apply them to the community to help it grow into a thriving society. This was designed to meet the core GBL element of strong storyline [3].

The traditional Course Menu was replaced by an interactive Community Map divided into 5 Neighborhoods rather than the usual weekly workshops. The Community Builder (student) would navigate the Curios City Community Map to find and engage in VR simulations to learn sociology concepts and then apply them to the Community in an academic deliverable. This was designed the meet the GBL element of using cutting edge technology to provide experiential web-based experiences with a deliverable [1].

Challenges throughout the community build take many forms including Tutorial, Avatar Creation, Case Study Video Interviews, Experiential Project Report, Social Change Paper, Praying in Color Spiritual Forums, VR Experience with Memo Reviews, and Conversational Essays. This meets the GBL element of interactive presentations, creativity opportunities, Learner creation contributions to a shared online platform, and simulation games [20].

The Community Builder begins the game by creating an Avatar that can be moved around the Community Map. This meets the core GBL element of opportunity for personalization [3]. The Community Builder then undergoes a tutorial to acclimate the learner to the game elements and course mechanics. This meets the deign GBL element of making the system easy to understand and use [1].

In the story, the Curios City Council also hires a renowned master Sociologist (instructor) to monitor the Community Builder's progress and make sure each sociology concept is applied in an effective and healthy manner. This was designed to meet the core GBL element of instructor evaluations interwoven into the storyline [1]. SOC 150 was designed to have four levels of nontraditional academic evaluation to engage the learner. These included Competence Scales, Educational Badges, Title Achievements, and a Community Completion Award to best maximize learning [6]. This met the core GBL element of achievement prizes rather than grades [1]. All 4 levels of evaluation combine for a Final Growth Report instead of a grade. This met the core GBL element of educational badges that impact the final grade [1].

There are no linear workshops in the SOC 150. Instead, the Neighborhood areas were designed to each reflect a different part of Curios City that be accessed in whatever order the Community Builder sees fit. This empowers the learner to control the course flow for her/himself and direct her/his own educational experience. This meets the GBL element of segmenting the course [3]. There are five Neighborhoods in total including Town Square, the Suburbs, Downtown, Uptown, and Campus town. Each Neighborhood was designed to have 3 Points of Interest and 1 Key Person. Each Point of Interest is a different building. Every Point of Interest is a gateway to a Challenge simulation. This meets the core GBL element of concept challenges instead of traditional assignments [20].

When the Community Builder successfully attempts a Challenge, s/he does this by guiding the Avatar to enter a VR simulation of a relevant Concept Challenge environment. For example, if the learner enters the Library Point of Interest, her/his Avatar appears in the hall before the Circulation desk with shelves of books all around them for the Library. This repeats with any Concept Challenge (i.e., enter City Hall see hallways of Office doors, enter the Park and see walking paths, etc.). If the learner completed the Library challenge and it is accepted by the Sociologist, the Point of Interest is replaced by an actual Library building Badge on the Community Map.

After the Community Builder completes all Points of Interest in a Neighborhood, then the learner can meet with the Key Person. This meets the GBL element of Boss battles [3]. There are 20 Challenges across the entire community build. The Community Builder must review all resources within the environment including readings, 360 videos, and VR simulations. This meets the GBL design element of using multi-media experiences [3]. After that the learner submits an assigned academic deliverable for the Sociologist to review. If the Challenge is with a Key Person, the Community Builder engages in an interactive conversation with the AI Chatbot about key sociology concepts learned in that Neighborhood that is recorded for the Sociologist to review. This is designed to meet the GBL element of interactive tests [15].

The Sociologist reviews the Community Builder's submissions using a Competence Scale designed specifically for that Challenge. This is designed to meet the GBL element of Competence-Based Learning [20]. The Sociologist uses a Competence Scale to determine whether a Challenge is good enough to be "Accepted". If the Challenge is "Accepted", then Community Builder earns the relevant Badge in the form of a building. So, if the learner completes the City Hall Challenge, then s/he earns a City Hall building which appears on the Community Map. This is designed to meet the GBL core element of using a rating system to replace traditional grading [18].

If the Community Builder's submission is not accepted, then the Community Builder receives a "Try Again" indicator with some Review Notes. The Sociologist will provide the Community Builder with individualized Review Notes that will help her/him be successful when the learner retakes the Challenge. The Community Builder can attempt the Concept Challenge again and resubmit for review by Sociologist until the Community Builder either passes the Concept Challenge or the SOC 150 community build 5-week timeframe ends. It is important to note, that the Community Builder does not have to wait until one Challenge submission is "Accepted" before working a different Challenge. This meets the GBL element of removing the stigma of failing and allows for learners to continue working on a concept until they master it [1].

The building Badges reflect the Community Builder completing a successful review of the sociology concepts linked to Points of Interest. These Badges include buildings on the map that include the "Welcome to Curios City!" Sign, Library, City Hall, Park, Church, Family Homes, Community Center, Welfare Department, Transportation Department, Café, Courthouse, Hospital, School, Office, and Fairgrounds. Completing a Key Person meeting also awards the Community Builder a Badge in the form of the Mayor, Pastor, Social Worker, Judge, or Dean standing in the neighborhood where they were based. Each educational Badge earns the Community Builder rewards towards the Final Growth Report.

The Community Builder starts out as a "Novice Community Builder". Every time the Community Builder completes an entire Neighborhood, s/he earns a Title Achievement which earns credit towards the Final Growth Report calculation. The Title Achievements are earned in this order no matter which Neighborhood the Community Builder finishes first, second, and so on. After the first Neighborhood completion, the Novice Community Builder becomes a "Developing Community Builder!". After the second Neighborhood completion, the Developing Community Builder becomes an "Outstanding Community Builder!". After the third Neighborhood completion, the Outstanding Community Builder becomes an "Expert Community Builder!". After the fourth Neighborhood completion, the Expert Community Builder becomes a "Master Community Builder!" After the fifth Neighborhood completion, the Master Community Builder becomes a "Legendary Community Builder!" This meets the GBL element of Feedback in the form of status gains [1].

If the Community Builder completes all Concept Challenges, earns all Educational Badges, and gathers all Title Achievements, s/he receives a Community Completion Award that gives the learner credit towards her/his Final Growth Report. All these factors combine into the Final Growth Report that the Community Builder can monitor at any time throughout the course. In addition, extra credit is built into the course in the guise of completing surveys. These appear on the Community Map as "Bridge to the Future" badges at the north, south, east, and west aspects.

IWU GBL VR Process

The instructional design approach to Gamification of SOC 150 at IWU took many stages. The first stage was to develop a shared vision of the class by the IDT. The team needed a multidisciplinary approach with different build members championing different aspects of the build whether it be story immersion, academic integrity, technology interface, or learner experience. This also involved the team member getting to know and understand each other's perspective, strengths, and potential blind spots.

The second stage was for the team to collaborate a storyline that would capture the course learning objectives (CLOs) in a believable way to encourage student buy in. This was a dynamic process that would be returned to several times throughout the rest of the build process. It was important to the instructional design team for the course to have educational integrity overlayed with engaging fun gameplay. All traditional language was systematically removed from the GBL build.

The third stage was to utilize the developed story as a guide to design game experiences that would effectively capture course concepts in an engaging way. Many challenges were designed and reworked. Many were thrown out even after significant work had taken place if they did not fit into the story while being anchored in the CLO. Many traditional aspects of online education were deconstructed in the process. There was nothing considered off limits as conventions like workshops, rubrics, gradebooks, linear flow, and more were removed from the build to make way for new exciting GBL elements based on research.

The fourth stage was to settle on the best technology that would deliver the GBL experience in a truly immersive way. The team agreed early on that the Introduction to Sociology GBL build would work best if done using VR simulations. Research into various VR educational programs and learning management supplements occurred with the team sharing resources. The instructional design team agreed the Engage platform would work best with this build. Engage is a leading metaverse platform founded in 2014 as an XR studio featuring educational programming [17] Engage is accessible through VR, desk-top computers, tablets, and mobile devices. The platform utilizes avatars (personalized self-representations), multiple virtual locations, and IFX (3D objects) [17]. Engage also has teleport function to reduce instances of cybersickness [17]. Engage was recently used to run a 10-week Communication course at Stanford University which resulted in two case studies reviewed by the SOC 150 Subject Matter Expert.

The fifth stage was to build the mechanics of the course in a way that brought the four previous levels together in a powerful way for prospective learners. There was a continual process of editing and reworking emanating from frequent instructional team meetings and email conversations.

Indiana Wesleyan University is a Christian university. When looking at any type of class build, it was important to make sure that it is biblically sound. There was an idea early in the build to have the class to mimic the Holy Trinity and how it works within our lives. By doing this, not only are biblically sound principles introduced into the class, but the learner is also exposed to the practicalities of how God works within lives.

In traditional educational systems, the teacher is the master authority over the course and material. Conversely, the student is a passive participant absorbing the information given. Christianity breaks this mode though calling for people to be active participants in their own faith and growth, while Christ comes alongside them. This active learner and partnering teacher dynamic became the basis for the GBL course build. Instead of the instructor being the master authority, giving information to the passive student, the instructor now comes alongside the student and actively working with them to create the thriving community.

In the GBL course, the City Council is equivalent to God having created Curios City for people to live and enjoy. Despite this, issues of prejudice, conflict, and inequality have taken root in Curios City. The City Council is an entity in relationship beyond the scope of the perception of the GBL build that has called upon the Community Builder to join in the creation process. The City Council can be seen though in the reflection of its creation Curios City. It wants good things for the people of Curios City.

The Tour Guide/Job Coach ("JC") is reflective of Jesus Christ. The Community Builder is called to be active participants in the community and JC comes alongside her/him. Even though Jesus is the master of all things, He never comes at people in such a manner. Instead, He walks with us, guides us, directs us, and provides an empathic ear. He allows us to fall and get back up and try again. In fact, He encourages to have peace amid the struggle. In the course, JC guides the Community Builder through the course and teaches her/him what the learner's role is, as well as how to accomplish it. JC never forces his viewpoint on the Community Builder, but rather offers ways to move forward on a good and rewarding path.

The Holy Spirit is represented by the Sociologist within the GBL build. This is the role that the instructor plays in the GBL course. The Holy Spirit convicts people of what is right or wrong; good or evil; healthy or unhealthy for their walk in this life. The Sociologist, in this role, provides feedback to the Community Builder on the best approach and application of course concepts, but ultimately it is up to the Community Builder what s/he does with that feedback. The Community Builder (student) can choose to follow or go his or her own way. The Sociologist works with the Community Builder strengthening her/his resolve, cheerleading and challenging the learner.

Conclusions

Despite detractors, GBL has been shown across multiple research studies to improve student motivation, learning, and retention if its design meets core GBL elements. These elements form a roadmap for academics to create new effective GBL learning opportunities. VR is an evolving technology that when utilized within GBL courses can take the learning opportunities to a whole new level. VR GBL has the potential to revolutionize the higher education system if enough educators and students are willing to pioneer these early courses and share their experiences. Continued research into what works and what doesn't will help develop best practices in VR GBL.

Future Research

IWU intends to run a research study with the first year of the GBL VR version of Introduction to Sociology. This would best occur using a quasi-experimental design of student experimental group within a GBL VR learning instructional course and a control student group non-GBL VR learning instructional condition. This would allow IWU to compare students in a control group of traditional online education utilizing workshops, rubrics, and assignment to an experimental group in a GBL VR design of the same course utilizing badges, achievements, and rating system.

A recent study into GBL course in higher education programming courses identified three key components of GBL. These entailed 1) usability of the game; 2) impact on knowledge acquisition; and 3) user experience [20]. Another study into using GBL is higher education hospitality programs identified five key components to survey student's perceptions on a gamified course experience being usability, fun, usefulness, reward, and satisfaction [1]. We intend to use these and other studies as a guidepost for our scholarly approach. Based on the above information, the following hypotheses have been put forward:

H1: Perceived usability of the GBL VR will positively affect student perception of the course.
H2: Perceived fun of the GBL VR will positively affect student perception of the course.
H3: Perceived value of the GBL VR will positively affect student perception of the course.
H4: Perceived motivation of the GBL VR will positively affect student perception of the course.
H5: Perceived knowledge acquisition of the GBL VR will positively affect student perception of the course.
H2: Perceived satisfaction of the GBL VR will positively affect student perception of the course.

A survey will be developed to examine each of these core GBL fundamentals and administered in the course to both the control and experimental groups. These survey questions will be charted on a 5-point Likert scale including [1] Strong Disagree, [2] Disagree, [3] Neutral, [4] Agree, and [5] Strongly Agree.

The Survey will follow these 4 key components:

Usability:
"I find it easy to navigate the course elements"
"I have no problems completing my work in the course."
"I think the instructions for the course are easily understood."

Fun:
"I find the course is an engaging approach to Sociology"
"I believe the class elements are fun."
"The course experiences make these concept interesting."

Value:
"I think the course elements are useful to study Sociology."
"I think the information presented about Sociology is valuable to know it deeply."
"I find the course allows me to apply my learning of Sociology."

Motivation:
"I feel motivated by the course feedback to achieve"
"I thought that my achievements in the course were reflected well"
"I felt the use of course elements were helpful in encouraging deep learning."

Knowledge Acquisition:
"I thought the course elements helped me understand course concepts"
"I felt I learned a lot in this course."
"I believe I will retain this information after the course is over."

Satisfaction:
"I found the course to be a positive experience."
"I would recommend the course to others."
"I would choose a course like this again in the future."

All data from the surveys across 1 year of coursework will be evaluated to determine whether the relationships between the variables of the IWU research study adequately reflect the correlations observed in the literature review.

References

[1] Aguiar-Castillo, L., Clavijo-Rodriguez, A., Hernandez-Lopez, L., De Saa-Perez, P., Perez-Jimenez, R. (2021). Gamification and deep learning approaches in higher education. *Journal of Hospitality, Leisure, Sport & Tourism Education 29. 100290.* Retrieved from https://doi.org/10.1016/j.jhlste.2020.100290

[2] Buckley, P., Doyle, E. (2016). Gamification and Student Motivation. *Interact. Learn. Environ. 24*, 1162–1175.

[3] Coffland, D., & Huff, T. (2022). Stats Kwon Do: A Case Study in Instructional Design, Multimedia and Gamification of Instruction. *TechTrends* 66, 945–956. https://doi.org/10.1007/s11528-022-00793-y

[4] Djeki, E.; Dégila, J.; Bondiombouy, C.; Alhassan, M.H. (2020). E-Learning Bibliometric Analysis from 2015 to 2020. *J. Comput. Educ.*

[5] Fernandez-Antolin, M., Manuel del Río, L., Gonzalez-Lezcano, R., (2020). The use of gamification in higher technical education: perception of university students on innovative teaching materials. *International Journal of Technology and Design Education*. 31:1019–1038. Retrieved from https://doi.org/10.1007/s10798-020-09583-0

[6] Fischer, H., Heinz, M., Schlenker, L., Follert, F., (2016). "Gamifying Higher Education. Beyond Badges, Points and Leaderboards". International Forum on Knowledge Asset Dynamics. Technische Universität Dresden, Media Center. Retrieved from https://www.researchgate.net/publication/306038063_Gamifying_Higher_Education_Beyond_Badges_Points_and_Leaderboards

[7] Guillén-Nieto, V.; Aleson-Carbonell, M. (2012). Serious Games and Learning Effectiveness: The Case of It's a Deal! *Computer Education, 58*, 435–448.

[8] Hagge, P., (2021). Student Perceptions of Semester-Long In-Class Virtual Reality: Effectively Using "Google Earth VR" in a Higher Education Classroom. *Journal of Geography in Higher Education*. 45, NO. 3, 342–360. Retrieved from https://doi.org/10.1080/03098265.2020.1827376

[9] Liu, D., (2022). Research on the Application of VR Technical Ability in Political Education in Colleges and Universities. *Scientific Programming.* Article ID 7587820, Retrieved from https://doi.org/10.1155/2022/7587820

[10] Mathes, D., (2021). Efficacy of Virtual Reality Learning. *Librarium Research and Learning.*

[11] Murillo-Zamorano, L., Bueno Muñoz, C., Ángel, J., Sánchez, L., Godoy-Caballero, A., (2021). Gamification and active learning in higher education: is it possible to match digital society, academia and students' interests? *International Journal of Educational Technology in High Education.* 18:15. Retrieved from https://doi.org/10.1186/s41239-021-00249-y

[12] Navarro-Espinosa, J., Vaquero-Abellán, M., Perea-Moreno, A., Pedrós-Pérez, G., Martínez-Jiménez, M., and Aparicio-Martínez, P., (2022). Gamification as a Promoting Tool of Motivation for Creating Sustainable Higher Education Institutions**.** *Int. J. Environ. Res. Public Health* 2022, *19*, 2599. Retrieved from https://doi.org/10.3390/ijerph19052599

[13] Reeve, J. (2002). *Self-determination theory applied to educational settings*.

[14] Ryan, R. M., & Deci, E. L. (2000). Intrinsic and extrinsic motivations: Classic definitions and new directions. *Contemporary Educational Psychology,* 25(1), 54–67.

[15] Simonds, J., E. Behrens, and J. Holzbauer (2020). Competency-based education in a traditional higher education setting: a case study of an introduction to psychology course. International Journal of Teaching and Learning in Higher Education 29: 412-428.

[16] Sims, R., Chang, B., Bennett, V., Krishnan, A., Aboubakar, A., Coman, G., Bahrami, A., Huang, Z., Clarke, C., & Karnik, A. (2022). Step into My Mind Palace: Exploration of a Collaborative Paragogy Tool in VR. In A. Dengel, M-L. Bourguet, D. Pedrosa, J. Hutson, K. Erenli, D. Economou, A. Pena-Rios, & J. Richter (Eds.), *Proceedings of 2022 8th International Conference of the Immersive Learning Research Network, iLRN 2022* [9815936] IEEE. https://doi.org/10.23919/iLRN55037.2022.9815936

[17] Stewart, N., (2022). Virtual reality, metaverse platforms, and the future of higher education. University of Ottawa. Media Development.

[18] Townsley, M. and D. Schmid (2020). Alternative grading practices: An entry point for faculty in competency-based education. Competency-based Education DOI: https://doi.org/10.1002/cbe2.1219.

[19] Vodenicharova, M., (2022). Gamed-based Learning in Higher Education. TEM Journal. Volume 11, Issue 2, pages 779-790, ISSN 2217-8309, DOI: 10.18421/TEM112-35, May 2022.

[20] Zhao, D., Muntean, C. , Chis, A., Rozinaj, G., Muntean, G. (2022). Game-Based Learning: Enhancing Student Experience, Knowledge Gain, and Usability in Higher Education Programming Courses. *IEEE Transactions on Education*, 65 (4),

The Politics and Consequences of Decentralized Vocational Education: The Modified System of Vocational Studies in Ghana

Nkrumak Micheal Atta Ofori

***Abstract*—** The Vocational System is a decentralized Studies System implemented in Ghana as vocation studies strategy for grassroot that focuses on providing individuals with the specific skills, knowledge, and training necessary for a particular trade, craft, profession, or occupation. This article asks how devolution of vocational studies to local level authorities produces responsive and accountable representation and sustainable vocational learning under the vocational Studies System. It focuses on two case studies: Asokore Mampong and Atwima kwanwoma Municipal. Then, the paper asks how senior high school are developing new material and social practices around the vocational studies System to rebuild their livelihoods and socio-economic wellbeing. Here, the article focusses on Kumasi District, drawing lessons for the two other cases. The article shows how the creation of representative groups under the Vocational Studies System provides the democratic space necessary for effective representation of community aspirations. However, due to elite capture, the interests of privilege few people are promoted. The state vocational training fails to devolve relevant and discretionary resources to local teachers and do not follow the prescribed policy processes of the Vocational Studies System. Hence, local teachers are unable to promote responsive and accountable representation. Rural communities continue to show great interest in the Vocational Studies System, but the interest is bias towards gaining access to vocational training schools for advancing studies. There is no active engagement of the locals in vocational training, and hence, the Vocational Studies System exists only to promote individual interest of communities. This article shows how 'failed' interventions can gain popular support for rhetoric and individual gains.

***Keywords*—** vocational studies system, devolution of vocational studies, local-level authorities, senior high schools and vocational learning, community aspirations and representation.

Nkrumak Micheal Atta Ofori is with the Yaa Pokuaa Technical Institution, Ghana (e-mail: nkrumahmichealattaofori@gmail.com).

Assessing Teachers' Interaction with Children in Early Childhood Education (ECE). Cambodian Preschool Teachers' Beliefs and Intensions

Shahid Karim, Alfredo Bautista, Kerry Lee

***Abstract*—**The association between teachers' beliefs and practices has been extensively studied across the levels of education. Yet, there is a lack of context-specific evidence on the relationship between teachers' beliefs and intentions regarding their interaction with children in early childhood education settings. Given the critical role of teachers' beliefs in their practices, the present study examined Cambodian preschool teachers' beliefs and intentions related to their interaction with children and what factors affect the relationship. Data was collected through a self-reported Beliefs and Intentions Questionnaire (BTQ) from preschool teachers teaching at different types of preschools in Cambodia. Four hundred nine preschool teachers teaching in public, private and community schools participated in the study through an online survey administered on Qualtrics. The quantitative analysis of the data revealed that teachers' beliefs predict their intentions in preschool. Teachers' teaching experience, level of education and professional training moderated the relationship between their beliefs and intentions. Differences existed between the groups of teachers teaching in different types of preschools and genders. Implications of the findings related to policy and preschool teachers' professional development are discussed.

***Keywords*—**teacher-child interaction, teaching beliefs, teaching intentions, preschool teaching accreditations, Cambodia.

Shahid Karim is with the The Education University of Hong, Hong Kong (e-mail: shahid.karim83@live.com).

Doing Bad Things for Good Reasons: An Examination of Unethical Pro-Organizational Behavior among Professional Workers

Kyle Payne

***Abstract*—** Unethical organizational behavior can be extremely costly. While generating many of the same costs associated with unethical organizational behavior, unethical pro-organizational behavior poses a unique challenge. It suggests that there is a "dark side" to constructs thought to be productive, like organizational identification. Recent research suggests that individuals who identify highly with their organization are more likely to engage in unethical pro-organizational behavior and that moral disengagement mediates this relationship. Based on a sample of 281 professional engineers, this study attempts to validate these findings by testing a proposed theoretical model in which organizational identification is positively associated with unethical pro-organizational behavior and in which moral disengagement mediates this relationship. It also proposes two boundary conditions not yet examined in this context – professional identification and work engagement – and it further examines moral identity as a boundary condition. The study's findings call into question previous findings that organizational identification by itself predicts unethical pro-organizational behavior. It validates previous findings of a significant relationship between moral identity and moral disengagement and a significant relationship between moral disengagement and unethical pro-organizational behavior. It also provides the first empirical evidence of a significant relationship between work engagement and moral disengagement. While pointing to variables that practitioners can manipulate to mitigate the risk of unethical pro-organizational behavior, the study highlights the complexity of predicting and responding to the dark side of organizational identification and suggests further research.

***Keywords*—** moral disengagement, organizational identification, unethical pro-organizational behavior, professional identification, moral identity, work engagement.

Kyle Payne is with the Bellevue University, United States (e-mail: kyle.d.payne@gmail.com).

Underage Internal Migration from Rural to Urban Areas of Ethiopia: The Perspective of Social Marketing in Controlling Child Labor

Belaynesh Tefera, Ahmed Mohammed, Zelalem Bayisa

***Abstract*—** This study focuses on the issue of underage internal migration from rural to urban areas in Ethiopia, specifically in the context of child labor. It addresses the significant disparities in living standards between rural and urban areas, which motivate individuals from rural areas to migrate to urban areas in search of better economic opportunities. The study was conducted in Addis Ababa, where there is a high prevalence of underage internal migrants engaged in child labor due to extreme poverty in rural parts of the country. The aim of this study is to explore the life experiences of shoe-makers who have migrated from rural areas of Ethiopia to Addis Ababa. The focus is on understanding the factors that push these underage individuals to migrate, the challenges they face, and the implications for child labor. This study adopts a qualitative approach, using semistructured face-to-face interviews with underage migrants. A total of 27 interviews were conducted in Addis Ababa, Ethiopia, until the point of data saturation. The criteria for selecting interviewees include working as shoemakers and migrating to Addis Ababa underage, below 16 years old. The interviews were audio-taped, transcribed into Amharic, and then translated into English for analysis. The study reveals that the major push factors for underage internal migration are socioeconomic and environmental factors. Despite improvements in living standards for underage migrants and their families, there is a high prevalence of child labor and lack of access to education among them. Most interviewees migrated without the accompaniment of their family members and faced various challenges, including sleeping on the streets. This study highlights the role of social marketing in addressing the issues of underage internal migration and child labor. It suggests that social marketing can be an effective strategy to protect children from abuse, loneliness, and harassment during their migration process. The data collection involved conducting in-depth interviews with the underage migrants. The interviews were transcribed and translated for analysis. The analysis focused on identifying common themes and patterns within the interview data. The study addresses the factors contributing to underage internal migration, the challenges faced by underage migrants, the prevalence of child labor, and the potential role of social marketing in addressing these issues. The study concludes that although Ethiopia has policies against child internal migration, it is difficult to protect underage laborers who migrate from rural to urban areas due to the voluntary nature of their migration. The study suggests that social marketing can serve as a solution to protect children from abuse and other challenges faced during migration.

***Keywords*—** underage, internal migration, social marketing, child labor, Ethiopia.

Belaynesh Tefera Nidaw is with the Addis Ababa University, Ethiopia (e-mail: belaynesh.tefera@aau.edu.et).

Quality of Life Among People with Mental Illness Attending a Psychiatric Outpatient Clinic in Ethiopia: A Structural Equation Model

Wondale Getinet Alemu, Lillian Mwanri, Clemence Due, Telake Azale, Anna Ziersch

***Abstract*—**

Background: Mental illness is one of the most severe, chronic, and disabling public health problems that affect patients' Quality of life (QoL). Improving the QoL for people with mental illness is one of the most critical steps in stopping disease progression and avoiding complications of mental illness. Therefore, we aimed to assess the QoL and its determinants in patients with mental illness in outpatient clinics in Northwest Ethiopia in 2023.

Methods: A facility-based cross-sectional study was conducted among people with mental illness in an outpatient clinic in Ethiopia. The sampling interval was decided by dividing the total number of study participants who had a follow-up appointment during the data collection period (2400) by the total sample size of 638, with the starting point selected by lottery method. The interviewer-administered WHOQOL BREF-26 tool was used to measure the QoL of people with mental illness. The domains and Health-Related Quality of Life (HRQoL) were identified. The indirect and direct effects of variables were calculated using structural equation modeling with SPSS-28 and Amos-28 software. A p-value of < 0.05 and a 95% CI were used to evaluate statistical significance.

Results: A total of 636 (99.7%) participants responded and completed the WHOQOL-BREF questionnaire. The mean score of overall HRQoL of people with mental illness in the outpatient clinic was (49.6 ± 10 Sd). The highest QoL was found in the physical health domain (50.67 ±9.5 Sd), and the lowest mean QoL was found in the psychological health domain (48.41±10 Sd). Rural residents, drug nonadherence, suicidal ideation, not getting counseling, moderate or severe subjective severity, the family does not participate in patient care, and a family history of mental illness had an indirect negative effect on HRQoL. Alcohol use and psychological health domain had a direct positive effect on QoL. Furthermore, objective severity of illness, having low self-esteem, and having a history of mental illness in the family had both direct and indirect effects on QoL. Furthermore, sociodemographic factors (residence, educational status, marital status), social support-related factors (self-esteem, family not participating in patient care), substance use factors (alcohol use, tobacco use,) and clinical factors (objective and subjective severity of illness, not getting counseling, suicidal ideation, number of episodes, comorbid illness, family history of mental illness, poor drug adherence) directly and indirectly affected QoL.

Conclusions: In this study, the QoL of people with mental illness was poor, with the psychological health domain being the most affected. Sociodemographic factors, social support-related factors, drug use factors, and clinical factors directly and indirectly, affect QoL through the mediator variables of physical health domains, psychological health domains, social relation health domains, and environmental health domains. In order to improve the QoL of people with mental illnesses, we recommend that emphasis be given to addressing the scourge of mental health, including the development of policy and practice drivers that address the above-identified factors.

***Keywords*—** quality of life, mental wellbeing, mental illness, mental disorder, Ethiopia.

Wondale Getinet Alemu is with the Flinders University, Ethiopia (e-mail: wondale22@gmail.com).

Stereological Evaluation of Liver of Rabbit Fetuses After Transplantation of Human Wharton's Jelly-Derived Mesenchymal Stromal/Stem Cells

Zahra Khodabandeh, Leila Rezaeian, Mohammad Amin Edalatmanesh, Asghar Mogheiseh, Nader Tanideh, Mehdi Dianatpour, Shahrokh Zare, Hossein Bordbar, Neda Baghban, Amin Tamadon

***Abstract*—** Background: In-utero xenotransplantation of stem cells in abnormal fetuses effectively treats several genetic illnesses. Objective: The current research aimed to evaluate structural and morphological alterations in the liver of rabbit fetuses following xenotransplantation of human Wharton's jelly-derived mesenchymal stromal cells (hWJ-MSCs) using a stereological technique. Methods: hWJ-MSCs were isolated from the human umbilical cord, and their authenticity was established by flow cytometry and differentiation. At gestational day 14, the rabbits were anesthetized, and hWJ-MSCs were injected into the uteri of 24 fetuses. Twenty-two fetuses were born successfully. Ten rabbit liver specimens were prepared from injected fetuses, including eight rabbits on day three following birth and two rabbits on the 21st post-natal day. The non-injected fetuses were considered positive controls. The livers of the control and hWJ-MSCs-treated rabbits were fixed, processed, stained, and examined through stereological approaches. Results: In the hWJ-MSCs-treated group, the mean liver weight and volume increased by 42% and 78% compared to the control group. The total volume of the hepatocytes increased by 63% and that of sinusoids by threefold in the treated rabbits. The total volume of the central veins increased by 70%. The total number corresponding to hepatocytes in the experimental group increased by 112% compared to the rabbits in the control. The total volume of the hepatocyte nuclei in the experimental group increased by 117% compared to the rabbits in the control. Conclusion: After xenotransplantation of human MSCs, host tissue microenvironments (here, the rabbit liver) were altered, and these included quantitative factors corresponding to the liver tissue and hepatocyte morphometric indices.

***Keywords*—** xenotransplantation, mesenchymal stromal, stem cell, Wharton 's jelly, liver.

Zahra Khodabandeh Jahromi is with the Shiraz University of Medical Sciences, Iran (e-mail: zahrabandeh@gmail.com).

ScRNA-seq RNA Sequencing-Based Program-Polygenic Risk Scores Associated with Pancreatic Cancer Risks in the UK Biobank Cohort

Yelin Zhao[1], Xinxiu Li[1], Martin Smelik[1], Oleg Sysoev[2], Firoj Mahmud[1†], Dina Mansour Aly[1†], Mikael Benson [1†*]

***Abstract*—** Background: Early diagnosis of pancreatic cancer is clinically challenging due to vague, or no symptoms, and lack of biomarkers. Polygenic risk score (PRS) scores may provide a valuable tool to assess increased or decreased risk of PC. This study aimed to develop such PRS by filtering genetic variants identified by GWAS using transcriptional programs identified by single-cell RNA sequencing (scRNA-seq).

Methods: ScRNA-seq data from 24 pancreatic ductal adenocarcinoma (PDAC) tumor samples and 11 normal pancreases were analyzed to identify differentially expressed genes (DEGs) in in tumor and microenvironment cell types compared to healthy tissues. Pathway analysis showed that the DEGs were enriched for hundreds of significant pathways. These were clustered into 40 "programs" based on gene similarity, using the Jaccard index. Published genetic variants associated with PDAC were mapped to each program to generate program PRSs (pPRSs). These pPRSs, along with five previously published PRSs (PGS000083, PGS000725, PGS000663, PGS000159, and PGS002264), were evaluated in a European-origin population from the UK Biobank, consisting of 1,310 PDAC participants and 407,473 non-pancreatic cancer participants. Stepwise Cox regression analysis was performed to determine associations between pPRSs with the development of PC, with adjustments of sex and principal components of genetic ancestry.

Results: The PDAC genetic variants were mapped to 23 programs and were used to generate pPRSs for these programs. Four distinct pPRSs (P1, P6, P11, and P16) and two published PRSs (PGS000663 and PGS002264) were significantly associated with an increased risk of developing PC. Among these, P6 exhibited the greatest hazard ratio (adjusted HR[95% CI] = 1.67[1.14-2.45], p = 0.008). In contrast, P10 and P4 were associated with lower risk of developing PC (adjusted HR[95% CI] = 0.58[0.42-0.81], p = 0.001, and adjusted HR[95% CI] = 0.75[0.59-0.96], p = 0.019). By comparison, two of the five published PRS exhibited an association with PDAC onset with HR (PGS000663: adjusted HR[95% CI] = 1.24[1.14-1.35], p < 0.001 and PGS002264: adjusted HR[95% CI] = 1.14[1.07-1.22], p < 0.001).

Conclusion: Compared to published PRSs, scRNA-seq-based pPRSs may be used not only to assess increased but also decreased risk of PDAC.

***Keywords*—** Cox regression, pancreatic cancer, polygenic risk score, scRNA-seq, UK Biobank.

1. Medical Digital Twin Research Group, Department of Clinical Science, Intervention and Technology (CLINTEC), Karolinska Institutet, Stockholm, Sweden.
2. Division of Statistics and Machine Learning, Department of Computer and Information Science, Linköping University; Linköping, Sweden

† These contributed equally as last authors.

* Correspondence: Mikael Benson is with the Medical Digital Twin Research Group, CLINTEC, Karolinska Institute, Stockholm, Sweden (mikael.benson@ki.se).

Hilotherapy in Orthognathic Surgery

N. Gharooni-Dowrani, B. Gharooni-Dowrani

***Abstract*—**The benefits of hilotherapy following orthogonathic surgery have been explored in recent years, demonstrating reduction in patient pain and swelling post-operatively. However, hilotherapy is not always widely accessible to all patients following orthognathic surgery. In this study, 50 patients were examined at Luton and Dunstable Hospital, half (25) of which used hilotherm masks post operatively and half of which opted for traditional ice packs in order to aid recovery. This study demonstrated that the use of hilotherapy reduced patient pain when analgesia need and use were analysed, as well as shortening inpatient stay. Although no current hilotherm masks are available without rental services in our trust, this study demonstrated the positive outcomes that they may bring, which may be worth future investment for our department.

***Keywords*—**orthognathic surgery, orthodontics, hilotherapy, OMFS.

Nikou Gharooni is with the Luton and Dunstable University Hospital, United Kingdom (e-mail: nikougharooni@gmail.com).

RADSENPRO Supplement Formulation Augments the Effectiveness of Radiation Therapy by Regulating Multiple Pathway Cross Talks in Cancer

Gururaj Deshpande, Ashiq B. G., Hemanth Kumar, Sumanth Vasista, Priyanka Bhargav, Sravan Kumar

***Abstract*—**

Introduction: Radiation therapy is one of the important modalities in cancer treatment. However, the long-term effectiveness remains variable, due to complex genomic interplay in cancer. Chemotherapy agents are used as radio-sensitizers adding to increased co-morbidity in patients and may not be a suitable option in cases of compromised liver functions and/or palliative management. There is a need for safe and tolerable formulations, which can augment radiation's effectiveness. Here, we introduce RADSENPRO, consisting of secondary metabolites with potential to improve efficacy in combination with radiotherapy. The formulation is optimized for dosing to synergize with radiation. The rate of improvement and the mechanism of action of the formulation is explored here.

Methods: SCC-4, UM-SCC-6, HSC-3 and MG63 cell lines were treated with 2 Gy radiation alone, and in combination with Radsenpro and cell viability was assayed using MTT-assay. Key cancer biomarkers for radiation sensitivity and resistance was assayed using ELISA and western blot techniques for both the cohorts and the molecular mechanism was elucidated. Phase-1 trial was conducted in healthy human volunteers to check for tolerability.

Results: Viability assay showed a marked improvement in cell death with RADSENPRO supplementation Further, biomarker assay revealed a marked reduction in oncogenic resistance markers such as AKT1, RAD51 and increased apoptotic markers with RADSENPRO treatment. The formulation was found to be safe and tolerable in all volunteers. Conclusion: The RADSENPRO formulation is a highly effective radio-sensitizer which can safely augment the effectiveness of radiation-therapy.

***Keywords*—** oncology, radiation, nutraceutical, chemoresistance.

Sumanth Vasista is with the Sal Biosciences Private Limited, India (e-mail: sumanthvasishta@gmail.com).